

2015

Surface-Enhanced Raman and Single-Molecule Spectroscopy Studies of Fugitive Artists' Pigments

Kristen A. Frano
College of William & Mary

Follow this and additional works at: <https://scholarworks.wm.edu/etd>



Part of the [Analytical Chemistry Commons](#), and the [Fine Arts Commons](#)

Recommended Citation

Frano, Kristen A., "Surface-Enhanced Raman and Single-Molecule Spectroscopy Studies of Fugitive Artists' Pigments" (2015). *Dissertations, Theses, and Masters Projects*. Paper 1539791830.
<https://doi.org/10.21220/4b3z-6793>

This Thesis is brought to you for free and open access by the Theses, Dissertations, & Master Projects at W&M ScholarWorks. It has been accepted for inclusion in Dissertations, Theses, and Masters Projects by an authorized administrator of W&M ScholarWorks. For more information, please contact scholarworks@wm.edu.

Surface-Enhanced Raman and Single-Molecule Spectroscopy Studies of Fugitive
Artists' Pigments

Kristen A. Frano

Pembroke, MA

Bachelor of Arts, Saint Anselm College, 2012

A Thesis presented to the Graduate Faculty
of the College of William and Mary in Candidacy for the Degree of
Master of Science

Department of Chemistry

The College of William and Mary
May 2015

APPROVAL PAGE

This Thesis is submitted in partial fulfillment of
the requirements for the degree of

Master of Science



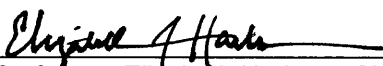
Kristen A. Frano

Approved by the Committee, April 2015

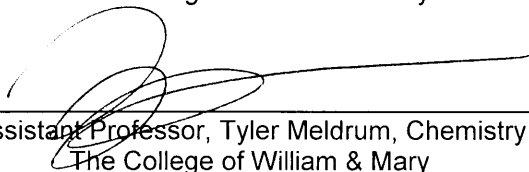


Committee Chair

Assistant Professor, Kristin Wustholz, Chemistry
The College of William & Mary



Associate Professor, Elizabeth Harbron, Chemistry
The College of William & Mary



Assistant Professor, Tyler Meldrum, Chemistry
The College of William & Mary

ABSTRACT

The values of a society, often represented in art such as oil paintings, are timeless. However, the materials used to create these paintings are unfortunately less permanent. For example, organic colorants (i.e., dyestuffs and pigments) are known to fade over time, often visibly altering the artwork from its original state. In addition to fading, due to their high tinting strength organic colorants are typically a small component of paint which may also contain inorganic pigments, oils, gums, waxes, and resins, making their identification a challenging task in conservation. Therefore, the problem of organic colorant fading in painting creates two challenges in art conservation: the first is the unambiguous detection of organic colorants, which aids conservators in their treatments and restoration of paintings. The second challenge involves developing a fundamental understanding of the mechanisms of fading, which can assist museum professionals with how to house precious artwork to prevent further photodamage. In this thesis, surface-enhanced Raman scattering (SERS) studies are used to identify faded pigments in oil paintings from the Colonial Williamsburg Foundation, and single-molecule spectroscopy (SMS) is used to study the photobleaching mechanism of red dyes and lake pigments. The collaboration between scientists, art conservators, and museum professionals to meet these challenges will greatly improve the ability to keep our cultural heritage intact, preserving it for future generations to come.

TABLE OF CONTENTS

Acknowledgements	iii
Chapter 1. Background	
Introduction	1
Theory of Raman scattering	8
Theory of surface-enhanced Raman scattering (SERS)	12
Summary of Part I of Thesis	14
References	15
Chapter 2. Organic Pigments in Transatlantic 18th-Century Oil Paintings: A Surface-Enhanced Raman Spectroscopy Study:	
Introduction	18
Experimental	21
Results and Discussion	23
Conclusions	31
Acknowledgments	34
References	34
Chapter 3. SERS Study of <i>Miracle of the Slave</i> from the Muscarelle Museum Collection	
Introduction	36
Experimental	38
Results and Discussion	39
Conclusions	42
Acknowledgments	43
References	43
Chapter 4. Direct Detection of Organic Red Lake Pigments in Paint Cross-Sections from Historic Oil Paintings	
Introduction	44
Experimental	45
Results and Discussion	48
Conclusions	55
Acknowledgments	56
References	56

Chapter 5.	Single-Molecule Spectroscopy Studies of Photobleaching in Historic Red Dyes and Lake Pigments	
	Introduction	57
	Experimental	63
	Results and Discussion	66
	Conclusions	81
	Acknowledgments	82
	References	82
Appendix		
	I: Table of Historic Organic Dyes and Pigments	84
	II: Using Raman Spectroscopy and Surface-Enhanced Raman Scattering (SERS): An Experiment for an Upper-Level Chemistry Laboratory	86
	III: All SMS Fit Parameters	95
	IV: Photobleaching Data	96

ACKNOWLEDGEMENTS

I wish to express my sincere appreciation to Dr. Kristin Wustholz, under whose guidance this investigation was conducted, for her patience, guidance and criticism throughout the investigation. I am also indebted to Professors Harbron and Meldrum for their careful reading and criticism of the manuscript. I am furthermore extremely appreciative of Dr. Bebout for her diligence as the Director of Graduate Studies for the Chemistry department.

I would also like to thank the members of the Wustholz lab, who make me excited to come into lab every day. A special thanks to Hannah Mayhew, Joo Yeon (Diana) Roh, Mary Matecki, Heidi Crockett, and Kan Tagami for their assistance and hard work in this research.

Shelley Svoboda of the Colonial Williamsburg Foundation has been an invaluable collaborator in the SERS aspect of this research, and I am truly grateful to her assistance, vast knowledge, and eagerness to provide us with samples and answer any questions we had.

I am lucky that I was able to work with a group of talented Masters students while at William & Mary. Their dedication to research and to mentoring undergraduates fosters an incredible environment for scholarship to thrive. A heartfelt thanks to Kylie Henline, who immediately helped me feel at home in a new place, and to Jessica Lampkowski, who I am so fortunate to begin and end this journey with.

Thank you to Mom and Dad, Scott, and Raven for all of your love and support.

CHAPTER 1: BACKGROUND

Introduction

The fading of natural, organic pigments in works of art upon exposure to light is a major challenge for the preservation of our cultural heritage, since the loss of pigments can significantly distort an artist's original aesthetic and intent. Thus, the detection of organic pigments in historic works of art is a vital task in conservation because the identification of these colorants can immediately assist conservators in understanding color changes and fading, authenticating artwork, and choosing techniques to use for future care. Organic pigment identification is also important in art history to broaden the understanding of historic trade routes and connections between archeological artifacts.

Organic lake pigments are particularly notorious for their propensity to fade. Lake pigments (i.e. madder lake, carmine lake) have been used as artists' materials since antiquity and are created from the precipitation of a water soluble organic dye with an inert metal-based mordant salt.¹ Although today's modern lake pigments are almost entirely made from synthetic dyes, lake pigments manufactured before the advent of synthetic aniline dyes in the 1850s were made from natural, organic dyes extracted from vegetables or insects. Although artists and scientists have long been aware of the fading properties of lake pigments, red lakes were prized for their lustrous appearance and often used by artists for flesh tones as a more aesthetically realistic alternative to more stable, red inorganic pigments.^{2,3} Due to their high tinting strength, red lakes are generally found in low concentrations in paintings. The identification of lake pigments in oil paintings is a

particularly difficult analytical task, as these colorants are generally found in low concentration in paint that may also include inorganic pigments, waxes, gums, and varnish.

Raman spectroscopy in art conservation

Analytical techniques such as UV/vis spectrometry,⁴ fluorescence spectroscopy,⁵⁻⁸ Raman spectroscopy,⁹⁻¹⁵ infrared spectroscopy,¹⁶ and high-performance liquid chromatography (HPLC)¹⁷⁻²¹ are often employed for the detection of organic colorants in art. Yet, many of these studies are often inhibited by poor sensitivity, low selectivity, a large sample requirement, and the inability to unequivocally distinguish among organic colorants. Raman spectroscopy can provide a unique vibrational fingerprint for a molecule from a relatively small sample size, enabling the unambiguous identification of pigments from paintings. For example, Raman spectroscopy is widely used for the identification of inorganic pigments in oil paintings^{11,22,23} and other cultural heritage objects including manuscripts,^{24,25} rock paintings,^{26,27} frescoes,²⁸⁻³⁰ and pottery³¹⁻³³ due to its selectivity and its ability to unequivocally identify inorganic colorants. Because Raman spectroscopy is a scattering technique and not an absorption technique, it may be used in a nondestructive manner in which a laser is incident directly onto an object, making it a useful tool for *in-situ* measurements in a wide range of environments thanks to advances in compact, handheld Raman spectrometers. Indeed, many high-quality spectral libraries and databases employing a variety of excitation wavelengths exist for inorganic pigments commonly found in cultural heritage objects.^{14,34,35} Reference spectra also exist for different binders and

varnishes, since paint matrices are often a complex mixture of different colorants and resins.^{34,36} Yet, Raman spectroscopy is not an effective technique for the identification of organic pigments in oil paintings.

Raman spectroscopy is inadequate for the identification of organic colorants because Raman scattering is an inherently weak technique. More importantly, competing fluorescence from excitation of the organic chromophore of the pigment overwhelms the Raman signal. In order to circumvent competing fluorescence, some spectral libraries of organic colorants employ laser wavelengths in the near-IR region of the electromagnetic spectrum (i.e., 1064 nm) in order to prevent the molecule from being excited into a fluorescent state.⁹ However, because only sub-nanogram amounts of organic pigment are needed for even intense coloration in oil paint, Raman scattering is generally not sensitive enough for the identification of organic colorants in paint samples, especially in areas with ultra-low concentrations of organic pigments such as flesh tones and smaller, stylistic details.³⁷ The ideal technique for the detection of organic colorants in oil paintings is sensitive, selective, requires small (i.e. microscopic) sampling, and possess the ability to unambiguously identify different organic pigments.

SERS in art conservation

Surface-enhanced Raman scattering (SERS) is emerging as a powerful technique for the identification of organic pigments in oil paintings. With the use of a noble metal substrate, SERS significantly increases the Raman signal from the analyte molecule and quenches the fluorescence that typically overwhelms the Raman signal upon visible excitation of an organic chromophore, making it a

sensitive and selective technique for the unequivocal identification of natural, organic pigments. Indeed, SERS is well suited to detect historic organic pigments given that crystal violet and rhodamine 6G, the dyes used to establish single-molecule sensitivity in SERS, were both synthesized in the late 19th century as textile dyes.³⁸ The first application of SERS to identify colorants of interest to cultural heritage occurred in 1987, when Guineau and Guichard saw large Raman signal enhancement with synthetic alizarin and textiles dyed with madder on a porous silver electrode.³⁹ However, few papers on SERS and art were published for almost the next twenty years, during which time substantial development was made in the field of nanofabrication methods. With recent advances in nanofabrication of metal substrates, SERS has made remarkable progress in the application of cultural heritage.

Varied nanofabrication methods have been used to create the noble metal substrate for SERS-based identification of organic pigments in artworks. The Lee and Meisel procedure for sodium citrate-reduced silver colloids is commonly for used for art analysis due to its low cost, simplicity, and stability.⁴⁰⁻⁵³ Other chemical syntheses for the study of cultural heritage objects use hydroxylamine hydrochloride or sodium borohydride as the reducing agent.^{49,54-57} Tollens mirrors have also been used as SERS substrates,⁴⁹ as well as metal films over nanospheres (FONs),⁵⁸ silver island films (AgIFs)^{37,59} and nanoparticles made by photo-reduction⁴³ or laser ablation.⁶⁰ These techniques often create precise and highly reproducible nanostructures, but they are costly and often require advanced instrumentation. Since the use of a SERS substrate requires sampling from a

painting or other cultural heritage object (albeit on a microscale), several new approaches have focused on nondestructive SERS. For instance, tip-enhanced Raman spectroscopy (TERS) coupled with atomic force microscopy (AFM) has been recently used for the *in-situ* identification of indigo and iron gall ink on historic paper.⁶¹ Detachable gels and films have also been used for the identification of red colorants in both textiles and a mock painting.^{62,63}

Early publications relating to SERS studies of organic colorants focus on alizarin and purpurin, the chromophores that comprise the red pigment madder lake. Cañamares and co-workers studied the Raman scattering of alizarin on silver colloids synthesized by a chemical reduction with hydroxylamine hydrochloride,⁵⁵ while Shadi and co-workers studied alizarin and purpurin using aggregated citrate-reduced silver colloids.⁵⁰ Following the successful SERS identification of alizarin and purpurin dyes, additional historic dyes were investigated in order to further examine SERS's potential to study organic artists' materials. The natural red dyestuffs cochineal,^{37,58} brazilwood,^{37,48} lac dye,^{54,58} kermes,^{37,49} eosin,^{37,64} and dragonsblood⁴⁸ have been identified with SERS. Appendix I lists the names, structures, and other details of historic organic red dyes referenced in SERS literature that are commonly found in cultural heritage materials.

In addition to water-soluble, organic dyes, lake pigments (e.g. madder lake and carmine lake) have also been identified with SERS in various binding media, representing a pivotal step in the development of SERS for art analysis. Leona and coworkers at the Metropolitan Museum of Art developed an effective method for the SERS detection of anthraquinones red lakes in paintings and textiles using a

hydrofluoric acid (HF) pretreatment.^{49,65,66} In this procedure, the sample is placed in a polyethylene holder and exposed to HF vapor for 5 minutes in a larger microchamber before silver colloids are added. The HF hydrolysis procedure is beneficial for red lakes in oil paint because it breaks down the mordant and attacks the binding medium.⁶⁵ This hydrolysis method has been successful for a variety of anthraquinone red lakes including madder lake, lac dye, and carmine lake in textiles and oil paintings from the Metropolitan Museum of Art.^{65,66} Although this technique readily identifies organic pigments, it compromises the integrity of samples since it partially attacks the oil binding medium.

Recently, focus has been placed on SERS techniques with limited pretreatment steps for the study of paint samples in order to maintain the integrity of a given sample. The elimination of the HF pretreatment is beneficial for two reasons: 1) it eliminates the chemical hazards associated with HF and 2) it fully maintains the sample integrity and allows for further analysis of the sample. In 2009, Brosseau *et al.* demonstrated the first instance of extractionless nonhydrolysis SERS on pigment grains from pastels and watercolors.⁵² In this study, citrate-reduced silver colloids are centrifuged to create a colloidal paste, which is directly applied to natural and synthetic reference materials (e.g. dried pigments, dyed textiles, and reference paints) establishing the ability of SERS to detect organic chromophores in increasingly complex matrices. High-quality SERS spectra were acquired from samples as small as a single pigment grain without the need for hydrolysis with HF. Brosseau and coworkers then applied the method to historic artists' materials, including samples from a pastel box attributed to Mary

Cassatt and historic watercolors samples from Winslow Homer's *For to Be a Farmer's Boy*.^{52,53} The detection of several organic watercolors in the faded sky in Homer's painting allowed for digital reconstruction of the painting to restore the sky to its original coloring, permitting the viewer to experience the artist's original intent. However, extractionless nonhydrolysis SERS was not successfully applied to oil paintings until Wustholz and coworkers demonstrated high-quality SERS spectra of anthraquinone red lakes, namely carmine lake, in dispersed samples from 18th-century portraits. This study reveals that SERS spectra of red lake pigments can be obtained from microscopic grains taken from complex, aged paint matrices containing other colorants, oils, and resins without the need for a pretreatment method that alters the integrity of the sample's binding medium.⁴⁰ Other previous studies by the Wustholz lab develop necessary pretreatment steps for the SERS identification of blue⁴¹ and yellow lake pigments in oil paintings.⁴⁶

Although the application of SERS for cultural heritage studies has made remarkable progress in only a decade of research, many unexplored areas exist. For instance, SERS investigations of historic synthetic organic colorants are still required in order to create a comprehensive SERS spectral database of artists' pigments. Furthermore, given that cross-section sampling (i.e., the removal of a sample from the painting that reveals its complete layer structure) is a valuable tool for conservators to learn a vast amount about a painting from a microscopic sample, SERS mapping of paint cross-sections embedded in resin represents an important but uninvestigated task. The application of SERS to explore these areas will increase our understanding of artists' materials. To understand the potential of

SERS in these tasks requires a comprehensive understanding of the Raman scattering effect, as well as the mechanisms associated with SERS that allows for Raman signal enhancement and ultimately the ability to detect organic pigments in oil paint.

Theory of Raman Scattering:

Raman spectroscopy is a vibrational spectroscopic technique that is complementary to infrared (IR) spectroscopy. Unlike IR spectroscopy where photons are absorbed, Raman is an inelastic photon scattering technique. The inherent weakness of Raman scattering requires a powerful excitation source, commonly a continuous wave visible laser (usually 400-1064 nm). Raman scattering results from an induced polarization (P) of the molecule as a result of incident light. Upon excitation with a laser, photons are promoted to what is known as a short-lived "virtual state"- an energy level that is greater than the energy between vibrational levels. Referring to Eqn. 1, the induced polarization scales as:

$$P = \alpha E \quad [1]$$

where α is the molecular polarizability for a given molecule and E is the incident electric field. The electric field E can be defined as:

$$E = E_0 \cos(2\pi\nu_0 t) \quad [2]$$

where E_0 is the electric field associated with the laser and ν_0 is the frequency of the laser. The molecular vibrations (Q_j) for a molecule with N atoms are termed normal modes, of which there are $3N-5$ for linear molecules and $3N-6$ for nonlinear molecules, and are defined by:

$$Q_j = Q_j^0 \cos(2\pi\nu_j t), \quad [3]$$

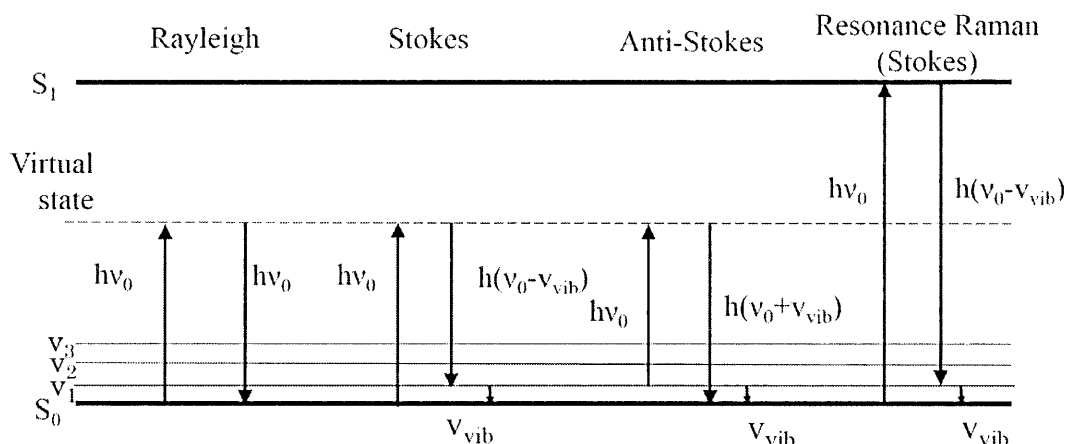


Figure 1 Schematic for Rayleigh, Raman (Stokes and anti-Stokes), and resonance where Q_j^0 is for a static molecule. The molecular polarizability changes for a molecule as vibrations occur, so (neglecting higher order terms) α can be defined as:

$$\alpha = \alpha_0 + \left(\frac{\delta\alpha}{\delta Q_j} \right) Q_j \quad [4]$$

with α_0 being the static polarizability and $\left(\frac{\delta\alpha}{\delta Q_j} \right)$ being the change in polarizability during vibration. Substituting these terms and a product-to-sum trigonometric function into Eqn. 1, the induced polarization P becomes:

$$P = \alpha_0 E_0 \cos 2\pi\nu_0 t + E_0 Q_j^0 \left(\frac{\delta\alpha}{\delta Q_j} \right) \frac{\cos 2\pi(\nu_0 + \nu_j)t + \cos 2\pi(\nu_0 - \nu_j)t}{2} . \quad [5]$$

The terms in Eqn. 5 demonstrate that upon laser excitation, light is scattered at three energies. The first term of Eqn. 5 represents elastic Rayleigh scattering, in which photons are scattered at the same energy as the exciting laser. The second term in Eqn. 5 represents anti-Stokes scattering, in which photons are scattered at a higher energy than the exciting laser, while the third term is Stokes scattering, in which photons are scattered at an energy lower than the exciting laser. The second

and third terms make up inelastic Raman scattering. The difference in energy between the incident photons and the scattered photons is referred to as the Raman shift, which is expressed in wavenumbers (cm^{-1}). A simple Jablonski diagram (Figure 1) is useful for visualizing Raman scattering.

In Raman spectroscopy, a plot of the intensity related to the number of photons inelastically scattered for a given Raman shift versus the Raman shift in cm^{-1} yields a spectrum for a molecule that represents a unique vibrational fingerprint. Stokes scattering is the most observed scattering at room temperature, since the intensity of anti-Stokes scattering is dependent on the population of the vibrational excited state of the ground electronic state according to the Boltzmann distribution:

$$\frac{I_{Anti-Stokes}}{I_{Stokes}} = \frac{(\nu_0 + \nu_j)^4}{(\nu_0 - \nu_j)^4} e^{\frac{-h\nu_j}{kT}} \quad [6]$$

which governs that for a molecule at room temperature the electronic ground state will be more populated relative to the first vibrational excited state. The intensity of Raman scattering (I_R) is defined as:

$$I_R \propto (\nu_0 \pm \nu_j)^4 \alpha_j^2 Q_j^2 \quad [7]$$

which demonstrates that the Raman intensity is proportional to the fourth power of the Raman frequency and scales to the square of the induced polarization.

Several insights about Raman scattering can be gained from an examination of Eqn. 5. First, the inherent weakness of Raman scattering relative to Rayleigh scattering can be inferred, since the change in molecular polarizability for a vibration $\left(\frac{\delta\alpha}{\delta Q_j}\right)$ will generally be smaller than the static polarizability of the

molecule (α_0). Indeed, the Rayleigh scattering cross section (i.e., the efficiency of a molecule to elastically scatter light) for simple diatomic gaseous molecules is on the order of 10^{-27}cm^2 ,⁶⁷ while the Raman scattering cross section (the efficiency of a molecule to Raman scatter photons) is on the order of 10^{-31}cm^2 .⁶⁸ In many cases, only 1 in about 10^6 - 10^{10} photons are Raman scattered.⁶⁹ Secondly, the $\left(\frac{\delta\alpha}{\delta Q_j}\right)$ term will vary for different vibrational modes, causing some modes to be more intense than others. Finally, the selection rule for a Raman active mode is $\left(\frac{\delta\alpha}{\delta Q_j}\right) \neq 0$. This selection rule differs from the selection rule for IR spectroscopy, in which for a mode to be IR active there must be a dynamic of dipole moment. The difference in selection rules of IR and Raman leads to different signal intensities on the same energy scale for different vibrations. For instance, in the molecule methyl oleate, the vibration of the C=O bond causes a significant change in the dipole moment in the molecule, leading to a strong infrared signal, while that same vibration causes a modest change in the polarizability of the molecule, leading to a relatively weak Raman signal.⁷⁰ Although Raman scattering is a less sensitive technique relative to IR spectroscopy, Raman has the advantages of a laser-dependent penetration depth that is longer than that of IR, as well as water compatibility, which is especially useful for aqueous biological samples.

One approach to increase the intensity of Raman scattering is by employing resonance Raman scattering (Figure 1). By choosing a laser wavelength that couples to an excited electronic state of the molecule, generally in the visible to near-IR regions of the electromagnetic spectrum, the amount of Raman scattered photons is increased to 1 in 10^3 - 10^6 photons. Resonance Raman requires a good

chromophore that does not fluoresce, since the fluorescence cross-section of a typical organic chromophore will be significantly larger than its scattering cross-section, and subsequently upon laser excitation fluorescence will subsequently overwhelm any Raman scattering. Currently, SERS is emerging as a powerful alternative to resonance Raman recently developed to enhance Raman signal and quench competing fluorescence from organic chromophores.

Theory of SERS spectroscopy

In 1977, two independent reports of anomalously intense Raman spectra of pyridine on electrochemically-roughened metal surfaces emerged.^{71,72} Since then, advances in the field of nanofabrication have allowed for the rapid growth of SERS. Its discovery has had a major impact on the fields of chemistry, nanoscience, and biology as a powerful analytical technique. SERS can enhance Raman scattering by factor of 10^6 - 10^{10} relative to normal Raman scattering,⁷³ but scientists deliberated to understand the mechanism by which this enhancement occurs.

Two mechanisms, an electromagnetic enhancement and a chemical enhancement, explain signal enhancement in SERS. The electromagnetic

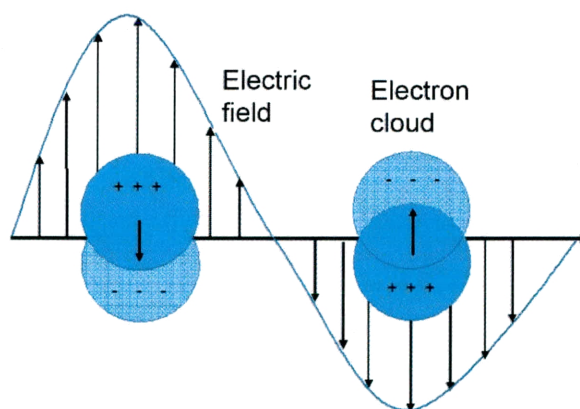


Figure 2 Illustration of localized surface plasmon resonance effect

mechanism (EM) is thought to contribute significantly to the enhancement of the Raman signal from an analyte. When the valence electrons at the surface of the metal substrate are excited by the incident electromagnetic field from the laser, the electron density at the surface of the metal substrate begins to collectively oscillate. This collective oscillation is known as the localized surface plasmon resonance (LSPR) (Figure 3). One major consequence of the excitation of the LSPR is an antenna effect: at the surface of the metal substrate: significant enhancements in the electric fields of the incident laser as well as the scattered frequency are observed. Since the intensity of Raman scattering is proportional to the square of the induced polarization of the molecule an enhancement in these electric fields will concomitantly enhance the Raman signal. The enhancement factor (EF), defined as the magnitude of the increase the Raman scattering when the analyte is adsorbed to the substrate, is defined as:

$$EF = \frac{|E_{out}|^2 |E'_{out}|^2}{|E_0|^4} \quad [8]$$

where E_{out} is the electric field at the laser frequency, E'_{out} is the electric field at the scattered frequency and E_0 is the electric field associated with the incident laser. Since both the incident and scattered frequencies are enhanced by E^2 , the enhancement is often referred to as the E^4 enhancement in the literature (i.e. if the electromagnetic field is enhanced by a factor of 10, then the overall Raman signal enhancement will be on the order of 10^4). Eqn. 8 is simplified to:

$$EF = \frac{I_{SERS}}{I_{NRS}} \quad [9]$$

or the simple ratio of the intensity of SERS (I_{SERS}) to the intensity of normal Raman scattering (I_{NRS}). Furthermore, for chromophores, a chemical enhancement via

charge transfer mechanisms when the excitation is resonant with the analyte-substrate electronic states (analogous to resonance Raman) can also account for an enhancement factor of approximately 10^2 . Chemical enhancement, however, is highly molecule-dependent. Electromagnetic and chemical enhancement factors combined can account for an EF of 10^{10} .⁷³ Indeed, with this enhancement, detection of organic dyes at the single-molecule level is possible,^{74,75} making SERS a highly sensitive technique for the detection of small quantities of organic colorants.

Summary of Thesis, Part I

The studies presented in the first part of this thesis represent novel methods or new applications of SERS for the detection of organic colorants in oil paintings. First, we use SERS to study a series of rare 18th-century New World oil paintings from the British American Southern colonies, a region largely unexplored in technical art history. The majority of the paintings show apparent fading due to overexposure to light or color changes due to past conservation treatments. We demonstrate that SERS can detect organic colorants (carmine lake, indigo) as well as the inorganic pigments Prussian blue and vermilion. The detection of these materials contributes to the understanding of artists' pigment availability, in addition to the Transatlantic flow of artists' materials between the Old and New World. This study represents one of the first comprehensive applications of SERS to technical art history.

The identification of synthetic organic pigments is also an under-researched area in SERS studies of oil paintings. In addition to natural, organic colorants from the 18th century, we also examine samples from a 19th-century oil painting, a copy of Tintoretto's *Miracle of the Slave*, recently acquired by the Muscarelle Museum of Art at The College of William & Mary. Areas of this painting are suspected to contain the first synthetic organic dye, mauveine. The detection of mauveine is useful for the dating of a painting, since the dye was first synthesized in 1856 by William Henry Perkin. Ultimately, we detect mauveine in this painting, which aids in the dating of the painting and ultimately with attributing it to a particular artist.

Finally, we develop a novel approach for the SERS-based detection of organic colorants in paint cross-sections embedded in polyester resin using SERS, Raman scattering, and light microscopy. Cross-section sampling from paintings is an extremely useful tool for conservators because it provides a vast amount of knowledge from a microscopic sample without visibly altering the artwork. The SERS mapping of paint cross-sections represents a challenging task in conservation science. Ultimately, the SERS-based detection of red organic colorants in cross-section samples from two paintings from the Colonial Williamsburg Foundation represents a crucial step for developing SERS as a spatial-mapping tool for organic pigments in cross sections.

References

1. Kirby, J. *The National Gallery Technical Bulletin* **1977**, *1*, 35.
2. Northcote, J. *Memoirs of Sir Joshua Reynolds*; M. Carey & Son: Philadelphia, 1817; .
3. Saunders, D.; Kirby, J. *The National Gallery Technical Bulletin* **1994**, *15*, 79.
4. Karapanagiotis, I.; Valianou, L.; Daniilia, S.; Chryssoulakis, Y. *J. Cult. Herit.* **2007**, *8*, 294.
5. Claro, A.; Melo, M. J.; Seixas de Melo, J. S.; van den Berg, K. J.; Burnstock, A.; Montague, M.; Newman, R. *J. Cult. Herit.* **2010**, *11*, 27.

6. Miliani, C.; Romani, A.; Favaro, G. *Spectrochim. Acta, Pt. A: Mol. Spectrosc.* **1998**, *54*, 581.
7. Claro, A.; Melo, M. J.; Schäfer, S.; de Melo, J. S. S.; Pina, F.; van den Berg, K. J.; Burnstock, A. *Talanta* **2008**, *74*, 922.
8. Melo, M. J.; Claro, A. *Acc. Chem. Res.* **2010**, *43*, 857.
9. Schmidt, C.; Trentelman, K. *Preservation Science* **2009**, *6*, 10.
10. Scherrer, N. C.; Stefan, Z.; Françoise, D.; Annette, F.; Renate, K. *Spectrochim. Acta, Pt. A: Mol. Spectrosc.* **2009**, *73*, 505.
11. Aibéo, C. L.; Goffin, S.; Schalm, O.; van der Snickt, G.; Laquière, N.; Eyskens, P.; Janssens, K. *J. Raman Spectrosc.* **2008**, *39*, 1091.
12. Ropret, P.; Centeno, S. A.; Bukovec, P. *Spectrochim. Acta, Pt. A: Mol. Spectrosc.* **2008**, *69*, 486.
13. Schulte, F.; Brzezinka, K.; Lutzenberger, K.; Stege, H.; Panne, U. *J. Raman Spectrosc.* **2008**, *39*, 1455.
14. Castro, K.; Pérez-Alonso, M.; Rodríguez-Laso, M. D.; Fernández, L. A.; Madariaga, J. M. *Anal. Bioanal. Chem.* **2005**, *382*, 248.
15. Vandenabeele, P.; Moens, L.; Edwards, H. G. M.; Dams, R. *J. Raman Spectrosc.* **2000**, *31*, 509.
16. Rosi, F.; Daveri, A.; Miliani, C.; Verri, G.; Benedetti, P.; Piqué, F.; Brunetti, B. G.; Sgamellotti, A. *Anal. Bioanal. Chem.* **2009**, *395*, 2097.
17. Sanyova, J.; Reisse, J. *J. Cult. Herit.* **2006**, *7*, 229.
18. Novotná, P.; Pacáková, V.; Bosáková, Z.; Štulík, K. *J. Chromatogr. A* **1999**, *863*, 235.
19. van Bommel, M. R.; Berghe, I. V.; Wallert, A. M.; Boitelle, R.; Wouters, J. *J. Chromatogr. A* **2007**, *1157*, 260.
20. Balakina, G. G.; Vasiliev, V. G.; Karpova, E. V.; Mamatyuk, V. I. *Dyes and Pigments* **2006**, *71*, 54.
21. Puchalska, M.; Polec-Pawlak, K.; Zdrożna, I.; Hryszko, H.; Jarosz, M. *J. Mass. Spectrom.* **2004**, *39*, 1441.
22. Benquerença, M.; Mendes, N. F. C.; Castellucci, E.; Gaspar, V. M. F.; Gil, F. P. S. C. *J. Raman Spectrosc.* **2009**, *40*, 2135.
23. Saverwyns, S. *J. Raman Spectrosc.* **2010**, *41*, 1525.
24. Clark, R. J. H. *Chem. Soc. Rev.* **1995**, *24*, 187.
25. El Bakkali, A.; Lamhasni, T.; Haddad, M.; Ait Lyazidi, S.; Sanchez-Cortes, S.; del Puerto Nevado, E. *J. Raman Spectrosc.* **2013**, *44*, 114.
26. Hernanz, A.; Gavira-Vallejo, J. M.; Ruiz-López, J. F.; Edwards, H. G. M. *J. Raman Spectrosc.* **2008**, *39*, 972.
27. Edwards, H. G. M.; Drummond, L.; Russ, J. *J. Raman Spectrosc.* **1999**, *30*, 421.
28. Edwards, H. G. M.; Gwyer, E. R.; Tait, J. K. F. *J. Raman Spectrosc.* **1997**, *28*, 677.
29. Edwards, H. G. M.; Farwell, D. W.; Seaward, M. R. D. *Spectrochim. Acta, Pt. A: Mol. Spectrosc.* **1991**, *47*, 1531.
30. Edwards, H. G. M.; Farwell, D. W.; Jenkins, R.; Seaward, M. R. D. *J. Raman Spectrosc.* **1992**, *23*, 185.
31. Zuo, J.; Zhao, X.; Wu, R.; Du, G.; Xu, C.; Wang, C. *J. Raman Spectrosc.* **2003**, *34*, 121.
32. Clark, R. J. H.; Curri, M. L.; Laganara, C. *Spectrochim. Acta, Pt. A: Mol. Spectrosc.* **1997**, *53*, 597.
33. Zuo, J.; Xu, C.; Wang, C.; Yushi, Z. *J. Raman Spectrosc.* **1999**, *30*, 1053.
34. Burgio, L.; Clark, R. J. H. *Spectrochim. Acta, Pt. A: Mol. Spectrosc.* **2001**, *57*, 1491.
35. Bell, I. M.; Clark, R. J. H.; Gibbs, P. J. *Spectrochim. Acta, Pt. A: Mol. Spectrosc.* **1997**, *53*, 2159.
36. Vandenabeele, P.; Wehling, B.; Moens, L.; Edwards, H.; De Reu, M.; Van Hooydonk, G. *Anal. Chim. Acta* **2000**, *407*, 261.
37. Whitney, A. V.; Van Duyne, R. P.; Casadio, F. *J. Raman Spectrosc.* **2006**, *37*, 993.
38. Casadio, F.; Leona, M.; Lombardi, J. R.; Van Duyne, R. *Acc. Chem. Res.* **2010**, *43*, 782.
39. Guineau, B.; Guichard, V. In *Identification de colorants organiques naturels par microspectrométrie Raman de résonance et par effet Raman exalté de surface (SERS)*; ICOM committee for conservation: 8th triennial meeting, Sydney, Australia, 6-11 September, 1987. Preprints; The Getty Conservation Institute: 1987; Vol. 2, pp 659-666.

40. Oakley, L. H.; Dinehart, S. A.; Svoboda, S. A.; Wustholz, K. L. *Anal. Chem.* **2011**, *83*, 3986.
41. Oakley, L. H.; Fabian, D. M.; Mayhew, H. E.; Svoboda, S. A.; Wustholz, K. L. *Anal. Chem.* **2012**, *84*, 8006.
42. Pozzi, F.; van den Berg, K. J.; Fiedler, I.; Casadio, F. *J. Raman Spectrosc.* **2014**, *45*, 1119.
43. Retko, K.; Ropret, P.; Cerc Korošec, R. *J. Raman Spectrosc.* **2014**, *45*, 1140.
44. Zaffino, C.; Bruni, S.; Guglielmi, V.; De Luca, E. *J. Raman Spectrosc.* **2014**, *45*, 211.
45. Centeno, S. A.; Shamir, J. *J. Mol. Struct.* **2008**, *873*, 149.
46. Mayhew, H. E.; Fabian, D. M.; Svoboda, S. A.; Wustholz, K. L. *Analyst*, 4493.
47. Cañamares, M. V.; Leona, M.; Bouchard, M.; Grzywacz, C. M.; Wouters, J.; Trentelman, K. *J. Raman Spectrosc.* **2010**, *41*, 391.
48. Bruni, S.; Guglielmi, V.; Pozzi, F. *J. Raman Spectrosc.* **2011**, *42*, 1267.
49. Leona, M.; Stenger, J.; Ferloni, E. *J. Raman Spectrosc.* **2006**, *37*, 981.
50. Shadi, I. T.; Chowdhry, B. Z.; Snowden, M. J.; Withnall, R. *J. Raman Spectrosc.* **2004**, *35*, 800.
51. Bruni, S.; Guglielmi, V.; Pozzi, F. *J. Raman Spectrosc.* **2010**, *41*, 175.
52. Brosseau, C. L.; Rayner, K. S.; Casadio, F.; Grzywacz, C. M.; Van Duyne, R. P. *Anal. Chem.* **2009**, *81*, 7443.
53. Brosseau, C. L.; Casadio, F.; Van Duyne, R. *J. Raman Spectrosc.* **2011**, *42*, 1305.
54. Cañamares, M. V.; Leona, M. *J. Raman Spectrosc.* **2007**, *38*, 1259.
55. Cañamares, M. V.; Garcia-Ramos, J. V.; Domingo, C.; Sanchez-Cortes, S. *J. Raman Spectrosc.* **2004**, *35*, 921.
56. Van Elslande, E.; Lecomte, S.; Le Hô, A. *J. Raman Spectrosc.* **2008**, *39*, 1001.
57. Cañamares, M. V.; Garcia-Ramos, J. V.; Domingo, C.; Sanchez-Cortes, S. *Vibrational Spectroscopy* **2006**, *40*, 161.
58. Whitney, A. V.; Casadio, F.; Van Duyne, R. P. *Appl. Spectrosc.* **2007**, *61*, 994.
59. Chen, K.; Vo-Dinh, K.; Yan, F.; Wabuyele, M. B.; Vo-Dinh, T. *Anal. Chim. Acta.* **2006**, *569*, 234.
60. Cesaratto, A.; Leona, M.; Lombardi, J. R.; Comelli, D.; Nevin, A.; Londero, P. *Angew. Chem. Int. Ed* **2014**, *53*, 14373.
61. Kurouski, D.; Zaleski, S.; Casadio, F.; Van Duyne, R. P.; Shah, N. C. *J. Am. Chem. Soc.* **2014**, *24*, 8677.
62. Doherty, B.; Brunetti, B. G.; Sgamellotti, A.; Miliari, C. *J. Raman Spectrosc.* **2011**, *42*, 1932.
63. Lofrumento, C.; Ricci, M.; Platania, E.; Becucci, M.; Castellucci, E. *J. Raman Spectrosc.* **2013**, *44*, 47.
64. Greeneltch, N. G.; Davis, A. S.; Valley, N. A.; Casadio, F.; Schatz, G. C.; Van Duyne, R. P.; Shah, N. C. *J Phys Chem A* **2012**, *116*, 11863.
65. Leona, M. *Proceedings of the National Academy of Sciences* **2009**, *106*, 14757.
66. Pozzi, F.; Lombardi, J. R.; Bruni, S.; Leona, M. *Anal. Chem.* **2012**, *84*, 3751.
67. Sneep, M.; Ubachs, W. *Journal of Quantitative Spectroscopy and Radiative Transfer* **2005**, *92*, 293.
68. Fouche, D.; Chang, R. *Appl. Phys. Lett.* **1971**, *18*, 579.
69. Engel, T. *Quantum Chemistry & Spectroscopy*, 3rd Ed. Pearson: 2013; pp 161.
70. McCreery, R. L. *Raman spectroscopy for chemical analysis*; John Wiley & Sons: 2005; Vol. 225.
71. Jeanmaire, D. L.; Van Duyne, R. P. *J. Electroanal. Chem.* **1977**, *84*, 1-20.
72. Albrecht, M. G.; Creighton, J. A. *J. Am. Chem. Soc.* **1977**, *99*, 5215.
73. Stiles, P. L.; Dieringer, J. A.; Shah, N. C.; Van Duyne, R. P. *Annu. Rev. Anal. Chem.* **2008**, *1*, 601.
74. Kneipp, K.; Wang, Y.; Kneipp, H.; Perelman, L. T.; Itzkan, I.; Dasari, R. R.; Feld, M. S. *Phys. Rev. Lett.* **1997**, *78*, 1667.
75. Nie, S.; Emory, S. R. *Science* **1997**, *275*, 1102.

CHAPTER 2: ORGANIC PIGMENTS IN TRANSATLANTIC 18TH-CENTURY OIL PAINTINGS: A SURFACE-ENHANCED RAMAN STUDY

Introduction

Recent research at the interface of art conservation and chemistry reveals numerous applications of surface-enhanced Raman scattering (SERS) to the identification of organic colorants in oil paintings. Studies that identify these organic pigments are especially important when color fading is observed over time.¹⁻³ For example, previous SERS studies of Old World, London-based 18th-century oil paintings have demonstrated the presence of several organic pigments (i.e. carmine lake, indigo), revealing information about the color changes in the painting and the artist's palette and methods. In particular, SERS analyses of *Portrait of Isaac Barre* by Sir Joshua Reynolds detected carmine lake in the sitter's flesh, as



Figure 1 (a) Natural-light image of *Portrait of Evelyn Byrd* (artist unidentified, probably 1725-1726, oil on canvas, 50-3/16 × 40-3/8 ", Colonial Williamsburg Foundation, CWF 1941-76) and (b) corresponding digitally-recolored visualization of the painting

well as the coat glaze applied over a layer of vermilion.^{4,5} These SERS findings establish Reynolds' continued use of carmine in flesh in 1766, despite his awareness of its fading properties and his clients' discontent.⁶

Previously, SERS studies of the *Portrait of Evelyn Byrd* by an unknown London-based artist, probably in 1725 or 1726, detected a mixture of both indigo and Prussian blue in the sitter's dress from an area of the painting previously protected by a frame, which explains the garment's present faded appearance (Figure 1). The contrast created by the fading of the dress disrupts the composition's original aesthetic and draws the viewer's eye to these areas and away from important, delicate features of the sitter. The identification of both indigo and Prussian blue in the *Portrait of Evelyn Byrd* also elucidates an interesting crossroads in the history of blue artists' pigments. Prior to the synthesis of Prussian blue in 1704 and its transition into frequent use by painters (ca. 1730s), artists frequently struggled with expensive blue pigments of unpredictable quality, difficult working properties, and the potential to fade.^{7,8} While very few oil paintings from the 18th century are identified as containing indigo paint, and traditional technical art history literature dismisses its use in paintings, extant technical manuals, documented palette layouts, and recent extensive research suggest that indigo played a role in oil painting between the 15th and 19th centuries.^{7,9,10} Hence, the detection of a mixture of indigo and Prussian blue represents a rare example of the use of indigo in London in the beginning decades of the 18th century and is consistent with contemporary findings establishing the use of indigo in oil painting. The detection of a mixture of indigo and Prussian blue is also compelling, given

that the literature suggests that once artists had access to Prussian blue they were likely to use it exclusively due to its many appealing characteristics.¹¹ Yet apparently adulteration of indigo with other colorants including Prussian blue was not uncommon.⁷

The *Portrait of Evelyn Byrd* and the *Portrait of Isaac Barre* SERS case studies reveal integral details regarding the artists' palettes and techniques, and offer explanations as to the apparent color fading present in these paintings, and most likely other 18th-century oil paintings. In an effort to gain a more comprehensive understanding of these artists' techniques and color changes in paintings from this era in addition to the flow of painting materials from the Old World to the New World, we investigate three rare 18th-century American oil paintings from the Southern British colonies, a region that, despite a recently published extensive historical analysis,¹² has largely been ignored in the realm of technical study. The majority of these paintings exhibit areas of faded color due to overexposure to light or color changes due to past treatments.

To determine what pigments were originally used in early Southern colonial paintings, we apply a SERS methodology to three paintings from the New World: *Portrait of Frances Parke Custis* by the Jaquelin-Brodnax Limner, ca. 1722; *Portrait of John Custis IV* by Williamsburg artist Charles Bridges, ca. 1735; and *Portrait of Elizabeth Allen* by Charleston, SC artist Jeremiah Theus, 1759. Cross-section and SERS analyses were performed as appropriate for the sampling regions. As is often the case with paintings of this age, the varnish cycles can demand regular treatment- therefore it is possible for past restoration materials to be present along

with historic materials. Indeed, several modern 20th-century pigments are identified in these paintings, the results of which follow the discussion of original historic materials. Ultimately, SERS is able to detect various historic pigments (i.e. carmine, vermilion, indigo, Prussian blue) in these three New World paintings. The presence of these pigments in both Old World and New World paintings can trace the flow of artists' materials across the Atlantic Ocean, which contributes to our understanding of artists' pigment availability during this period as well as the current appearance of these paintings.

Experimental

Materials, Synthesis, and Sample Preparation

Natural indigo, carmine naccarat, vermilion, Prussian blue, and cold-pressed linseed oil were obtained from Kremer Pigments (NYC). Reference paints were prepared in linseed oil by grinding them to even mixtures on a marble slab and applying them to glass slides (Fisher). Dispersed samples with particle diameters on the micron scale (i.e. invisible to the naked eye) were obtained with surgical blades (Feather Safety Razor Company, #15). Microscopic samples from the *Portrait of Frances Parke Custis* by the Jaquelin-Brodnax Limner (ca. 1722, oil on canvas, 36 × 30-1/4", Washington-Custis-Lee Collection, Washington and Lee University, U1918.15), the *Portrait of John Custis IV* by Charles Bridges (ca. 1735, oil on canvas, 36 × 27-1/2", Washington-Custis-Lee Collection, Washington and Lee University, U1918.1.4), and the *Portrait of Elizabeth Allen* by Jeremiah Theus (1759, oil on canvas, 30-3/16 × 25-1/4", Colonial Williamsburg Foundation, CWF 2012-91) were investigated using SERS. Cross-section samples were mounted in

polyester resin (Ward's Bio-Plastic), polished (Micro-Mesh, Inc., 12,000 grit), examined with a microscope (Nikon Eclipse E600) under white-light (OPELCO, fiber-optic halogen source) and UV illumination (100 W Hg lamp) at 200 × magnification, and imaged with a camera (Nikon D80).

Glassware was cleaned with aqua regia and rinsed thoroughly with ultrapure water (ThermoScientific, EasyPure II, 18.2 MΩ cm⁻¹) prior to base bathing. Silver nitrate (Acros Organic, 99%) and sodium citrate trihydrate (Sigma Aldrich) were used to synthesize citrate-reduced Ag colloids in accordance with the Lee-Meisel procedure.¹³ The colloids were centrifuged (Eppendorf, MiniSpin, 1-mL aliquots with ~0.97 mL of supernatant removed) for two cycles at a relative centrifugal force of ~12,000 g at 15 min per cycle. Blue solid samples were transferred to a 1-mL centrifuge tube (Fisher) and treated with 0.75 μL of concentrated H₂SO₄ for 45 minutes. To the indigo solution was added 0.75 μL of centrifuged colloids, and 0.75 μL of the resulting solution was pipetted onto a clean glass coverslip (Fisher). SERS measurements of untreated reference and art samples were performed on clean glass coverslips (Fisher) that were coated with 0.75 μL of centrifuged colloids.

SERS Measurements

SERS measurements were performed on an inverted confocal microscope. Excitation at 632.8 nm from a HeNe laser (Research Electro-Optics, LHRP-1701) was filtered (Semrock, LL01-633-25) and focused to the sample using a 20× objective (Nikon CFI, N.A.= 0.5). Scattering from the sample was collected through the objective, filtered (Semrock, LP02-633RS-25), focused to the entrance slit of

the spectrograph (Princeton Instruments, SP2356), and dispersed using a 600 g/mm grating blazed at 500 nm. The observed Raman frequencies were calibrated using a cyclohexane standard. Excitation power (P_{exc}) and acquisition times (t_{acq}) were varied in order to maximize signal-to-noise ratios while avoiding molecular photobleaching.

Results and Discussion

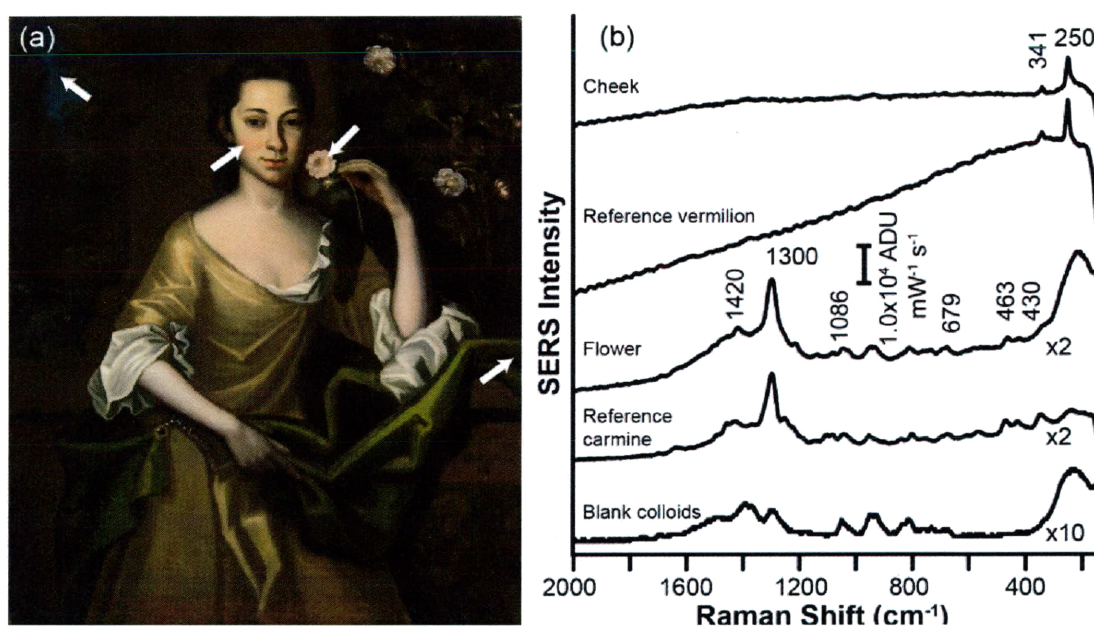


Figure 2 (a) *Portrait of Frances Parke Custis* by the Jaquelin-Brodnax Limner (ca. 1722, oil on canvas, 36 × 30-1/4", Washington-Custis-Lee Collection, Washington and Lee University, U1918.15) with sample locations indicated by arrows. (b) Corresponding SERS spectra of red samples obtained using 632.8-nm excitation at $P_{exc} = 20 \mu W$. Labeled peaks are consistent with carmine lake and vermilion. The spectrum of blank Ag colloids, which exhibits background SERS peaks due to adsorbed citrate, is shown for reference.

In order to investigate the flow of materials and painting techniques from the Old World to the New World British American Southern colonies, we first examined samples from the *Portrait of Frances Parke Custis* (Figure 2), an oil painting by the Jaquelin-Brodnax Limner that was painted in colonial Virginia ca. 1722. Preliminary examination of the painting revealed color losses in the flesh areas and obvious color changes in the sitter's green drape that indicate an organic pigment sensitive to light fading. Both cross-section and SERS analyses were performed to determine the extent of these changes. Figure 2 presents SERS spectra from microscopic, dispersed samples obtained from the flower and flesh regions of the painting, as well as blank Ag colloids. A sample from the sitter's cheek exhibits peaks at 250 and 341 cm^{-1} , consistent with the SERS spectrum for reference vermilion paint.^{14,15} The flower in the sitter's hand exhibits SERS peaks at 1420

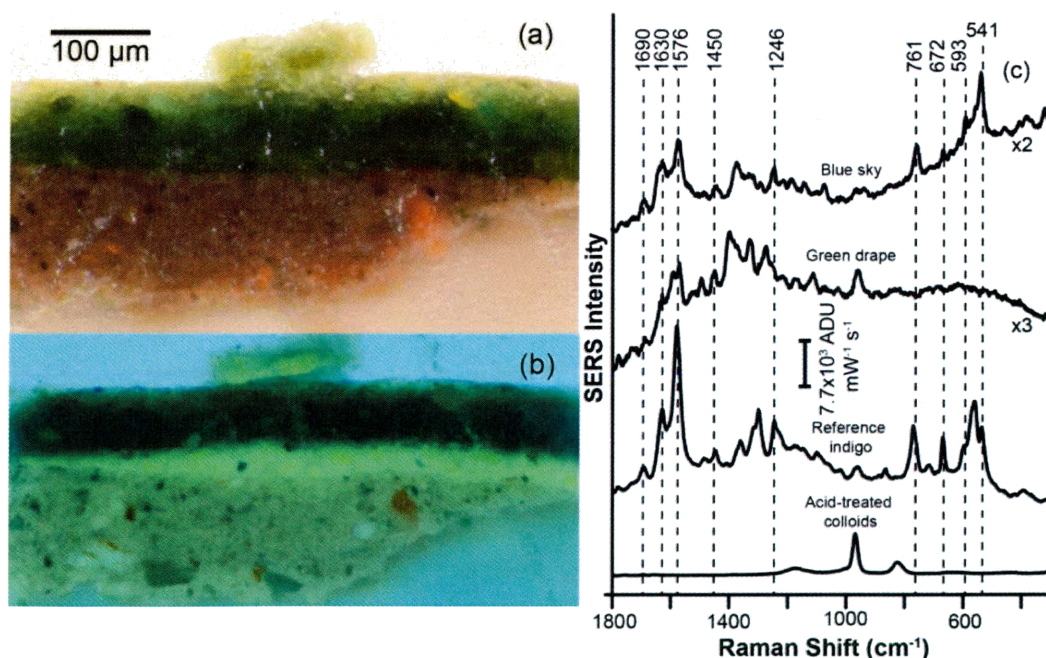


Figure 3 Cross-section from the sitter's green drape imaged in (a) white and (b) UV light. (c) SERS spectra of H_2SO_4 -treated blue samples from the *Portrait of Frances Parke Custis* obtained using 632.8-nm excitation at $P_{\text{exc}} \approx 30 \mu\text{W}$. Labeled peaks are consistent with a reference sample of H_2SO_4 -treated indigo paint. The SERS spectrum of Ag colloids treated with H_2SO_4 is shown to demonstrate peaks attributed to adsorbed sulfate.

cm^{-1} (w), 1300 cm^{-1} (s), 1086 cm^{-1} (w), 679 cm^{-1} (w), 463 cm^{-1} (m), and 430 cm^{-1} (m), consistent with carmine lake paint.^{4,5,16,17}

Though vermilion is the only red pigment we were able to identify in the sitter's flesh area, it is likely that the paint originally also contained an organic red lake component based on the slightly faded appearance of the flesh and the faint color difference between the sitter's face and arms. Since carmine lake was detected in the rose in the sitter's hand, it is probable that the flesh also contained this lake pigment. Indeed, previous studies of two other Virginia portraits of William Nelson and Elizabeth Burwell Nelson by Robert Feke in 1749 identified carmine in the sitters' flesh,⁵ suggesting that the presence of carmine lake in flesh areas from *Portrait of Frances Parke Custis* is even more likely. A cross-section sample from the sitter's green drape in *Portrait of Frances Parke Custis*, obtained from an area previously protected by a frame, is imaged in white (Figure 3a) and UV (Figure 3b) light. The cross-section analysis reveals a layering system built on a red ground with an initial thin, yellow green layer followed by a thicker blue-green optical mixture. Figure C presents corresponding SERS spectra of microscopic disperse samples obtained from the green drape and sky regions in the *Portrait of Frances Parke Custis*. In consistency with our previous SERS studies of the colorants indigo and Prussian blue, blue samples were pretreated with H_2SO_4 before the application of Ag colloids in order to solubilize the pigments. Specifically, we previously demonstrated the use of H_2SO_4 to convert insoluble indigo paint to soluble indigo carmine, enabling the SERS-based detection of indigo historic oil paint samples.¹⁸ A H_2SO_4 -treated sample obtained from the blue sky in the upper

left corner of the painting reveals SERS peaks at 1690 cm^{-1} (w), 1630 cm^{-1} (m), 1576 cm^{-1} (s), 1450 cm^{-1} (w), 1246 cm^{-1} (m), 761 cm^{-1} (m), 672 cm^{-1} (w), 593 cm^{-1} (w), 541 cm^{-1} (s), consistent with pretreated indigo paint.¹⁸ SERS peaks at 1173 cm^{-1} , 967 cm^{-1} , 824 cm^{-1} are attributed to adsorbed sulfate.^{19,20} The SERS spectrum of a pretreated sample obtained from the shadow in the sitter's green drape also contains peaks consistent with pretreated indigo paint. Yet, several vibrational modes that are characteristic of indigo (i.e. $< 800\text{ cm}^{-1}$) are not observed, indicating that the color may be degraded. These results taken together indicate the presence of indigo in the blue sky and green drape in the *Portrait of Frances Parke Custis*, the latter of which may have suffered from fading. Indigo in 1722 Williamsburg would most likely have been imported from the Caribbean or from England.²¹ Because technical studies have diminished the presence of indigo in oil paintings, the detection of indigo in the 1722 *Portrait of Frances Parke Custis* reflects both the Jaquelin-Brodnax Limner's pigment preferences and handling knowledge in addition to material availability.

The *Portrait of John Custis IV* (Figure 4a) by Charles Bridges ca. 1735 is another example of an early colonial Virginia oil painting. Custis was one of the wealthiest Virginians of the period, and his love of horticulture is reflected in his portrait. Bridges was an English-born painter who is the first documented professional artist in the colony. Microscopic dispersed samples obtained from the tulip stem and sitter's cheek in *Portrait of John Custis IV* were examined using SERS. Figure 3 demonstrates that H_2SO_4 -treated blue and green samples from the edge of the tulip leaf exhibits SERS peaks at 2072 cm^{-1} (vs), 585 cm^{-1} (w), and

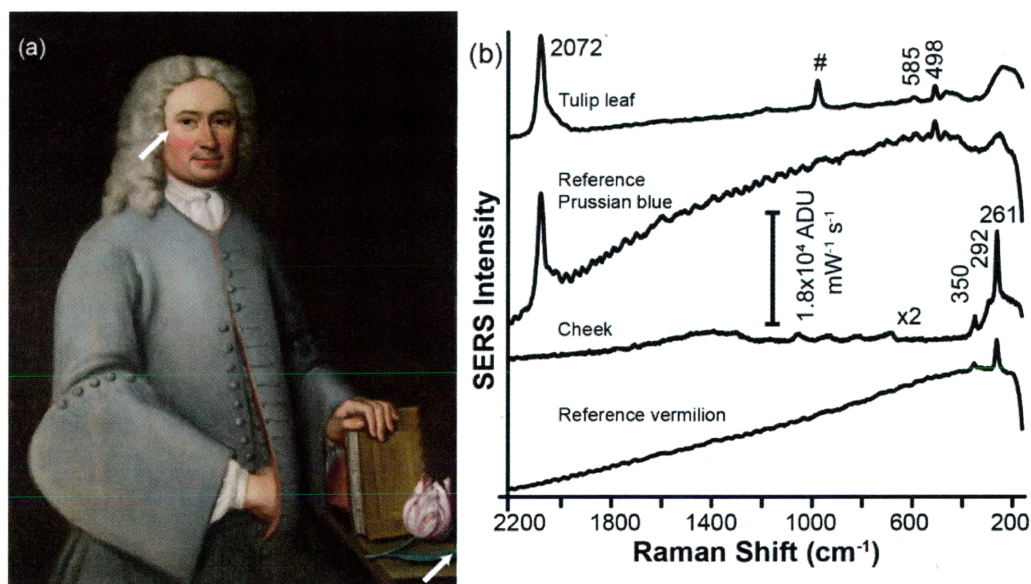


Figure 4 (a) *Portrait of John Custis IV* by Charles Bridges (ca. 1735, oil on canvas, 36 × 27-1/2", Washington-Custis-Lee Collection, Washington and Lee University, U1918.1.4) with sample location indicated by the arrow. (b) SERS spectrum of the H₂SO₄-treated paint sample obtained at 632.8-nm excitation and $P_{exc} = 20 \mu W$. Labeled peaks correspond to reference Prussian blue paint treated with H₂SO₄. The peak at $\sim 1000 \text{ cm}^{-1}$ (#) is attributed to sulfate.

498 cm^{-1} (w), consistent with the reference spectrum of pretreated Prussian blue paint.^{18,19} To our knowledge, the identification of Prussian blue in the *Portrait of John Custis IV* represents the earliest known use of the pigment in an oil painting made in the Southern colonies and perhaps New England as well. Furthermore, although visual inspection of the fleshtones in the portrait suggested the presence of a red lake pigment, SERS measurements did not detect any remaining lake and instead revealed the presence of vermilion.

Finally, an additional 18th-century New World example investigated includes the *Portrait of Elizabeth Allen* (Figure 5a), a portrait painted in 1759 by Jeremiah Theus, a Swiss-born artist who worked throughout his lifetime in the Charleston, South Carolina area. A H₂SO₄-treated sample from the lining of the sitter's blue sleeve demonstrates peaks at 2070 cm^{-1} (s), 582 cm^{-1} (w), and 498 cm^{-1} (w),

consistent with SERS bands for pretreated Prussian blue paint.¹⁸ Period Charleston newspaper records indicate Prussian blue was imported from London.²² Interestingly, although large quantities of indigo were raised in Charleston, and the sitter's husband owned large rice and indigo plantations, no indigo was detected in this portrait.

Samples from the wide, dark shadow at the bottom edge of the sitter's red drape exhibits SERS peaks for vermilion at 259 cm^{-1} (s) and 348 cm^{-1} (w), as well as peaks at 1416 cm^{-1} (m), 1300 cm^{-1} (s), 1103 cm^{-1} (w), 1083 cm^{-1} (w), and 468 cm^{-1} (w), consistent with reference carmine lake paint.^{4,5,16} Cross-section analysis reveals Theus' indirect painting technique to create a lower layer of opaque vermilion followed by a layer of the more expensive, transparent carmine lake

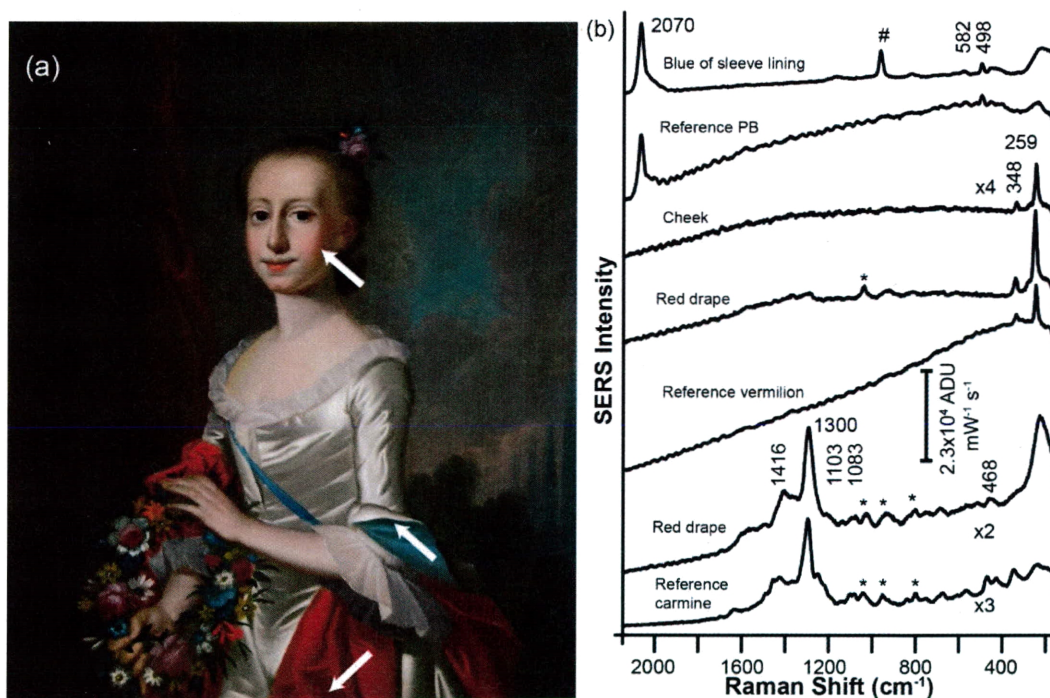


Figure 5 (a) *Portrait of Elizabeth Allen* by Jeremiah Theus, (1759, oil on canvas, 30-3/16 × 25-1/4", Colonial Williamsburg Foundation, CWF 2012-91). (b) Corresponding SERS spectra from samples obtained at 632.8-nm excitation. Labeled peaks are consistent with reference Prussian blue paint treated with H_2SO_4 , vermilion, and carmine lake paints. Peaks attributed to sulfate (#) and citrate (*) are indicated.

pigment. The South Carolina Gazette documents that in Charleston, a major port city, carmine was imported from London and readily available for purchase.²³ Vermilion was also the only red pigment detected in the sitter's cheek, despite the indicated presence of a red lake via visual inspection.

During our SERS studies of red and blue pigments from three New World portraits from the Southern British American colonies, we acquired several SERS spectra that did not match any reference spectra in our library of historic materials. Considering the physical history of paintings of this age, previous conservation treatment, which can introduce modern materials, is expected. Indeed, we

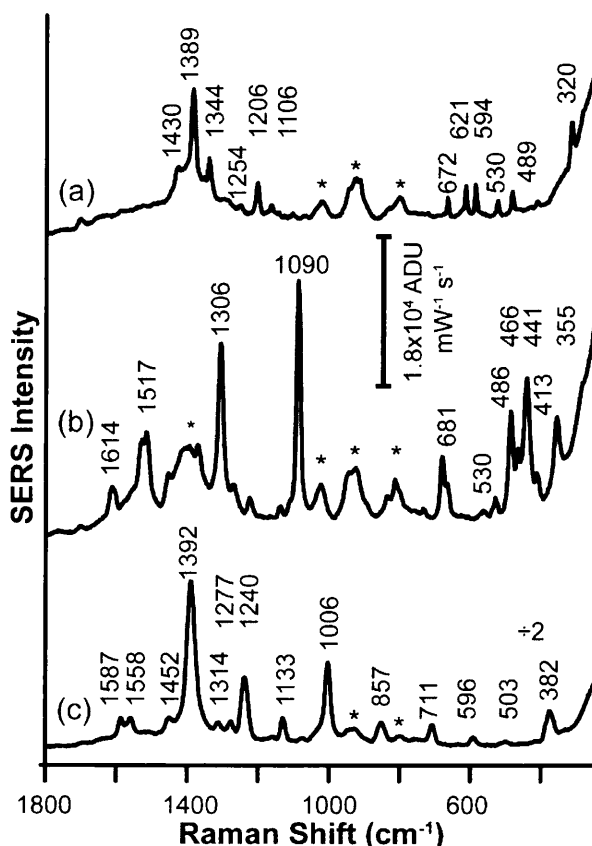


Figure 6 SERS spectra of red and purple samples obtained from *Portrait of John Custis IV*. Samples from the cheek flesh exhibit SERS bands consistent with (a) dioxazine violet, and (b) an azo dye. Samples from the tulip exhibit SERS bands consistent with a perylene derivative (e.g., PR 123, PR 179). Peaks denoted by an asterisk are attributed to citrate.

identified various modern 20th-century materials in these three 18th-century paintings using SERS. Several SERS spectra of modern, synthetic organic pigments identified in the *Portrait of John Custis IV* (Figure 4a) are presented in Figure 6. In Figure 6a, SERS spectra of samples from the cheek region from the painting exhibit peaks at 1430 cm⁻¹ (m), 1389 cm⁻¹ (s), 1344 cm⁻¹ (m), 1254 cm⁻¹ (w), 1206 cm⁻¹ (w), 1106 cm⁻¹ (w), 672 cm⁻¹ (w), 621 cm⁻¹ (w), 594 cm⁻¹ (w), 530 cm⁻¹ (w), 489 cm⁻¹ (w), and 320 cm⁻¹ (w), consistent with previously published FT-Raman spectra for the modern synthetic pigment dioxazine violet.²⁴ Another sample from the cheek region contains SERS peaks at 1614 cm⁻¹ (w), 1517 cm⁻¹ (m), 1306 cm⁻¹ (s), 1090 cm⁻¹ (s), 681 cm⁻¹ (m), 530 cm⁻¹ (w), 486 cm⁻¹ (m), 466 cm⁻¹ (w), 441 cm⁻¹ (m), 413 cm⁻¹ (w), and 355 cm⁻¹ (m) (Figure 6b), consistent with a modern synthetic azo dye.²⁴ Figure 6c presents the SERS spectrum obtained from the red of the tulip. Peaks at 1587 cm⁻¹ (w), 1558 cm⁻¹ (w), 1452 cm⁻¹ (w), 1392 cm⁻¹ (s), 1314 cm⁻¹ (w), 1277 cm⁻¹ (w), 1240 cm⁻¹ (m), 1133 cm⁻¹ (w), 1006 cm⁻¹ (m), 857 cm⁻¹ (w), 711 cm⁻¹ (w), 596 cm⁻¹ (w), 503 cm⁻¹ (w), and 382 cm⁻¹ (w) are consistent with a red synthetic perylene dye (e.g., PR 123, PR 179).²⁴⁻²⁶ Interestingly, numerous samples from this series of paintings contain perylene dye. Table 1 presents a summary of all historic and modern pigments identified in the paintings using SERS. Because the microscopic dispersed samples are carefully obtained from regions in the painting that only contain original materials, it is likely that these modern materials are present in extremely small concentrations. Indeed, the SERS spectra of modern materials are only observed in extremely localized areas of the dried colloids spots, proving the remarkable sensitivity of SERS for

the detection of both historic and modern organic colorants in miniscule art samples. Indeed, perylene dyes have been used in single-molecule SERS experiments.²⁷⁻²⁹ To our knowledge, these results represent the first application of SERS for the identification of 20th-century synthetic, organic colorants in historic oil paintings. Ultimately, the detection of historic and modern pigments in this collection of 18th-century New World and Old World paintings expands our knowledge of their original materials, their appearances due to color changes, and their past conservation treatments.

Conclusions

SERS studies of three early oil paintings from the Southern British colonies reveal fascinating findings in the context of technical art history and aesthetics. Our SERS results reveal that the use of carmine is prevalent in these 18th-century Transatlantic oil paintings, not only in broad-scale quantity-rich areas of the composition, but also the more challenging fleshtones and small but important detail regions. Indeed, period writing by Reynolds as well as early painting manuals confirm the high aesthetic value of carmine. Our findings establish the presence of carmine not only in the high-style environment of London,^{4,5} but also in the flesh of New World portraits by Robert Feke⁵ and in broad-scale textiles and small detail regions of New World portraits. Despite the fact that several other red lakes were likely available in London and the Southern colonies during the 18th-century, our investigation did not find any evidence of a lake alternatives to carmine lake, consistent with previous studies of 18th-centuries Old World oil paintings.³⁰

Table 1. Summary of results for the SERS-based identification of natural and synthetic organic pigments

Painting	Sample Location	Pigment
<i>Portrait of Isaac Barre</i> , Joshua Reynolds, 1766	Flesh from sitter's cheek and finger	carmine lake
	Sitter's red coat	carmine lake, vermilion
<i>Portrait of Evelyn Byrd</i> , unknown British artist, probably 1725-1726	Sitter's blue dress	Prussian blue, indigo
<i>Portrait of Frances Parke Custis</i> , the Jaquelin- Brodnax Limner, ca. 1722	Rose glaze: flower in sitter's hand	carmine lake
	Flower bud	perylene
	Flesh from sitter's hand	perylene
	Flesh from sitter's cheek	perylene, vermilion
	Blue sky	indigo
	Green drape	indigo
<i>Portrait of John Custis IV</i> , Charles Bridges, ca. 1735	Tulip	perylene
	Flesh from sitter's cheek	vermilion, azo dye, dioxazine violet
	Tulip leaf	Prussian blue
<i>Portrait of Elizabeth Allen</i> , Jeremiah Theus, 1759	Red drape	carmine lake, vermilion, perylene
	Lavender flower (hair accessory)	perylene
	Flesh from sitter's lips	perylene
	Flesh from sitter's cheek	vermilion
	Rose glaze: flower in sitter's hand	perylene
	Blue lining from sitter's sleeve	Prussian blue

The identification of indigo and Prussian blue in both Old World and New World paintings reveals an interesting crossroads in the history of blue pigments. Past literature informing technical art history largely dismisses the use of indigo in oil paintings, although recent research suggests that it did play at least a minor role in oil paintings between the 15th and 19th centuries.^{7,9} Therefore, the detection of indigo in the *Portrait of Evelyn Byrd* provides a rare example of the use of indigo

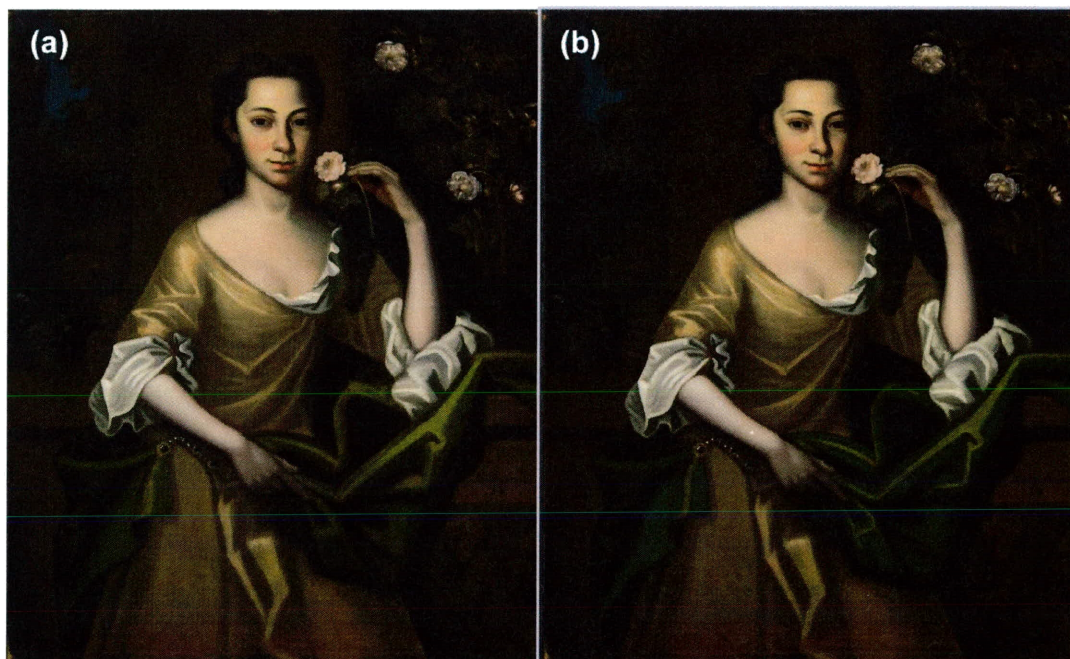


Figure 7 Normal-light image of *Portrait of Frances Parke Custis* by the Jaquelin-Brodnax Limner (ca. 1722, oil on canvas, 36 × 30-1/4", Washington-Custis-Lee Collection, Washington and Lee University, U1918.15) and (b) corresponding digitally-recolored visualization of the painting.

in London in the early 18th-century, almost two decades after the synthesis of Prussian blue. This finding is interesting, since artists were likely to use Prussian blue exclusively once they had access to it and knew of its more appealing characteristics.¹¹ The *Portrait of Frances Parke Custis* was also painted during the 1720s, but in colonial Virginia. The presence of indigo in this painting reflects both the Jaquelin-Brodnax Limner's choice of pigments and material availability in Virginia at the time, and its detection in this painting with SERS enables a digital recolorization of the sitter's green drape (Figure 7). Interestingly, SERS reveals that the slightly later portraits by Charles Bridges and Jeremiah Theus use exclusively Prussian blue, consistent with reports that date the pervasive use of Prussian blue by painters to the 1730s.^{7,8} The lack of indigo in these later portraits is fascinating, considering the large amount of indigo that was grown in the

Southern colonies during this time period. Ultimately, we establish the presence of indigo in oil paintings in the Southern colonies even after the advent of Prussian blue, and our identification of Prussian blue in Williamsburg and Charleston represents a shift in artists' blue pigment materials in the mid-18th century.

Acknowledgements

Painting samples and images are courtesy of the Colonial Williamsburg Foundation and the Washington-Custis-Lee Collection, Washington and Lee University, Lexington, VA.

References

1. Brosseau, C. L.; Casadio, F.; Van Duyne, R. P. *J. Raman Spectrosc.* **2011**, *42*, 1305.
2. Casadio, F.; Leona, M.; Lombardi, J. R.; Van Duyne, R. *Acc. Chem. Res.* **2010**, *43*, 782.
3. Pozzi, F.; van den Berg, K. J.; Fiedler, I.; Casadio, F. *J. Raman Spectrosc.* **2014**, *45*, 1119.
4. Frano, K. A.; Mayhew, H. E.; Svoboda, S. A.; Wustholz, K. L. *Analyst* **2014**, *139*, 6450.
5. Oakley, L. H.; Dinehart, S. A.; Svoboda, S. A.; Wustholz, K. L. *Anal. Chem.* **2011**, *83*, 3986.
6. Talley, M. K. In Penny, N., Ed.; Reynolds; Royal Academy of Arts: 1986; pp 65.
7. van Eikema Hommes, M. *Changing Pictures: Discoloration in 15th-17th Century Oil Paintings*; Archetype Publications Ltd.: London, 2004; .
8. Veliz, Z. In Kirby, J., Nash, S. and Cannon, J., Eds.; Trade in Artist's Materials: Markets and Commerce in Europe to 1700; Archetype Publications Ltd.: London, 2010.
9. Quinby, I. M. G., Ed.; In *American Painting to 1766: A Reappraisal*; University Press of Virginia: 1971.
10. Balfour-Paul, J. *Indigo*; Archetype Publications, Ltd.: London, 2006; .
11. Kirby, J. *The National Gallery Technical Bulletin* **1993**, *14*, 62.
12. Weekley, C. *Painters and Paintings in the Early American South*; The Colonial Williamsburg Foundation in association with Yale University Press: New Haven, CT, 2013; .
13. Lee, P. C.; Meisel, D. *J. Phys. Chem.* **1982**, *86*, 3391.
14. Burgio, L.; Clark, R. J. H. *Spectrochim. Acta, Pt. A: Mol. Spectrosc.* **2001**, *57*, 1491.
15. Bell, I. M.; Clark, R. J. H.; Gibbs, P. J. *Spectrochim. Acta, Pt. A: Mol. Spectrosc.* **1997**, *53*, 2159.
16. Brosseau, C. L.; Rayner, K. S.; Casadio, F.; Grzywacz, C. M.; Van Duyne, R. P. *Anal. Chem.* **2009**, *81*, 7443.
17. Brosseau, C.; Gamberdella, A.; Casadio, F.; Grzywacz, C. M.; Wouters, J.; Van Duyne, R. P. *Anal. Chem.* **2009**, 3056.
18. Oakley, L. H.; Fabian, D. M.; Mayhew, H. E.; Svoboda, S. A.; Wustholz, K. L. *Anal. Chem.* **2012**, *84*, 8006.
19. Hintze, P. E.; Kjaergaard, H. G.; Vaida, V.; Burkholder, J. B. *J Phys Chem A* **2003**, *107*, 1112.
20. Miller, Y.; Chaban, G. M.; Gerber, R. B. *J Phys Chem A* **2005**, *109*, 6565.
21. The Boston News-Letter, 1700-1740, America's Historical Newspapers, Feb 21 2015.
22. South Carolina Gazette, 1735, Accessible Archives, Feb 21 2015.
23. South Carolina Gazette, 1752, Accessible Archives, Feb 21 2015.

24. Scherrer, N. C.; Stefan, Z.; Francoise, D.; Annette, F.; Renate, K. *Spectrochim. Acta, Pt. A: Mol. Spectrosc.* **2009**, *73*, 505.
25. Schulte, F.; Brzezinka, K.; Lutzenberger, K.; Stege, H.; Panne, U. *J. Raman Spectrosc.* **2008**, *39*, 1455.
26. Aroca, R. F.; Constantino, C. J. L.; Duff, J. *Appl. Spectrosc.* **2000**, *54*, 1120.
27. Constantino, C. J. L.; Lemma, T.; Antunes, P. A.; Aroca, R. *Spectrochimica Acta Part A: Molecular and Biomolecular Spectroscopy* **2002**, *58*, 403.
28. Constantino, C. J. L.; Lemma, T.; Antunes, P. A.; Aroca, R. *Anal. Chem.* **2001**, *73*, 3674.
29. Lemma, T.; Aroca, R. F. *J. Raman Spectrosc.* **2002**, *33*, 197.
30. Kirby, J. O.; White, R. *National Gallery Technical Bulletin* **1996**, *17*, 56.

CHAPTER 3: SERS STUDY OF *MIRACLE OF THE SLAVE* FROM THE MUSCARELLE MUSEUM COLLECTION

Introduction

The accidental discovery of mauveine by William Henry Perkin in 1856 began the synthetic dye industry that exists today. As a student tasked to synthesize the anti-malaria drug quinine from coal tar extracts, Perkin oxidized toluidine-containing aniline with potassium dichromate to yield a black precipitate from which he extracted a vibrant purple solution that he used to dye a piece of silk.¹ Throughout its history, this dye has been referred to as “Perkin’s dye”, “Perkin’s mauve”, and “aniline purple”, but is best known simply as mauve or mauveine. Mauveine represents the first instance of a purely synthetic dye whose

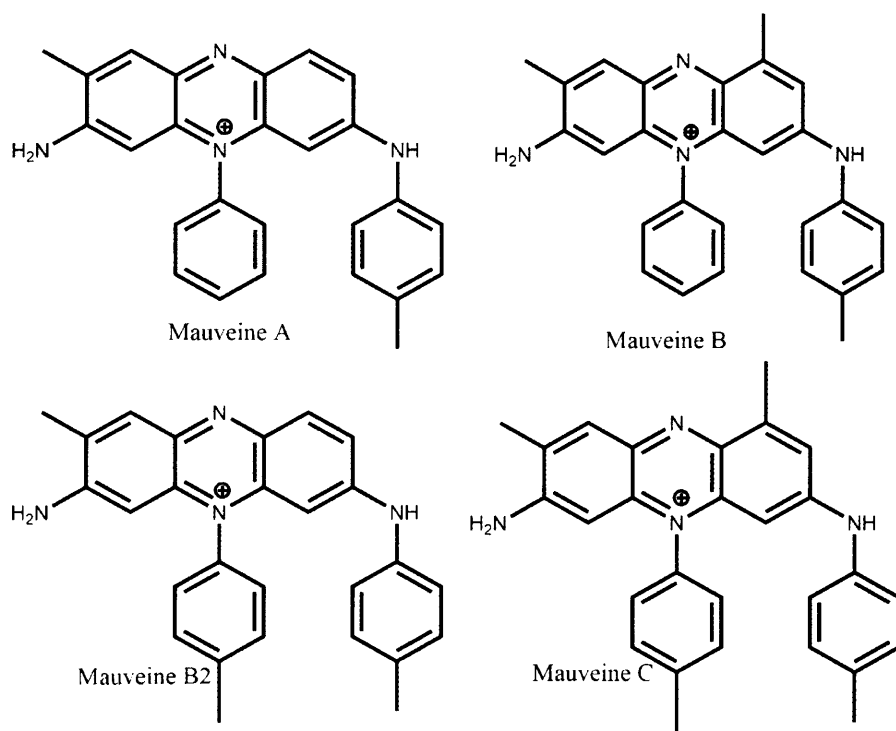


Figure 1 Mauveine chromophores (adapted from Reference 5)

structure is not found anywhere in nature. Originally thought to be a mixture of two molecules, mauveine is actually a mixture of four chromophores (see Figure 1).² While a synthesis for quinine would not be developed for another 88 years, Perkin's fortuitous synthesis of mauveine generated the beginning of the chemical industry and catalyzed the synthesis of thousands of organic dyes.

Mauveine is an icon of the Victorian age in Great Britain, since its success as a textile dye is due in large part to the advent of the Industrial Revolution in the early 19th-century and the consequential increase in trade during the growth of the British Empire.³ Furthermore, the dye grew in popularity thanks to fashions worn



Figure 2 Copy of *Miracle of the Slave*, artist unattributed, recently acquired by the Muscarelle Museum of Art at The College of William & Mary. Arrows show regions sampled for this study.

by Queen Victoria and the Empress Eugenie of France. Mauveine was also sold as an acetate salt for dyeing,^{1,4} although there is virtually nothing written from that period about its prevalence in painting or its use as a lake pigment.

The successful detection of mauveine in paintings and other cultural heritage objects is extremely useful, as its presence dates an object to after March of 1856. Furthermore, because the patent for the dye process was finalized in 1857 and Perkin sold his factory in 1873 after several years of commercial decline, it is estimated that public demand for mauveine and presumably other coal tar dyes was at its peak between 1857 and 1864.² Although several structural studies of mauve samples exist,²⁻⁴ in addition to a recently published TLC-SERS study of mauveine dye,⁵ mauveine has yet to be identified in art. For this study, we obtained paint samples from a recent acquisition of the Muscarelle Museum of Art at the College of William and Mary (Figure 2). The painting is a copy of Tintoretto's *Miracle of the Slave*, and currently has no documented artist. To aid in attributing this painting to a particular artist, we use SERS to identify mauveine or other coal tar dyes to date the painting post-1856. Because mauveine is no longer commercially available, we compare our findings to reference material from a modern synthesis as well as previously published spectra.

Experimental

Materials, synthesis, and sample preparation

Since mauveine is not commercially available, a reference solution of mauveine was created using a modern synthesis.⁶ Specifically, a 1:2:1 mixture of aniline, o-toluidine, and p-toluidine was made to recreate the impure aniline that

Perkin would have used and added to a small (~1 mL) amount of acetic acid. Another solution containing 5 mL of ethanol and 10 drops of Clorox bleach (acting as the oxidizing agent) was added to the acetic acid solution and allowed to mix for approximately one hour until the solution reached a deep purple color. Samples from the Copy of *Miracle of the Slave* (artist unattributed, oil on canvas), a recent acquisition by the Muscarelle Museum of Art, were obtained with surgical blades (Feather Safety Company) and investigated with SERS.

Citrate-reduced Ag colloids were synthesized in accordance with the Lee-Meisel procedure and centrifuged to a colloidal paste as previously described in Chapter 2. For mauveine dye reference sample, 0.75 μL of Ag colloids were added to 0.40 μL of the synthesized dye. Microscopic dispersed art samples were placed on clean glass coverslips and coated in 0.75 μL of Ag colloids for SERS analysis. All references and samples were allowed to dry before analysis.

SERS Measurements

SERS measurements were consistent with the SERS study previously described in Chapter 2. Typical excitation powers (P_{exc}) of 10-30 μW were used for SERS measurements. Acquisition times (t_{acq}) were varied from ~30-90 s for SERS measurements in order to maximize signal-to-noise ratios while avoiding irreversible molecular photobleaching.

Results and Discussion

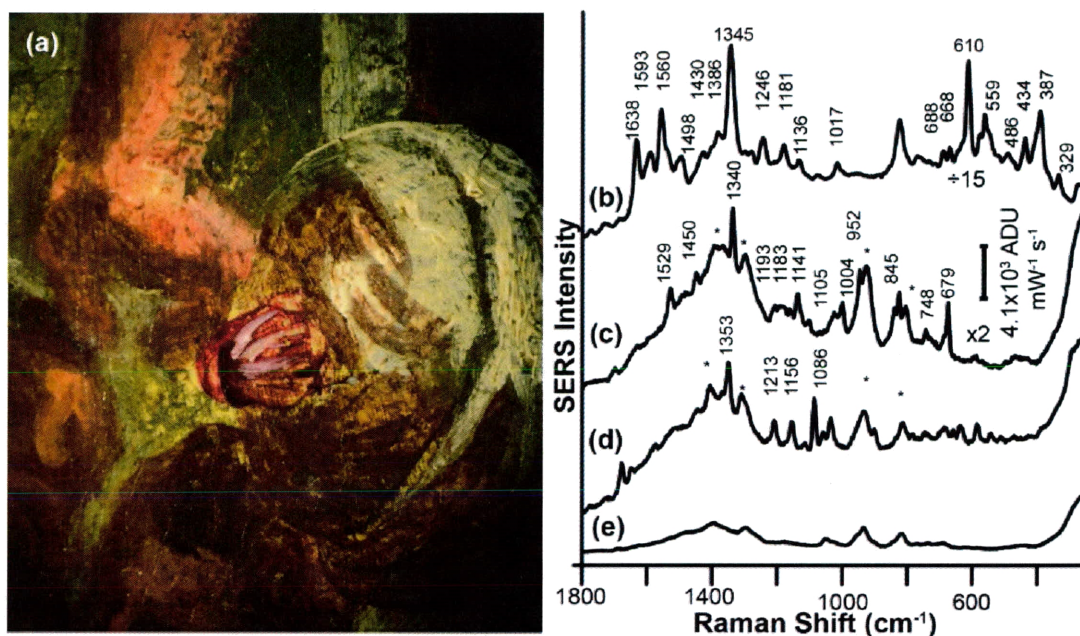


Figure 3 (a) Detail from turban in the Copy of *Miracle of the Slave*; (b) SERS spectrum of reference mauveine; (c) SERS spectrum of lower region of turban; (d) SERS spectrum of upper region of turban; (e) blank Ag colloids.

Deep red and purple samples from two areas of the turban in the center of the painting, shown in detail in Figure 3, were suspected to contain mauveine. Figure 3b presents the SERS spectrum for the synthesized mauveine obtained with 632.8 nm excitation. Peaks at 1386 cm⁻¹ (w), 1345 cm⁻¹ (vs), 1246 cm⁻¹ (w), 1181 cm⁻¹ (w), 1136 cm⁻¹ (w), 1017 cm⁻¹ (w), 668 cm⁻¹ (w), and 559 cm⁻¹ (m) are consistent with a previously published SERS study of mauveine from a historically-accurate synthesis.^{5,7} Figure 3c presents a SERS spectrum from the lower region of the turban, and has major peaks at 1529 cm⁻¹ (w), 1450 cm⁻¹ (w), 1340 cm⁻¹ (s), 1193 cm⁻¹ (w), 1183 cm⁻¹ (w), 1141 cm⁻¹ (w), 1105 cm⁻¹ (w), 1004 cm⁻¹ (w), 952 cm⁻¹ (m), 845 cm⁻¹ (w), 748 cm⁻¹ (w), and 679 cm⁻¹ (m).

Figure 3c is inconsistent with a variety of reference spectra for red and purple historic and synthetic organic colorants, including carmine lake, madder lake, lac, brazilwood, logwood, Tyrian purple, kermes, crystal violet, cobalt violet, rhodamine B, dioxazine violet, and perylene dye. Although peaks at 1340 cm^{-1} , 1183 cm^{-1} , 1141 cm^{-1} , and 679 cm^{-1} are consistent with the mauveine reference spectrum, and peaks at 1529 cm^{-1} , 1450 cm^{-1} , 1193 cm^{-1} , 1004 cm^{-1} , and 845 cm^{-1} are in good agreement with previously published SERS spectra of mauveine,⁵ several major peaks for mauveine (i.e. 1638 cm^{-1} , 1593 cm^{-1} , 1560 cm^{-1} , 610 cm^{-1} , 559 cm^{-1} , 434 cm^{-1} , and 387 cm^{-1}) are absent. It is likely that the historic sample has experienced degradation over time, causing certain bonds in the chromophores to irreversibly break. It is also possible that the distribution between the chromophores differs between the modern synthesis and the historic sample.

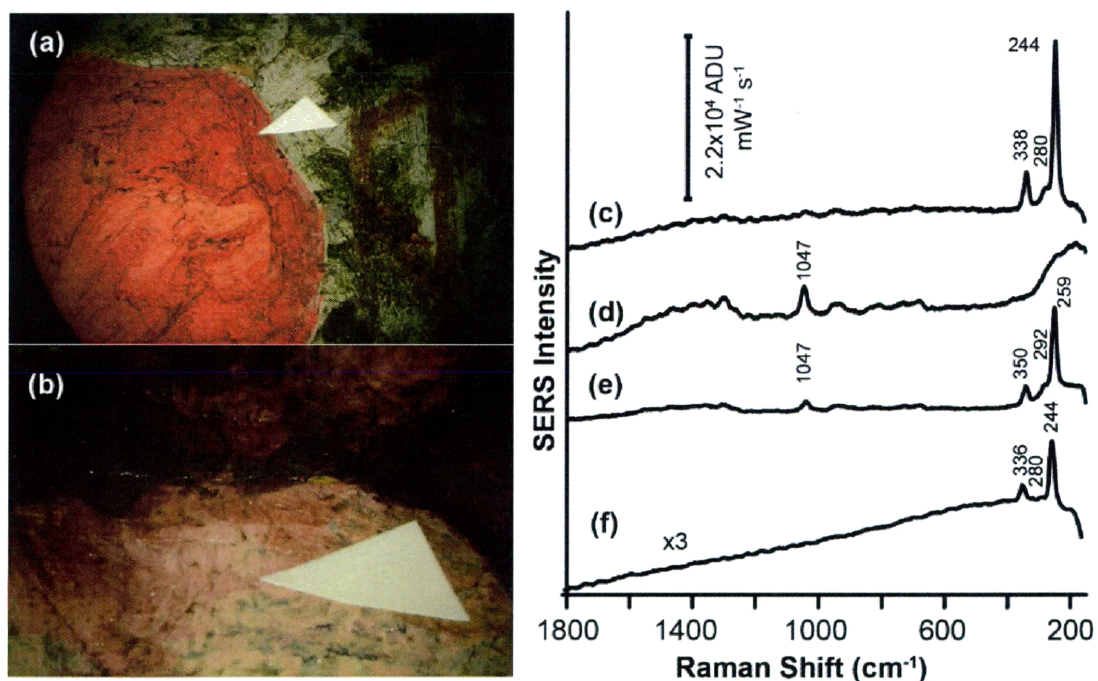


Figure 4: (a) sample detail from coral cape in the Copy of *Miracle of the Slave*; (b) sample detail from flesh of mother; (c) and (d) SERS spectrum from coral cape, consistent with vermilion and lead white; (e) SERS spectrum from flesh of the mother, consistent with lead white and vermilion; (f) SERS spectrum of vermilion reference paint.

However, due to the lack of spectral correlation between historic natural red lakes as well as the apparent similarities to synthesized mauveine, the pigment from the lower part of the turban is attributed to be a synthetic purple colorant, either mauveine or another aniline derivative. Figure 3d presents a SERS spectrum from the upper region of the turban, and exhibits major peaks at 1353 cm^{-1} (s), 1213 cm^{-1} (w), 1156 cm^{-1} (w), 1086 cm^{-1} (m), in modest agreement with the reference mauveine SERS spectrum. Based on the lack of agreement with any reference historical natural red lakes, we suspect this sample also contains mauveine or an aniline derivative. However, since we were unable to obtain consistent and reproducible SERS spectra from this sample, the results from the upper region of the turban are inconclusive.

Nonfluorescent red samples from the areas of the coral cape at the top edge of the painting and the flesh from the back of the mother in lower left corner of the painting (both areas shown in detail in Figure 4a and 4b, respectively) were also investigated. Figure 4c shows SERS spectra from the coral cape and flesh of the mother. Peaks at 1047 cm^{-1} (w), 338 cm^{-1} (m), 280 cm^{-1} (w), and 244 cm^{-1} (s) indicate an inorganic mixture of vermilion and lead white, consistent with a SERS spectrum of vermilion paint as well as previous Raman studies.^{8,9}

Conclusions

SERS results indicate the presence of an inorganic red mixture, as well as the presence of suspected degraded mauveine in the Copy of *Miracle of the Slave*. These initial findings of mauveine or aniline derivative suggests that the painting

was made after the synthesis of mauveine in 1856. The detection of mauveine in this painting further confirms the belief of the museum curators that this painting is by a notable post-Impressionist. This detection of mauveine or similar aniline dye in an oil painting represents the first SERS-based identification of mauveine in artwork, and expands the SERS spectral library of natural, organic colorants to 19th-century synthetic organic dyes. Our lab will continue to examine samples (primarily yellow lake pigments embedded in polyester resin) from this painting obtained by conservator and paint analyst Susan Buck in the near future.

Acknowledgements

Painting samples and images are courtesy of Aaron de Groft at the Muscarelle Museum of Art at The College of William & Mary and Shelley Svodoba at the Colonial Williamsburg Foundation.

References

1. Filarowski, A. *Resonance* **2010**, *15*, 850.
2. Sousa, M. M.; Melo, M. J.; Parola, A. J.; Morris, P. J. T.; Rzepa, H. S.; Seixas de Melo, J. Sérgio *Chem. Eur. J.* **2008**, *14*, 8507.
3. Seixas, d. M.; Takato, S.; Sousa, M.; Melo, M. J.; Parola, A. J. *Chem. Commun.* **2007**, 2624.
4. Meth-Cohn, O.; Smith, M. J. *Chem. Soc., Perkin Trans. 1* **1994**, 5.
5. Cañamares, M. V.; Reagan, D. A.; Lombardi, J. R.; Leona, M. J. *Raman Spectrosc.* **2014**, *45*, 1147.
6. Anonymous In *In Mauve Synthesis and Silk Dyeing*; 2011 Introductory Chemistry & Art Workshop: Colorants & Paints- Monday; 2011.
7. Scaccia, R. L.; Coughlin, D.; Ball, D. W. *J. Chem. Educ.* **1998**, *75*, 769.
8. Burgio, L.; Clark, R. J. H. *Spectrochim. Acta, Pt. A: Mol. Spectrosc.* **2001**, *57*, 1491.
9. Bell, I. M.; Clark, R. J. H.; Gibbs, P. J. *Spectrochim. Acta, Pt. A: Mol. Spectrosc.* **1997**, *53*, 2159.

CHAPTER 4: DIRECT DETECTION OF ORGANIC RED LAKE PIGMENTS IN PAINT CROSS-SECTIONS FROM HISTORIC OIL PAINTINGS

Introduction

Although SERS has been established as a sensitive technique to unequivocally identify organic pigments in historic oil paintings, the detection of these pigments from a microscopic sample from the surface of a painting does little to provide conservators with contextual information regarding the stratigraphic structure that is necessary to gain insight into an artist's palette and methodology. Cross-section sampling from a painting is an extremely important tool for conservators and is generally rationalized by the vast amount of knowledge that can be learned from even a microscopic (microns to millimeters) sample without visibly altering the artwork.¹ In this process, paint cross-sections are mounted in a polyester resin and then polished to expose the paint stratigraphy.

There are many analytical techniques that are used to analyze these cross-sections. For example, optical microscopy,¹ attenuated total reflection Fourier-transform infrared spectroscopy (ATR-IR),²⁻⁶ normal Raman scattering (NRS),^{3,7-11} visible light imaging (VIS-imaging),¹² and secondary ion mass spectrometry (SIMS)¹³ are often performed to study cross-section samples, and are frequently coupled with energy dispersive x-ray analysis (EDX) or micro-x-ray fluorescence (XRF). However, while these approaches are able to detect inorganic pigments, organic binders, proteins, and lipids, they do not allow for the unambiguous detection of natural, organic colorants in paint cross-sections.

Because extractionless nonhydrolysis SERS has proven successful for the unequivocal detection of red lakes in small, dispersed sample grains from the

surface of paintings,¹⁴ we employ that same technique here, along with light microscopy and NRS, for the detection of organic red lakes in cross-sections from oil paintings mounted in polyester resin. Although recently SERS was used to study natural red lake colorants (i.e. kermes, madder) in cross-sections from Italian 13th century polychrome statues and 16th-century mural paintings,¹⁵ in order for SERS to be a valid technique for cross-section analysis, investigations of additional colorants and binding media are required. For this study, we examined prepared reference paint cross-sections made from red pigments typical of the 18th century (i.e. carmine lake, vermilion, madder lake), as well as samples from two 18th-century oil paintings from the Colonial Williamsburg Foundation's collection. The first, the *Portrait of Elizabeth Burwell Nelson*, is by Robert Feke, the first American-born artist of European descent. The second, the *Portrait of Isaac Barré* by Sir Joshua Reynolds, was previously studied with extractionless nonhydrolysis SERS and was found to contain carmine lake paint in dispersed samples from the sitter's cheek and finger flesh.¹⁴ We also examine a 19th century sample from *Young Woman in a Red Dress* by Gabriel de Cool. This successful application of extractionless nonhydrolysis SERS along with NRS and light microscopy for the detection of organic red lake pigments in polyester resin represents a crucial step towards developing SERS as a spatial mapping tool for red lakes in paint cross-sections.

Experimental

Materials, synthesis, and sample preparation

Reference materials including madder lake, carmine naccarat, vermilion, linseed oil, and charcoal black were obtained from Kremer Pigments. Flake white pigment was obtained from RGH Artists' Oil Paints. Reference paint samples of carmine lake, vermilion, madder lake, and flake white were prepared with linseed oil on a marble slab with a glass muller. To create reference cross-section samples, a preparation layer of flake white and charcoal black was applied to a primed wood panel (8" × 10"), followed by applications of carmine lake, madder lake, or a mixture of carmine lake and vermilion paints to create a stratified structure. A mastic varnish (Kremer) was applied to the panel after sufficient drying. Cross-section samples from the *Portrait of Isaac Barré* (by Sir Joshua Reynolds, oil on canvas, 1766, 50-1/8 × 40-1/16"; CWF 2010-103), the *Portrait Elizabeth Burwell Nelson (Mrs. William Nelson)* (by Robert Feke, oil on canvas, probably 1749-1751, 49-5/8 × 39-5/8"; CWF 1986-246), and dispersed samples from *Young Woman in a Red Dress* (by Gabriel de Cool, oil on canvas, 1890, 39 × 20 1/2"; Private Collection) were investigated with SERS. Samples were obtained from oil paintings with surgical blades (Feather Safety Company).

Citrate-reduced Ag colloids were synthesized in accordance with the Lee-Meisel procedure and centrifuged to a colloidal paste as previously described in Chapter 2. Microscopic dispersed art samples were placed on clean glass coverslips and coated in 0.75 μL of Ag colloids for SERS analysis. Using a surgical microscope (Zeiss, OPMI 1FC), approximately 0.25-0.50 μL of Ag colloids were directly applied to specific regions of interest in the mounted samples. Samples were allowed to dry (~20 minutes) before SERS measurements.

Cross-section analysis

Cross-sections were mounted in a plastic tray with polyester resin (Ward's Bio-Plastic), resulting in approximately 12.7 mm × 12.7 mm × 12.7 mm (~2500 mm³) sample cubes. Cubes were ground down on a belt grinder (Wilton, 335 grit) to an approximate size of 12.7 mm × 9.5 mm × 3.1 mm (374 mm³), and then finely polished with bonded abrasive cloths (Micro-Mesh, Inc., 320-12,000 grit). Cross-section samples were examined with a microscope (Nikon Eclipse E600) under white light (OPELCO, fiber optic halogen source) and UV illumination (100 W Hg lamp) at 10× magnification and imaged with a camera (Nikon D7000). To remove Ag colloids from the cross-section samples and expose a fresh surface of paint, samples were polished again using a 1500 grit bonded abrasive cloth.

SERS Measurements

SERS measurements were consistent with the SERS study previously described in Chapter 2 and 3. A color camera (Edmund Optics, EO-0413C) was used to record images of the samples and to localize the exciting laser to specific regions of interest. In particular, those regions containing natural, organic pigments exhibited fluorescence upon examination with a microscope under UV illumination. SERS spectra were monitored across the cross-section samples using a manual x,y translation stage (Nikon TiU) in order to examine the distribution of colorants and SERS intensities. Typical excitation powers (P_{exc}) of 10-20 μ W and ~1 mW were used for SERS and normal Raman measurements, respectively. Acquisition times (t_{acq}) were varied from ~30-90 s for SERS measurements in order to

maximize signal-to-noise ratios while avoiding irreversible molecular photobleaching.

Results and Discussion

Figure 1 presents a cross-section sample containing paint layers of lead white, a mixture of carmine and vermilion, and a pure carmine glaze. Approximately 0.25 μL of Ag colloids were added to an edge of the sample, enabling SERS measurements in various localized regions within the cross-section. Major peaks at 1454 cm^{-1} (m), 1300 cm^{-1} (s), 1103 cm^{-1} (w), 1083 cm^{-1} (w), 669 cm^{-1} (w), 471 cm^{-1} (m), and 428 cm^{-1} (m) were observed in regions 1 and 2 of the sample, consistent with previous SERS studies of carmine lake paint.^{14,16,17} In region 3 of the sample, an area not coated by Ag colloids, strong fluorescence from carmine lake is observed. Although vermilion is a nonfluorescent pigment, the NRS signal is overwhelmed by the fluorescence from the organic pigment. These results show that SERS provides the ability to detect an organic pigment with pinpoint accuracy while maintaining the integrity of the stratigraphy within the sample. In order to test this SERS-based approach to identify red lakes in cross-sections from historic oil paintings, we investigated a cross-section sample from the flower bud in the *Portrait of Elizabeth Burwell Nelson* by Robert Feke. Figure 2 presents a cross-section sample imaged in white and UV light. Although the sample does not possess a defined paint layer system, the fluorescence under UV

illumination indicates the presence of a red lake. Figures 2D and 2E present SERS spectra from regions 1 and 2 of the sample, respectively, with 632.8 nm excitation.

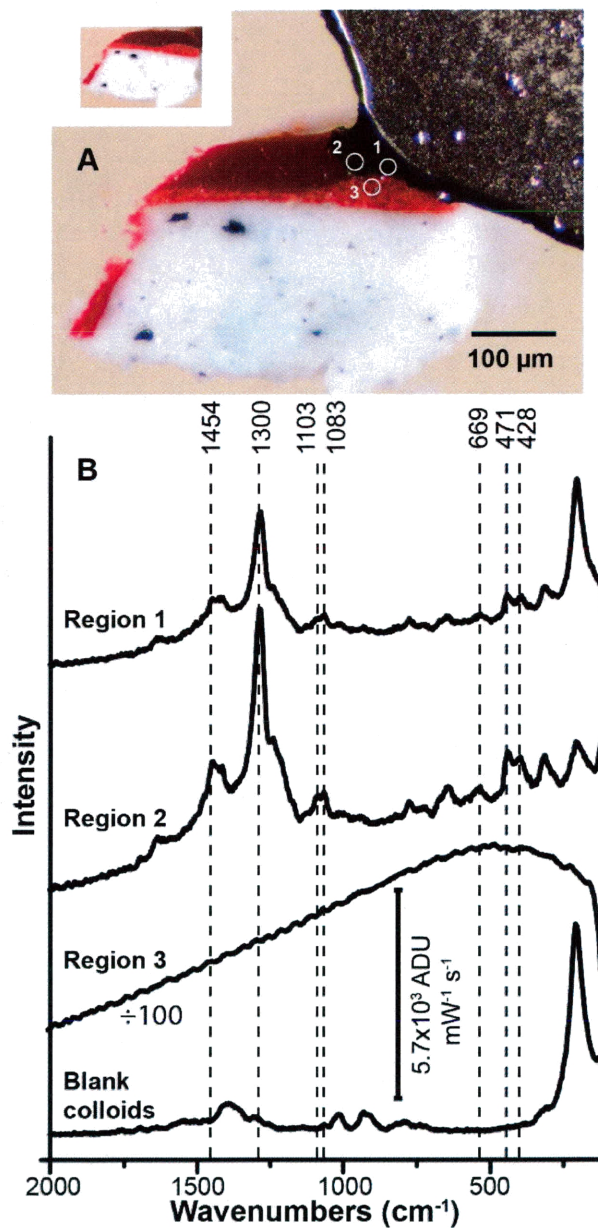


Figure 1: (A) Reference cross-section containing oil paint layers of lead white, a mixture of carmine and vermilion, and pure carmine (shown with and without colloids). (B) SERS spectra from three different regions of the cross-section as well as bare Ag colloids, obtained at 632.8 nm excitation.

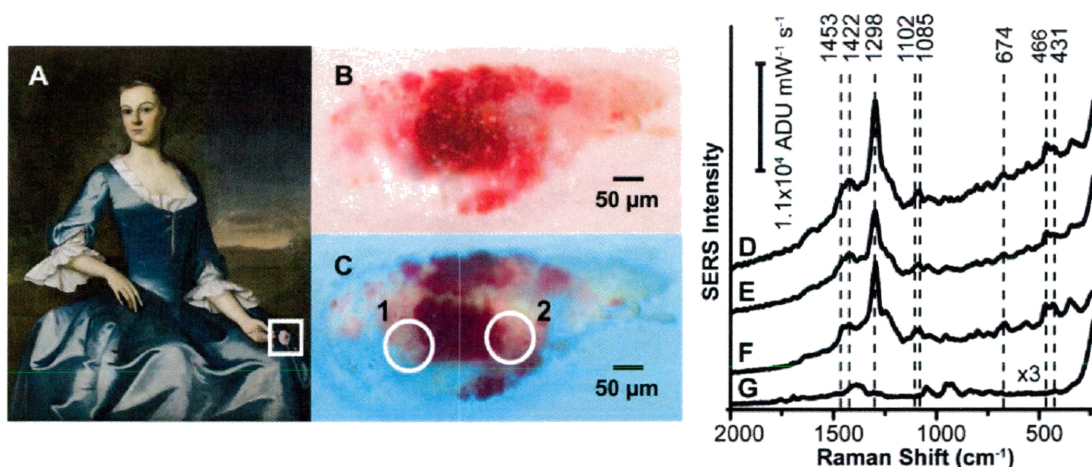


Figure 2. (A) *Portrait of Elizabeth Burwell Nelson* by Robert Feke, probably 1749-1751. Rose bud sample imaged in (B) white and (C) UV light. SERS spectra from (D) region 1 and (E) region 2 of the sample obtained using 632.8 nm excitation. SERS spectra of (F) a reference carmine-containing cross-section mounted in polyester resin and (G) blank Ag colloids applied to the polyester resin block. Peaks attributed to carmine lake are highlighted.

Labeled peaks are consistent with the spectrum for carmine lake paint in polyester resin (Figure 2F), and previous SERS studies of carmine lake.^{14,16,17} Figure G shows the spectrum for blank colloids to establish peaks due to citrate. In order to apply this SERS-based approach to a cross-section with a defined layer system, we investigated a sample from the *Portrait of Isaac Barré* by Sir Joshua Reynolds. A previous SERS study of this painting revealed the presence of carmine lake in the sitter's cheek and finger flesh in microscopic dispersed paint samples.¹⁴ Figure 3 presents a cross-section from the sitter's coat imaged in white and UV light. The cross-section reveals a preparation ground layer followed by a nonfluorescent paint layer and then a paint layer containing an organic red lake, as indicated by the fluorescence under UV illumination. Figure 3D presents a SERS spectrum from region 1 indicated in Fig 3B. This region exhibits major peaks consistent with carmine lake and linseed oil (~ 870 cm^{-1}), as well as peaks

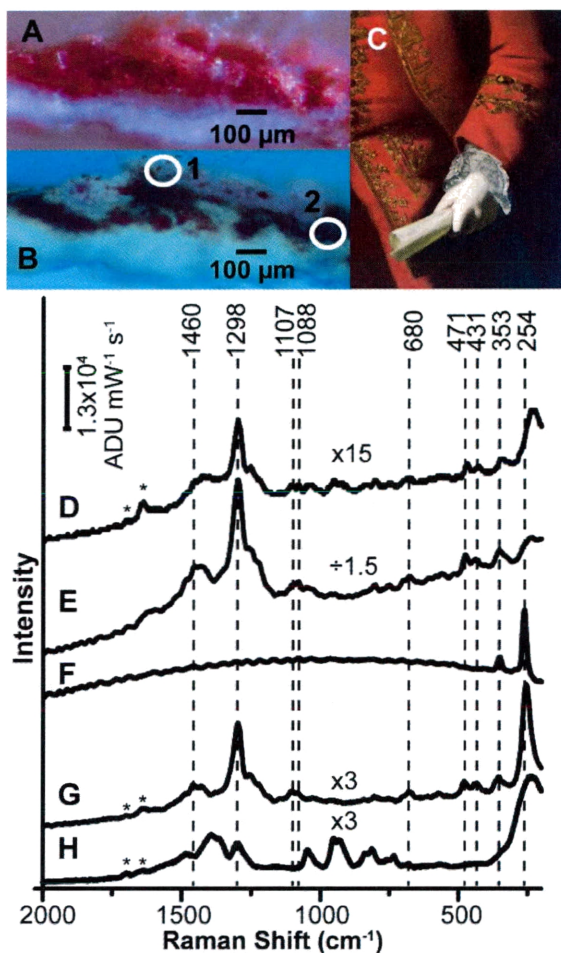


Figure 3: (A) Painting cross-section imaged in white and (B) UV light from the (C) detail of coat in the *Portrait of Isaac Barré* by Sir Joshua Reynolds, 1766; (D) SERS spectrum from *Portrait of Isaac Barré* cross-section; (E) SERS spectrum of same cross-section sample after colloids were removed by polishing and reapplied; (F) Raman spectrum from area containing vermilion in *Portrait of Isaac Barré* after colloids were removed; (G) Reference carmine and vermilion containing cross-section mounted in polyester resin; (H) SERS spectrum of blank Ag colloids applied to a polyester resin cube.

attributed to resin ($\sim 1640\text{ cm}^{-1}$ and $\sim 1700\text{ cm}^{-1}$) and citrate.^{14,16,18} This detection of carmine lake is consistent with the previous extractionless nonhydrolysis SERS study of the sitter's flesh.

Although these results demonstrate that carmine lake can be identified in cross-sections from historic artworks mounted in polyester resin, they do not account for the spatial distribution of colorants within the sample. To determine

SERS's potential as a spatial mapping tool, spectra were recorded in a variety of locations within the colloid spot on the cross-section. Inhomogeneous SERS intensities for carmine lake were observed throughout the sample, indicating that the signal originates from a localized areas in the sample and not from carmine lake dissolved into the sample to produce homogeneous signal. These results demonstrate that SERS has the potential to detect carmine lake while maintaining the integrity of the cross-section sample.

While these results represent the first *in situ* SERS-based detection of carmine lake in a mounted cross-section from a historic oil painting, attempts to repeat the measurements in Figures 2 and 3 were unsuccessful approximately one week after the application of Ag colloids. It is our thought that interactions between the nanoparticles and the polyester resin allow for the diffusion of the nanoparticles through the resin matrix, rendering the sample SERS inactive. In order to determine the future viability of these cross-section samples, we used a polishing cloth to gently remove the existing nanoparticles and expose a fresh surface of paint. White light microscopy revealed that although a small quantity of residual colloids remained, the integrity of the layer system of the sample remains intact. Ag nanoparticles were reapplied to the new paint layer after repolishing. Figure 3E shows the SERS spectrum of region 1 in the repolished cross-section. Remarkably, SERS peaks from carmine lake in polyester resin are still readily observed following colloid removal, repolishing, and reapplication.

UV microscopy (Figure 3B) also reveals the presence of a nonfluorescent, red inorganic colorant in the cross-section from the sitter's coat. NRS

measurements of the nonfluorescent red areas of the cross-section (region 2 in Figure 3B) demonstrate the presence of vermilion (Figure 3F).^{19,20} However, corresponding SERS measurements performed after the addition of Ag colloids did not exhibit peaks due to vermilion. Poor SERS signal is attributed to modest resonance Raman enhancement or insufficient adsorption of the inorganic colorant to the Ag nanoparticle substrate. Indeed, previous SERS studies with the inorganic pigment Prussian blue demonstrated the need for sample pretreatment with acid in order to solubilize the pigment to increase the SERS enhancement.²¹ Ultimately, the combination of light microscopy with NRS and SERS provides for the unambiguous detection of carmine lake and vermilion in different regions of the cross-section. This data represents the first instance of *in situ* SERS detection of colorants in mounted paint cross-sections from historic oil paintings within multiple regions of the sample and without the need for sample pretreatment. Furthermore, the SERS substrate can be removed via polishing and then reapplied for further analysis.

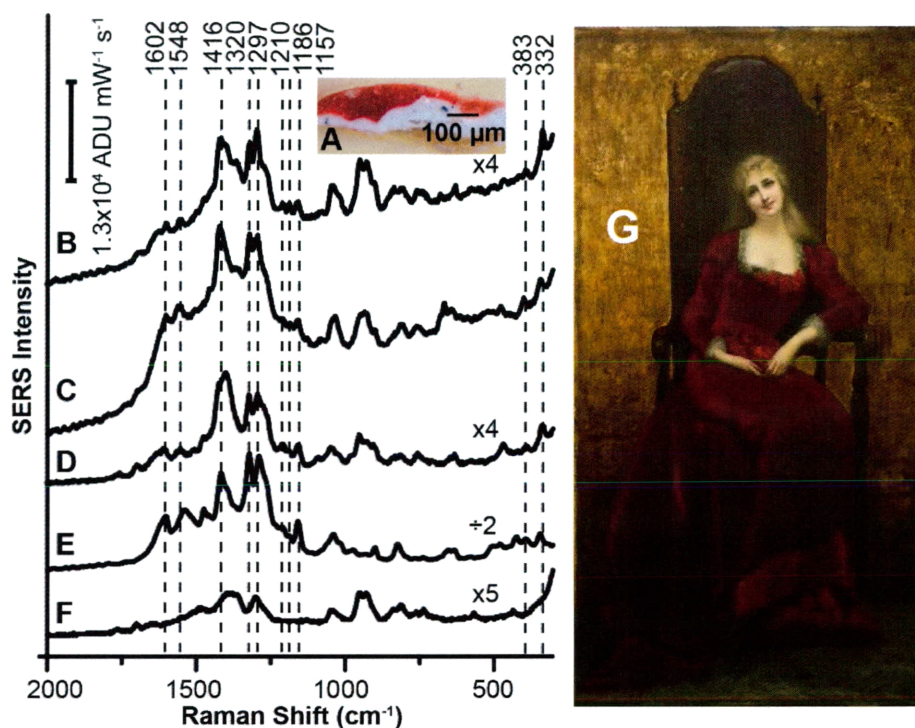


Figure 4 (A) Reference cross-section sample containing madder lake imaged in white light. (B) Corresponding SERS spectrum of A. (C) SERS spectrum of a dispersed paint sample from *Young Woman in a Red Dress* by Gabriel de Cool (1890). SERS spectra of reference madder lake (D) paint and (E) pigment. (F) SERS spectrum of blank Ag colloids applied to a polyester resin block. (G) *Young Woman in a Red Dress* (by Gabriel de Cool, oil on canvas, 1890, 39 × 20-1/2in.; Private Collection)

In order to establish that this SERS-based approach is successful for colorants other than carmine lake, we investigated madder lake. Figure 4A displays a reference cross-section in polyester resin containing madder lake paint. The corresponding SERS spectrum is presented in Figure 4B, with major peaks at 1602 cm^{-1} (w), 1548 cm^{-1} (w), 1416 cm^{-1} (s), 1320 cm^{-1} (s), 1297 cm^{-1} (s), 1210 cm^{-1} (w), 1186 cm^{-1} (w), 1157 cm^{-1} (w), 383 cm^{-1} (w) and 332 cm^{-1} (m), being in excellent agreement with the SERS spectra of alizarin and purpurin, the chromophores components of madder lake.²²⁻²⁴ To test the viability of this approach on a real art sample, we investigated a dispersed paint sample from *Young Woman in a Red Dress* by Gabriel de Cool with extractionless

nonhydrolysis SERS. Figure 4C shows the SERS spectrum from a microscopic sample from the flower region in the painting, consistent with major peaks for madder lake in polyester resin, as well as dispersed madder lake paint (Figure 4D) and pigment (Figure 4E). This suggests that extractionless nonhydrolysis SERS provides the ability to detect madder lake paint in both small dispersed samples and embedded cross-sections. This work represents the first detection of madder lake with extractionless nonhydrolysis SERS.

Conclusions

These results demonstrate the ability of extractionless nonhydrolysis SERS to successfully detect natural red lake pigments in paint cross-sections from historic oil paintings. By the direct, *in-situ* application of Ag colloids to cross-section samples embedded in polyester resin, SERS is able to unambiguously detect carmine lake, madder lake, and vermilion paint in specific regions within multiple paint layers. This provides conservators with a comprehensive knowledge of an artist's materials and methods with a single sample and without the need for pretreatment. That SERS can detect these pigments while maintaining the integrity of the stratigraphy of the layer system of a sample represents an important step towards developing SERS as a spatial mapping tool for the identification of organic pigments in paint cross-sections. Future work by the Wustholz lab will attempt to combine this light microscopy, NRS, and SERS approach to image both organic and inorganic colorants in paint cross-sections.

Acknowledgements

Painting images of *Elizabeth Burwell Nelson* and *Isaac Barré* are courtesy of CWF.

Images of *Young Woman in a Red Dress* courtesy of S. Svoboda.

References

1. Wolbers, R. C.; Buck, S. L.; Olley, P. In Stoner, J. H., Rushfield, R., Eds.; *The Conservation of Easel Paintings*; Routledge: New York, NY, 2012; pp 326.
2. Spring, M.; Ricci, C.; Peggie, D. A.; Kazarian, S. G. *Anal. Bioanal. Chem.* **2008**, *392*, 37-45.
3. Daher, C.; Drieu, L.; Bellot-Gurlet, L.; Percot, A.; Paris, C.; Le Hô, A. *J. Raman Spectrosc.* **2014**, *45*, 1207.
4. Sloggett, R.; Kyi, C.; Tse, N.; Tobin, M. J.; Puskar, L.; Best, S. P. *Vibrational Spectroscopy* **2010**, *53*, 77.
5. Joseph, E.; Prati, S.; Sciutto, G.; Ioele, M.; Santopadre, P.; Mazzeo, R. *Anal. Bioanal. Chem.* **2010**, *396*, 899-910.
6. Mazzeo, R.; Joseph, E.; Prati, S.; Millemaggi, A. *Anal. Chim. Acta* **2007**, *599*, 107.
7. Lau, D.; Livett, M.; Praver, S. *J. Raman Spectrosc.* **2008**, *39*, 545.
8. Aibéo, C. L.; Goffin, S.; Schalm, O.; van der Snickt, G.; Laquière, N.; Eyskens, P.; Janssens, K. *J. Raman Spectrosc.* **2008**, *39*, 1091.
9. Ropret, P.; Centeno, S. A.; Bukovec, P. *Spectrochim. Acta, Pt. A: Mol. Spectrosc.* **2008**, *69*, 486.
10. Conti, C.; Colombo, C.; Matteini, M.; Realini, M.; Zerbi, G. *J. Raman Spectrosc.* **2010**, *41*, 1254.
11. Burgio, L.; Clark, R. J. H.; Sheldon, L.; Smith, G. D. *Anal. Chem.* **2005**, *77*, 1261.
12. van, d. W.; van Veen, M. K.; Heeren, R. M. A.; Boon, J. J. *Anal. Chem.* **2003**, *75*, 716.
13. Keune, K.; Boon, J. J. *Anal. Chem.* **2004**, *76*, 1374.
14. Oakley, L. H.; Dinehart, S. A.; Svoboda, S. A.; Wustholz, K. L. *Anal. Chem.* **2011**, *83*, 3986.
15. Idone, A.; Aceto, M.; Diana, E.; Appolonia, L.; Gulmini, M. *J. Raman Spectrosc.* **2014**, *45*, 1127.
16. Brosseau, C.; Gamberdella, A.; Casadio, F.; Grzywacz, C. M.; Wouters, J.; Van Duyne, R. P. *Anal. Chem.* **2009**, 3056.
17. Brosseau, C. L.; Rayner, K. S.; Casadio, F.; Grzywacz, C. M.; Van Duyne, R. P. *Anal. Chem.* **2009**, *81*, 7443.
18. Vandenaabeele, P.; Ortega-Avilès, M.; Castelleros, D. T.; Moens, L. *Spectrochim. Acta, Pt. A: Mol. Spectrosc.* **2007**, *68*, 1085.
19. Bell, I. M.; Clark, R. J. H.; Gibbs, P. J. *Spectrochim. Acta, Pt. A: Mol. Spectrosc.* **1997**, *53*, 2159.
20. Burgio, L.; Clark, R. J. H. *Spectrochim. Acta, Pt. A: Mol. Spectrosc.* **2001**, *57*, 1491.
21. Oakley, L. H.; Fabian, D. M.; Mayhew, H. E.; Svoboda, S. A.; Wustholz, K. L. *Anal. Chem.* **2012**, *84*, 8006.
22. Bruni, S.; Guglielmi, V.; Pozzi, F. *J. Raman Spectrosc.* **2010**, *41*, 175.
23. Pozzi, F.; Lombardi, J. R.; Bruni, S.; Leona, M. *Anal. Chem.* **2012**, *84*, 3751.
24. Bruni, S.; Guglielmi, V.; Pozzi, F. *J. Raman Spectrosc.* **2011**, *42*, 1267.

CHAPTER 5: SINGLE-MOLECULE SPECTROSCOPY STUDIES OF PHOTBLEACHING IN HISTORIC RED DYES AND LAKE PIGMENTS

Introduction

Although SERS has the ability to identify natural, organic pigments in faded regions of paintings, an understanding of the complex photobleaching mechanisms of these pigments is equally crucial. In fading, the chromophores that provide color to an object are photobleached upon exposure to light over time. Photobleaching is an irreversible process that photochemically alters the structure of a chromophore to a colorless form. Fading often accounts for color changes that distort an artist's original aesthetic vision, as observed in the SERS studies of faded garments from the *Portrait of Evelyn Byrd* and the *Portrait of Frances Parke Custis*. Therefore, an understanding of the molecular photodegradation pathways of colorants is crucial, enabling museums to establish proper storage and exposure conditions for cultural heritage objects and to prevent further photodamage.

Various artists' materials are known to exhibit fading with time upon exposure to light. Natural red lake pigments such as madder lake and carmine lake have been used as artists' materials since antiquity and are highly susceptible to

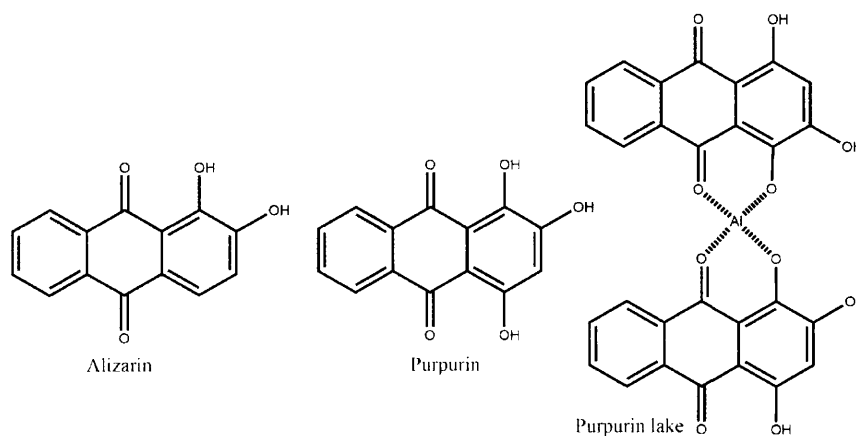


Figure 1 Hydroxyanthraquinone chromophores: alizarin, purpurin, and purpurin lake

fading. Lake pigments are created from the precipitation of water-soluble dyes (e.g., alizarin, purpurin, and carminic acid extracts from natural sources) with a mordant salt such as alum (i.e., $\text{KAl}(\text{SO}_4)_2$). The resulting water-insoluble pigments were highly prized by artists due to their high tinting strength and lustrous qualities. Indeed, red lakes were used in fleshtones and small, yet important, detail regions in paintings, even after scientists and artists knew of their fading potential.¹

In an effort to understand molecular photobleaching of red lake pigments, we investigate the fading of several hydroxyanthraquinone-based chromophores (Figure 1). Although several publications on anthraquinone dye fading exist,^{2,3} many of these reports assess color changes with time rather than examine mechanistic details. For example, dye structure is known to play an important role in the photophysics of hydroxyanthraquinones.⁴ Furthermore, lake pigments made with tin (i.e., SnCl_2) and aluminum (i.e., $\text{KAl}(\text{SO}_4)_2$) mordants exhibit significant fading compared to pigments containing copper, chrome, or iron.⁵ The presence of oxygen has also been observed to greatly impact the fading of hydroxyanthraquinones, but the mechanistic details of these changes are not well understood.⁶

The influence of different mordant salts on the photophysics and photochemistry of lake pigments is an underexplored area in conservation science. Studies of purpurin ($\phi_f = 0.004$) and purpurin with Al^{3+} ions in solution observed that purpurin complexed with Al^{3+} (Figure 1) demonstrates increased fluorescence ($\phi_f = 0.29$), where ϕ_f is the fluorescence quantum yield. It is hypothesized that mordant salts containing heavy-atoms can facilitate triplet-state blinking and

photobleaching, but relatively few spectroscopic studies of hydroxyanthraquinone dyes and related lake pigments have been performed. Ultimately, several persistent questions remain about fading in art: (1) what are the detailed structure-property relationships in chromophore photobleaching?, (2) what is the role of mordant salt (chelating metal ion) in photophysics and photochemistry?, and (3) what is the impact of molecular oxygen on these dynamics?

Various spectroscopic tools are used to monitor fading (e.g., colorimetry, UV/Vis, fluorescence), but ensemble-averaged approaches are complicated by the heterogeneous paint matrix, in which a variety of materials have undergone ageing and associated photochemical and photophysical changes with time. Understanding the detailed relationships among paint structure,⁷ chromophore local environment,⁸ and external environmental factors⁹⁻¹⁴ (e.g., oxygen, pollutants, age) will likely be hidden under the averaging over an ensemble with conventional spectroscopy. Moreover, hydroxyanthraquinones exist in multiple protonation states in condensed phases and are known to undergo excited state intramolecular proton transfer (ESIPT).^{4,15,16} Single-molecule spectroscopy (SMS) is uniquely suited to study chromophores in complex environments.

SMS is a powerful technique recently developed for the detection of single molecules, the ultimate limit of detection. Given that fluorescence is a sensitive technique where a bright signal appears against a dark background, SMS is an obvious technique for the study of individual chromophores. The first instance of SMS detection of fluorophores at room temperature was reported in 1990,¹⁷⁻¹⁹ and although despite experimental difficulties and generally poor S/N ratio, SMS has

significant advantages over ensemble averaging for investigating heterogeneous systems. For example, SMS studies commonly investigate the conformation of biomolecules, including protein folding and DNA, to remove problems associated with ensemble-averaging and non-synchronicity.²⁰⁻²²

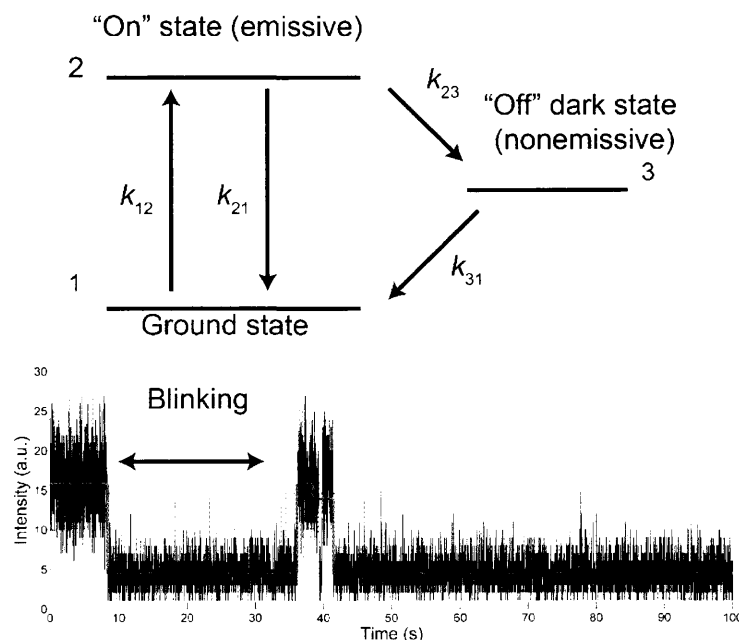


Figure 2 Jablonski diagram of fluorescence for an emission to an “on” state and transfer to nonemissive “off” state and their corresponding rate constants. A schematic of blinking dynamics is shown below

With SMS, the photophysics of single molecules are probed by measuring the dynamics of molecular “blinking”, defined as fluctuations in the emission intensity under continuous excitation of a single molecule.²³ The possible photophysical pathways for a single molecule upon excitation are represented in Figure 2. Upon excitation, a molecule is promoted to a fluorescent state “on” state, and emission intensity is observed. However, a molecule can transition to an “off” nonemissive state. Once the molecule returns to the ground state, the molecule can be promoted to a fluorescent state again. Single-step photobleaching can also

be observed, where the molecule reaches a permanent, nonfluorescent bleach state. To quantify molecular photophysics, the durations of emissive and non-emissive events (on times and off times, respectively) are compiled into histograms. The functional form of the resulting histogram relates to the underlying kinetic model. For example, when blinking occurs via a triplet state, the population and depopulation of on and off states obey first-order kinetics. Hence, the on-times and off-times histograms are fit by single exponential functions with rate constants corresponding to triplet population and depopulation.^{24,25} However, many systems exhibit event distributions that are not single exponential, indicating that the observed blinking behavior corresponds to more complex processes. More recently, various SMS studies have revealed on-time and off-time distributions that appear to follow heavy-tailed functions (e.g., power law, Weibull and log-normal distributions), indicating that the rate constants for population and depopulation are not described by a single value but vary with time, leading to a distribution of the rate constants k_{23} and k_{31} in Figure 2.^{26,27}

Previous studies in our group have demonstrated that SMS studies of rhodamine dyes on TiO₂ substrates coupled with robust statistical analysis and Monte Carlo simulations reveal dispersive electron-transfer kinetics in model dye-sensitized solar cells (DSSCs).²³ In this approach, the combination of experiment and computation reveals the underlying distributed kinetics of chromophores in DSSCs. For example, the log-normal distribution of events corresponds to a Gaussian distribution of activation energies for forward electron transfer and back electron transfer.²³ Distributions corresponding to alternative heavy-tailed

functions indicate different kinetic behavior. For instance, a power law distribution of events relates to the exponential distribution of rate constants.²⁸

To complement our SERS studies of pigment identification in historic oil paintings, we use this combined SMS and computational approach to study chromophore photophysics and photochemistry of natural red dyes and their corresponding lake pigments in air and anoxic environments, since the presence of oxygen are known to play a role in chromophore fading,⁹⁻¹³ In particular, we investigate the photophysical properties of alizarin and purpurin dyes (the main chromophores in madder lake) as well as purpurin lake pigment, in order to examine the role that dye-mordant interactions play in photobleaching. The processes responsible for fading are incredibly complex, as they are highly dependent on dye structure and the surrounding environment. While SMS investigates molecular photophysics unobscured by environmental heterogeneity and ensemble averaging, to our knowledge, no SMS studies of artists' natural, organic dyes and their lake pigments have been performed. Using the combined SMS and computational approach, we seek to elucidate the complex photophysical and photobleaching pathways responsible for the fading of artists' red hydroxyanthraquinone dyes and lake pigments. An understanding of fading in these systems has the potential to benefit artists, conservators, and museum curators and visitors. Studies of the photophysics of hydroxyanthraquinones also benefit organic DSSC technology, drug delivery, and colorimetric sensing. SMS studies of alizarin, purpurin, and purpurin lake are performed to explore the impact

that the chromophore structure, mordant, and oxygen has on the photophysics and photobleaching of these colorants.

Experimental

Synthesis of purpurin lake and sample preparation

Purpurin, alizarin, potassium carbonate, aluminum potassium sulfate, and methanol were purchased from Sigma Aldrich. Ultrapure water ($18.2 \text{ M}\Omega \text{ cm}^{-1}$) was obtained with a water purification system (ThermoScientific, EasyPure II). Glass coverslips (Fisher Scientific 12-545-102) were cleaned in a base bath for 24 hours, thoroughly rinsed with ultrapure water, and dried using clean dry air (McMaster Carr, filter 5163K17).

Because lake of purpurin dye is not commercially available, a historically-accurate synthesis was performed.²⁹ Briefly, approximately 60 mg of purpurin dye was added to a 0.2M solution of potassium carbonate (K_2CO_3) in ultrapure water in an Erlenmeyer flask. Next, a 0.2M solution of potassium alum ($\text{KAl}(\text{SO}_4)_2 \cdot 12(\text{H}_2\text{O})$) was added drop-wise to the purpurin and K_2CO_3 solution until the it reached a pH of ~ 5 . The solution was vacuum filtered and the resulting product was crushed into a fine powder with a mortar and pestle. The resulting water-insoluble solid is brighter and pinker relative to the dark, reddish-brown purpurin dyestuff.

Dye solutions of alizarin and purpurin were prepared in ethanol and ethyl acetate, respectively. However, since lake pigments are generally insoluble in water, several solvents including ethyl acetate, ethanol, DMA, xylenes, and

isopropanol were tested to solubilize the pigment, but were deemed unsuitable for single-molecule experiments due to their inability to even partially dissolve purpurin lake, or for their ability to chemically transform the molecule. (e.g., purpurin lake is fully dissolved in dimethylamine, but in this basic solvent the neutral form of the chromophore seemed to be converted to its anion form).³⁰ Purpurin lake is partially soluble in a 3:1 solution of MeOH and ultrapure water.³¹ Therefore, consistent with previous studies, purpurin lake solutions were prepared in a 3:1 solution of MeOH and ultrapure water and flushed with inert argon gas to remove dissolved oxygen. SMS samples were prepared by spin-coating 35 μL of a 10^{-8} - 10^{-9} M chromophore solution onto a clean glass coverslip using a spin coater (Laurell Technologies, WS-400-6NPP-LITE) operating at 3000 rpm. Samples were mounted in a custom-design flow cell for environmental control and flushed with dry N_2 for single-molecule experiments in anoxic environments.

Single-molecule confocal microscopy

Samples for SMS studies were placed on a nanopositioning stage atop an inverted confocal microscope (Nikon TiU). Laser excitation at 532 nm (Spectra-Physics, Excelsior) was focused to a diffraction-limited spot using a variable numerical aperture (NA) 100 \times oil immersion objective (Nikon Plan Fluor, NA= 0.5-1.3) set to NA= 1.3. Excitation powers (P_{exc}) corresponding to 0.80 μW , 1.4 μW , \sim 2.6 μW were used for purpurin lake, alizarin dye, purpurin dye in air and N_2 respectively. Fluorescence from the sample was collected through the objective, spectrally filtered using an edge filter (Semrock, LP03-532RS-2S), and focused onto an avalanche photodiode detector (APD) with a 50 μm aperture (MPD,

PDM050CTB) to provide confocal resolution. A custom LabView program was used to manipulate the nanopositioning stage and collect emission. Emission from single molecules was established based on the observation of diffraction-limited spots, blinking dynamics, and irreversible single-step photobleaching.

Blinking dynamics were acquired using 10-30 ms integration times for up to 200 s. Consistent with previous analyses, blinking dynamics were analyzed using the change-point detection method (CPD), which reports statistically-significant intensity change points, rather than a threshold method since previous studies have established that thresholding is problematic.²³ Deconvolved states with intensities greater than one standard deviation above the rms noise (i.e. 20% of the maximum emission) are denoted as on states, while the lowest deconvolved state is deemed the nonemissive “off” state. The durations of the first and last events are disregarded, since they are artificially set by the observation period. Control blinking experiments are performed on bare glass to determine the average background noise. Dye molecules are discounted in the final Clauaset analyses if they have at least one on segment lower than the calculated average background noise from the control blinking traces. For example, blinking traces of blank glass with experimental parameters for purpurin lake had a calculated average background signal of $3.40(\pm 0.06)$ counts per 10 ms, so any purpurin lake molecules with emissive events corresponding to < 3.40 counts per 10 ms are discounted. Matlab with custom code was used for all data analyses and fitting procedures. If Matlab determines that the intensity of the last deconvolved

segment is the lowest in the whole trace for a molecule, then the molecule is considered photobleached.

Results and Discussion

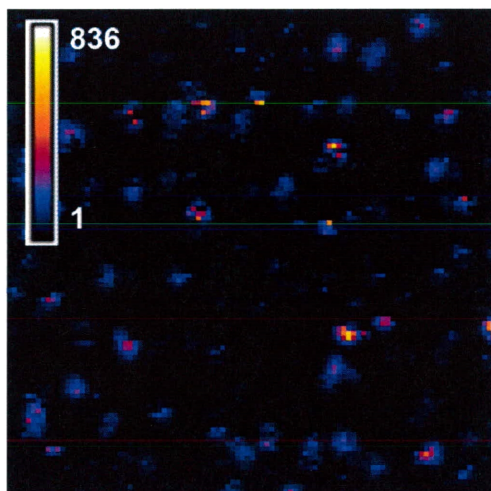


Figure 3 False-colored $10 \times 10 \mu\text{m}^2$ image of fluorescence from 10^{-9} alizarin on glass obtained with 532 nm excitation and laser power (P_{exc}) of $0.80 \mu\text{W}$. Color scale corresponds to counts per 30 ms.

SMS studies of alizarin and purpurin in anoxic environments

To study the effect of dye structure on chromophore blinking and bleaching, SMS studies of alizarin and purpurin (Figure 1) were performed by spin coating nanomolar quantities of the dyes onto clean glass slides and flushing the samples with nitrogen. Figure 3 presents a representative false-colored fluorescence image of single alizarin molecules on glass recorded using a single-molecule confocal microscope employing 532-nm excitation at $1.4 \mu\text{W}$, a 100-nm step size, and a 30 ms integration time. Corresponding SMS studies of purpurin excitation $2.6 \mu\text{W}$ excitation power, a 100-nm step size, and a 10 ms integration time. The blinking dynamics of 138 alizarin molecules and 91 purpurin molecules are analyzed with the CPD method.³² Consistent with previous SMS studies of single rhodamine

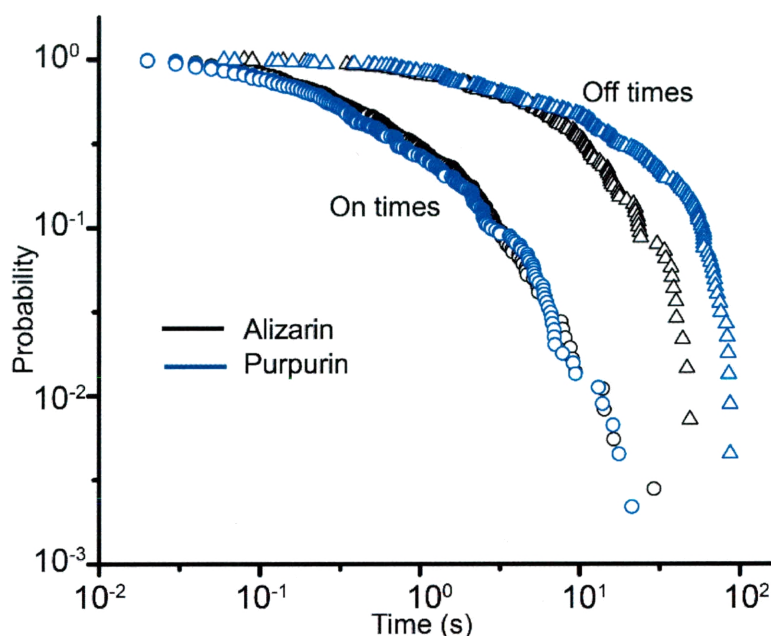


Figure 4 Probability distributions for alizarin (black) and purpurin (blue) in N_2 . On times are denoted with circles and off time are denoted with triangles.

molecules on glass and TiO_2 , the resulting on- and off-time histograms are transformed into complementary cumulative probability distribution functions (CCDFs) (Figure 4). These probability distributions describe the probability of an event occurring in a time less than or equal to a given t .

The on-time probability distributions for alizarin and purpurin appear quite similar, but the off times are distinct. To understand these differences the probability distributions are fit to a variety of heavy-tailed probability distribution functions (i.e., power law, Weibull, log-normal). In this method, the goodness of fit to each function is quantified by a p value.³³ Values of $p < 0.05$, which suggest that the data has less than a 5% chance of arising from the corresponding probability distribution function, are considered statistically insignificant. Table 1 shows the fit parameters corresponding to log-normal and Weibull functions for alizarin and purpurin. Based on a significant p value of 0.05, on times for alizarin are best

characterized by the log-normal distribution. A nonzero p -value for purpurin indicates that on times are also best described by the log-normal distribution.

Figure 4 also shows that while on times for alizarin and purpurin are similar, corresponding off times appear significantly distinct, reflected by their respective fit parameters (Table 1). For alizarin, off times are characterized by the Weibull function, based on an unusually high p value ($p = 0.93$), while a nonzero p value ($p = 0.026$) for purpurin off times indicates that the data is also best fit by the Weibull function.

	Fit Parameters		p - value	
	Log-normal $\frac{1}{t\sigma\sqrt{2\pi}} e^{-\frac{(\ln(t)-\mu)^2}{2\sigma^2}}$	Weibull $\frac{A}{B} \left(\frac{t}{B}\right)^{A-1} e^{-\left(\frac{t}{B}\right)^A}$	Log-normal	Weibull
Alizarin ON	$\mu = -0.86 \pm 0.08$ $\sigma = 1.49 \pm 0.05$	$A = 0.69$ $B = 0.91$	0.05	0
Alizarin OFF	$\mu = 1.4 \pm 0.1$ $\sigma = 1.49 \pm 0.09$	$A = 0.75$ $B = 8.66$	0.01	0.9
Purpurin ON	$\mu = -1.00 \pm 0.07$ $\sigma = 1.52 \pm 0.05$	$A = 0.65$ $B = 0.80$	0.004	0
Purpurin OFF	$\mu = 1.8 \pm 0.1$ $\sigma = 1.2 \pm 0.8$	$A = 0.62$ $B = 15.11$	0	0.026

Table 1. Best-fit parameters and p -values for log-normal and Weibull functions for alizarin and purpurin in N_2 on glass. Statistically significant p -values are highlighted and in bold. Errors represent one standard deviation.

Appendix III shows the complete fit parameters for power-law, Weibull, and log-normal functions. It should be noted that although p values for the power-law function in Appendix III are often above 0.05, indicating statistical significance, the large t_{min} parameters indicate that only a small percentage of the data is actually fit by power law. Therefore, we further omit any further discussion of power law.

The data in Figure 4 and Table 1 suggest that the off times, governed by equation 1:

$$\tau_{off} = \frac{1}{k_{31}} \quad [1]$$

where k_{31} is the rate from the dark state back to the ground state, are affected by the structural differences in the two molecules (Figure 1). On times are insensitive to changes in structure, as their statistical parameters (Table 1) of μ (mean of the event distribution) and σ (standard deviation) are within error. To understand the differences in the photophysics of these molecules, a discussion of excited state intramolecular proton transfer (ESIPT) is necessary.

Excited State Intramolecular Proton Transfer (ESIPT)

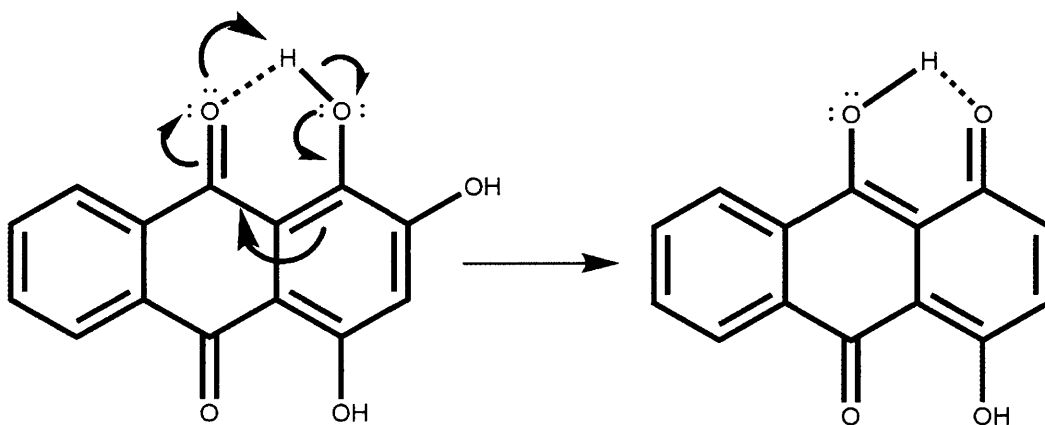


Figure 5 ESIPT in alizarin and purpurin (blue), where (a) excited molecule before ESIPT and (b) is the phototautomer formed after ESIPT

Several ensemble-averaged fluorescence studies of hydroxyanthraquinones (e.g. alizarin) have observed ESIPT.^{4,8,34} Thus, we expect ESIPT plays a role in the blinking dynamics of alizarin and purpurin. ESIPT reactions are among the fastest chemical reactions, with rates observed on a femtosecond time scale.³⁴ The highly conjugated nature of anthraquinones results

in low-lying molecular orbital energy states and easily-accessible excited states, making ESIPT a likely process for many hydroxyanthraquinones. In ESIPT, a proton transfer from the substituted hydroxyl group to the anthraquinone ketone can occur upon photoexcitation of the molecule (Figure 5).³⁴ An energy level diagram corresponding to ESIPT is shown in Figure 6. In the ground state S_0 , the molecule absorbs light and is excited to a fluorescent S_1 state, where a local emission (LE) is observed. However, in the excited state, the molecule can undergo fast ESIPT to form the phototautomer in Figure 5b. Emission in the excited tautomer state T^* is also observed at a lower energy than the local emission. The local emission that occurs from $S_1 \rightarrow S_0$ is characterized as the short wavelength emission (SWE), while the emission that occurs from $T^* \rightarrow T$ is termed long wavelength emission (LWE). This dual fluorescence is characteristic of ESIPT.

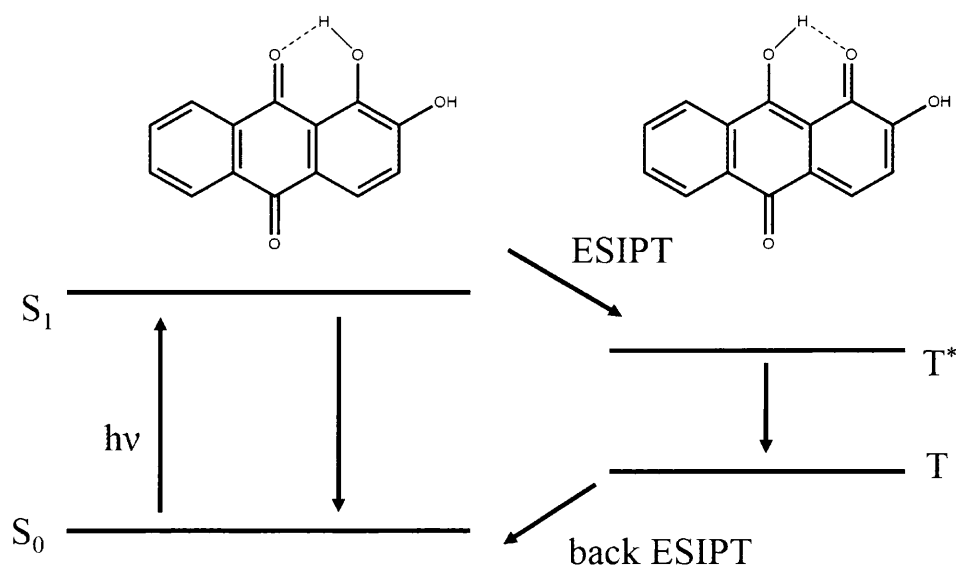


Figure 6 Four energy level diagram characteristic of ESIPT. Molecule is excited from S_0 to S_1 , and in the course of ESIPT converts to the phototautomer T^* (adapted from Reference 34)

To test the hypothesis that ESIPT plays a role in blinking, solvent-dependence emission studies were performed. Figure 7a shows that alizarin exhibits dual fluorescence ($\lambda_{LE} = 534$ nm, $\lambda_{ESIPT} = 594$ nm), consistent with ESIPT. Indeed, Miliani *et al.* determined that dual emission of alizarin is solvent- and wavelength-dependent.^{35,36} In nonpolar solvents such as benzene, the locally excited structure of alizarin is stabilized, and a large ratio of the local emission to the emission from the tautomer is observed (Figure 7). However, in more polar solvents such as ethanol and acetonitrile, the alizarin tautomer is stabilized, and a high ratio of the emission from the tautomer to the local emission is observed. Furthermore, Figure 8 shows an unusually large Stokes shift of 70 nm for alizarin in ethanol, indicating that ESIPT occurs in alizarin.

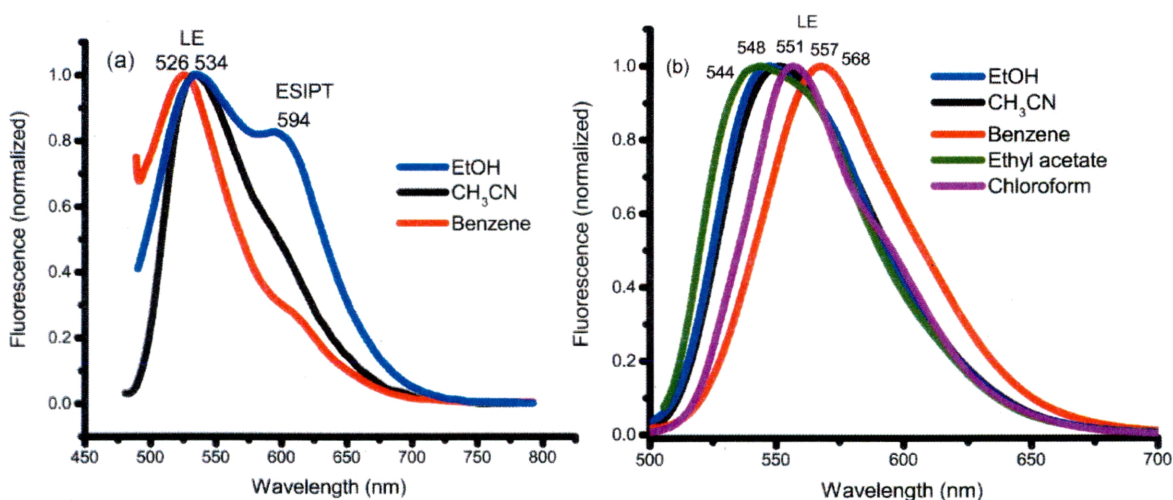


Figure 7 Emission studies of alizarin and purpurin in ethanol. Alizarin exhibits solvent-dependent dual fluorescence from the local emission and the phototautomer, while purpurin maintains the same λ_{em} over a range solvents

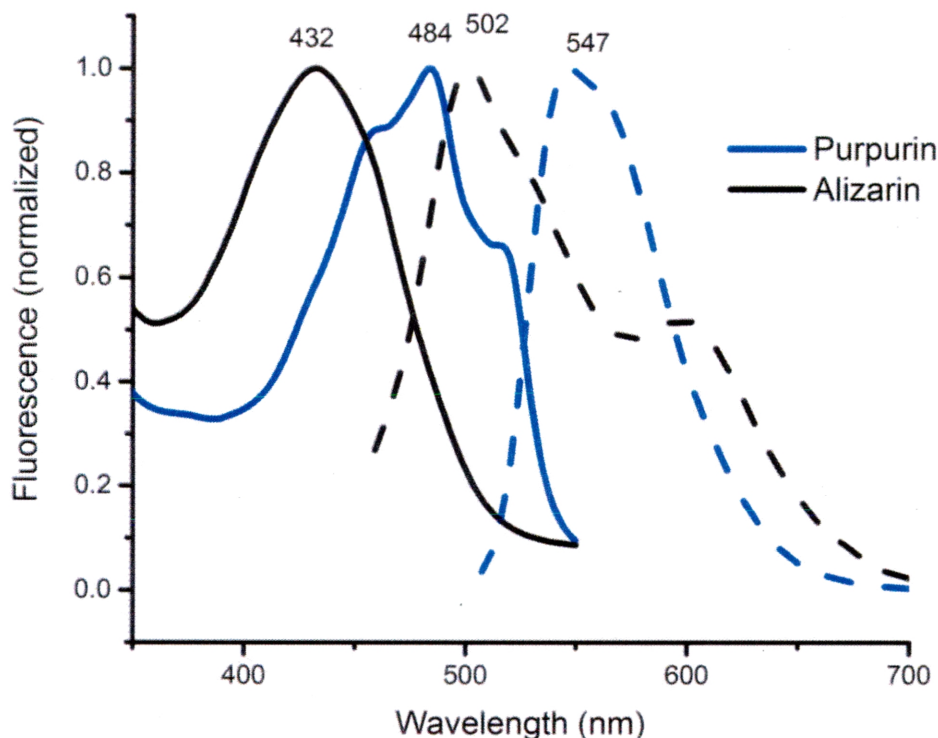


Figure 8 Absorbance (solid line) and emission studies (dashed line) of alizarin and purpurin in benzene. Both dyes exhibit unusually large Stokes shifts, indicating ESIPT.

In the same solvent-dependent studies of purpurin, it appears purpurin exhibits very different photophysical behavior than alizarin. While clear dual fluorescence is not observed, consistent with reports that purpurin does not undergo ESIPT,⁴ there appear to be modest secondary peak at $\lambda_{em} = \sim 564$ nm in the fluorescence spectra of purpurin in polar solvents, indicating that ESIPT possibly occurs in purpurin. Furthermore, Figure 8 demonstrates that purpurin in ethanol has an unusually large Stokes shift (63 nm), suggesting that ESIPT does occur in both purpurin and alizarin. Given that ensemble-averaging limits the ability to accurately probe subpopulations of molecules, additional investigation is required to determine if ESIPT plays a role in the photophysics of purpurin. Given that ESIPT occurs in alizarin and possibly in purpurin, we hypothesize this mechanism accounts for the dark state in the blinking of these molecules, since at

532-nm excitation our single-molecule detector is not able to detect the LWE from the phototautomer.

Although the distributions of on times for purpurin and alizarin are similar, the distribution of the off times are distinct. The probability distributions in Figure 4 show that purpurin experiences longer off times than purpurin. If ES IPT is a process that occurs in purpurin, this suggests that alizarin is able to undergo back proton transfer more efficiently than purpurin due to the shorter distribution of off times for alizarin. As the substituted hydroxyl group in purpurin is the only structural difference between the molecules, it appears to play a role in the rates of back proton transfer. In ES IPT, the basic anthraquinone ketone acts as the acceptor for the acidic proton. However, during back proton transfer, the newly formed ketone in the phototautomer acts as the proton acceptor. We hypothesize that in purpurin, the ability of this ketone to accept a proton (i.e., its basicity) is directly affected by the para-hydroxyl substituent, causing a difference in the off times of purpurin and alizarin molecules.

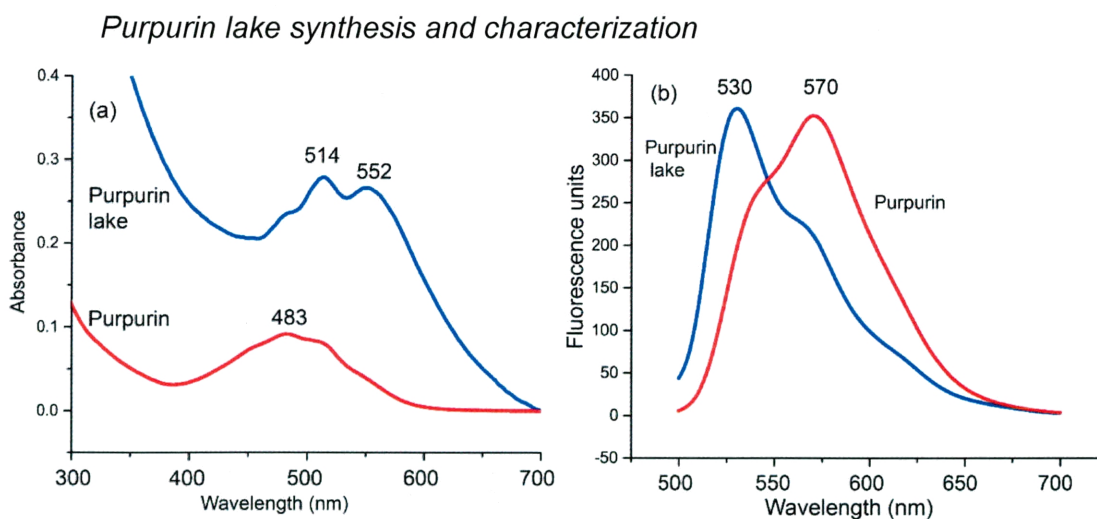


Figure 9 (a) Absorbance and (b) corresponding fluorescence spectra of purpurin and purpurin lake solutions in 3:1 MeOH/H₂O

To determine the differences in photophysics of an aluminum lake pigment relative to the bare chromophore, we studied purpurin lake using SMS. Ensemble-averaged UV/vis and fluorescence spectroscopy measurements were performed to compare the synthesized purpurin lake with the pure chromophore. Figure 9 shows the absorbance and corresponding fluorescence spectra of purpurin and purpurin lake, consistent with the absorbance and fluorescence maxima (λ_{abs} and λ_{em} , respectively) of previous fluorescence studies of purpurin.³¹ For purpurin $\lambda_{\text{abs}} = 483$ nm and $\lambda_{\text{em}} = 570$ nm, while for purpurin lake, there are two distinguishable peaks in the absorbance spectrum at $\lambda_{\text{abs}} = 514$ and $\lambda_{\text{abs}} = 552$, and $\lambda_{\text{em}} = 530$. SERS studies of the lake pigment and the purpurin dyestuff were done to determine any differences in vibrational modes due to structural changes to the molecule upon chelation to aluminum. Figure 10 presents the SERS spectra of purpurin and purpurin lake. The only peaks that are significantly distinct (i.e., >10 cm^{-1} apart) correspond to the 810 cm^{-1} (w) of purpurin and 826 cm^{-1} (w) of purpurin

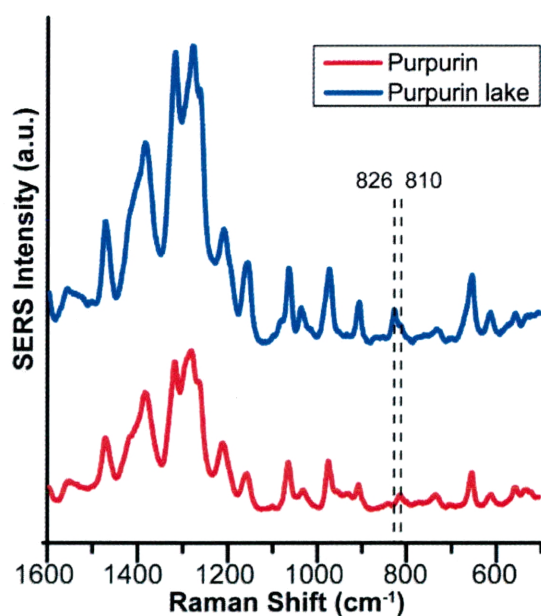


Figure 10 SERS spectra of purpurin and purpurin lake pigment obtained using 632.8 nm

lake. While no Raman theoretical calculations exist solely for purpurin dye, calculations for alizarin dye indicate that the 810 cm^{-1} peak for purpurin could correspond to CC stretching or C-H and C-O out-of-plane bending.³⁷ These results indicate that our synthesized purpurin lake is modestly spectroscopically distinct from the purpurin dyestuff, although future tests involving x-ray crystallography are planned to determine if our synthesized purpurin lake is structurally consistent with the structure for purpurin lake generally cited in the literature (Figure 1).

SMS of single purpurin lake molecules

Due to the insolubility of purpurin lake, several control experiments were performed to determine a consistent concentration to yield single molecules, as a proportional reduction of dye molecules in a false-colored fluorescence image was not generally observed with a reduction in dye concentration. For each new dye solution made, concentration tests were performed to determine what concentration should be used for single-molecule experiments. A 10^{-8} M solution in 3:1 solution of MeOH and ultrapure water typically used for SMS studies of purpurin lake, although due to its inability to completely dissolve in any available solvent, we suspect this concentration is lower. Based on the observed number of molecules for purpurin and purpurin lake solutions at 10^{-8} M concentrations, we estimate that the concentration of purpurin lake is actually $\sim 10\times$ lower than the calculated concentration that assumed total solubility.

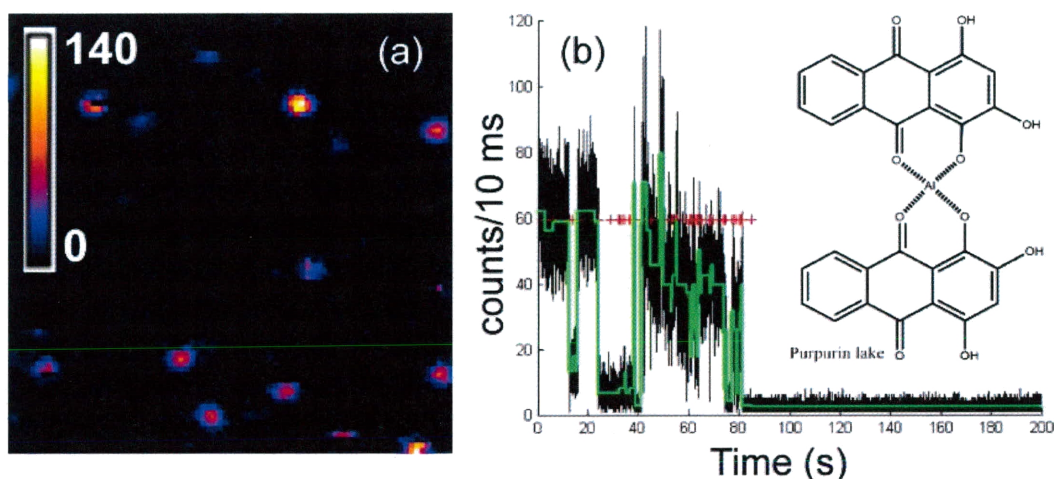


Figure 11 (a) False-colored $8 \times 8 \mu\text{m}^2$ images of fluorescence from 10^{-8} M purpurin lake on glass, obtained using 532-nm excitation and a laser power (P_{exc}) of $0.80 \mu\text{W}$. Color scale corresponds to counts per 10 ms. (b) Blinking dynamics using the CPD method for a single purpurin-lake molecule on glass is shown for the same acquisition parameters

Figure 11 presents a representative false-colored fluorescence image of purpurin lake molecules on glass using 532-nm excitation at $0.8 \mu\text{W}$, a 100-nm step size, and a 10 ms integration time, as well as representative time-dependent emission for a single purpurin lake molecule. Blinking dynamics of 52 purpurin lake molecules were recorded, compiled into CCDFs and fit to various functions to quantify their photophysical distributions. Figure 12 shows the probability distributions for purpurin and purpurin lake in N_2 . The on-time probability distributions are comparable, confirmed by the similarities (Table 2) in the statistical parameters for log-normal fit, μ and σ , for on time distributions, but the off times appear distinct. This pattern is analogous to the relationship between alizarin and purpurin in N_2 .

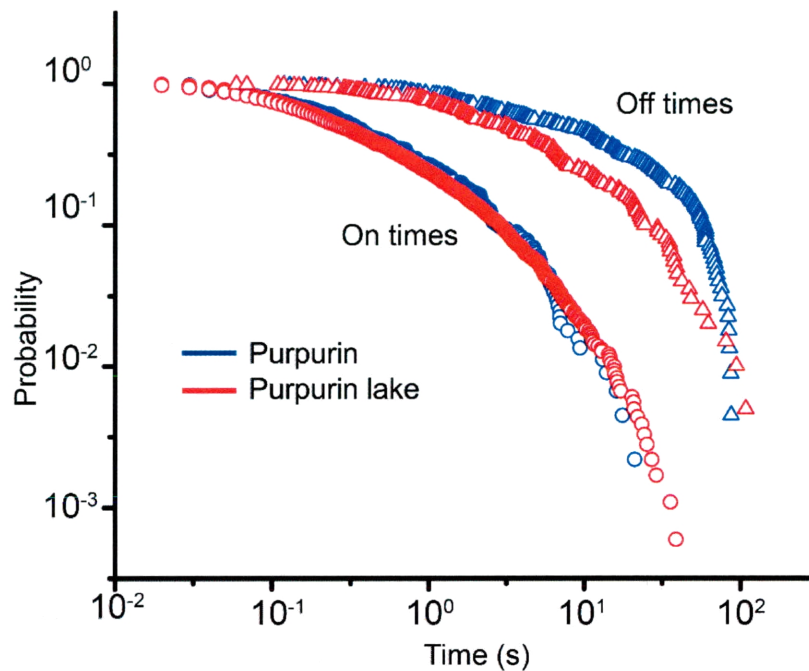


Figure 12 Probability distributions for purpurin in N₂ (blue) and purpurin lake in air (red). On time are denoted by circles and off time are denoted with triangles.

	Fit Parameters		<i>p</i> - value	
	Log-normal $\frac{1}{t\sigma\sqrt{2\pi}} e^{-\frac{(\ln(t)-\mu)^2}{2\sigma^2}}$	Weibull $\frac{A}{B} \left(\frac{t}{B}\right)^{A-1} e^{-\left(\frac{t}{B}\right)^A}$	Log-normal	Weibull
Purpurin ON	$\mu = -1.00 \pm 0.07$ $\sigma = 1.52 \pm 0.05$	A = 0.65 B = 0.80	0.004	0
Purpurin OFF	$\mu = 1.8 \pm 0.1$ $\sigma = 1.2 \pm 0.8$	A = 0.62 B = 15.11	0	0.026
Purpurin lake ON	$\mu = -1.09 \pm 0.04$ $\sigma = 1.53 \pm 0.03$	A = 0.64 B = 0.76	0	0
Purpurin lake OFF	$\mu = 1.1 \pm 0.1$ $\sigma = 1.59 \pm 0.08$	A = 0.63 B = 6.72	0.5	0.003

Table 2. Best-fit parameters and *p*-values for log-normal and Weibull functions for purpurin and purpurin lake in N₂. Statistically significant *p*-values are highlighted and in bold. Errors represent one standard deviation.

Although for purpurin lake on times, $p = 0$ for the log-normal and Weibull distributions, due to statistical similarities of the purpurin lake on-time probability distribution to the purpurin in N₂, we attribute that for purpurin lake, the on-time

distribution is best fit by log-normal distribution. Purpurin lake off times show a statistically significant p value for log-normal fit, but also has a nonzero p value corresponding to the Weibull function (although visual inspection of the fits does not strongly indicate log-normal distribution over Weibull). Indeed, statistical parameters for alizarin and purpurin lake in N_2 are closer than purpurin and purpurin lake indicating that purpurin lake behaves similar to alizarin and possibly undergoes ESIPT.

SMS studies of purpurin in air

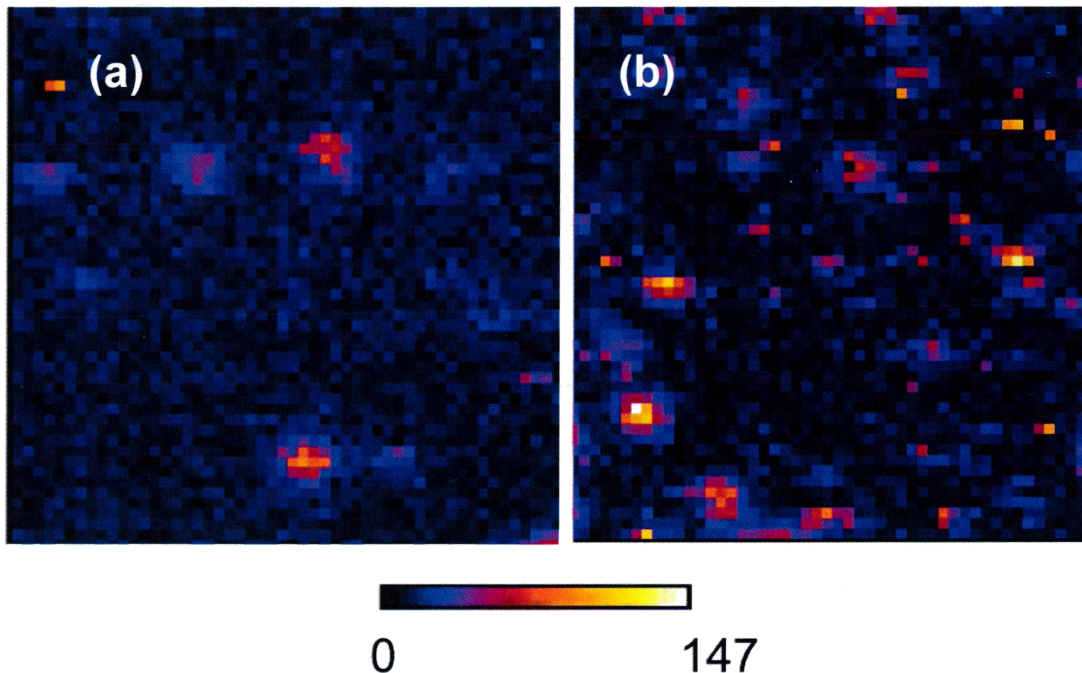


Figure 13 (a) False-colored images of fluorescence from 10^{-9} M purpurin on glass in (a) N_2 ($5 \times 5 \mu m^2$) and (b) air ($5 \times 5 \mu m^2$), obtained using 532-nm excitation and a laser power (P_{exc}) of $\sim 2.6 \mu W$. Color scale corresponds to counts per 10 ms.

Studies of purpurin were performed in both air and N_2 to determine the effect that oxygen has on fading, since the presence of oxygen has been known to influence fading.^{6,9} Figure 13 presents representative false-colored fluorescence

images of single purpurin molecules on glass in air (13a) and N_2 (13b) recorded using 532-nm excitation at 2.6 μW , 100-nm step size, and 10 ms integration time. Blinking dynamics were collected for 61 molecules in air and 91 molecules in N_2 and converted to CCDFs. Figure 14 shows the probability distributions for purpurin in N_2 and air. Purpurin on times are particularly sensitive to the presence of oxygen, given the difference between the probability distributions of purpurin in air and purpurin in N_2 . However, the statistical parameters (Table 3) indicate the similarity of the probability distributions for off times, as the respective μ and σ fall within error. The probability distributions of on times indicate that in air, purpurin spends less time in the on state than purpurin in N_2 , suggesting that oxygen facilitates a dark state in the molecule. While the only statistically significant p value for purpurin in air ($p = 0.08$) indicates the off times are best fit to a log-normal distribution, given the similarities in the statistical parameters for off times of

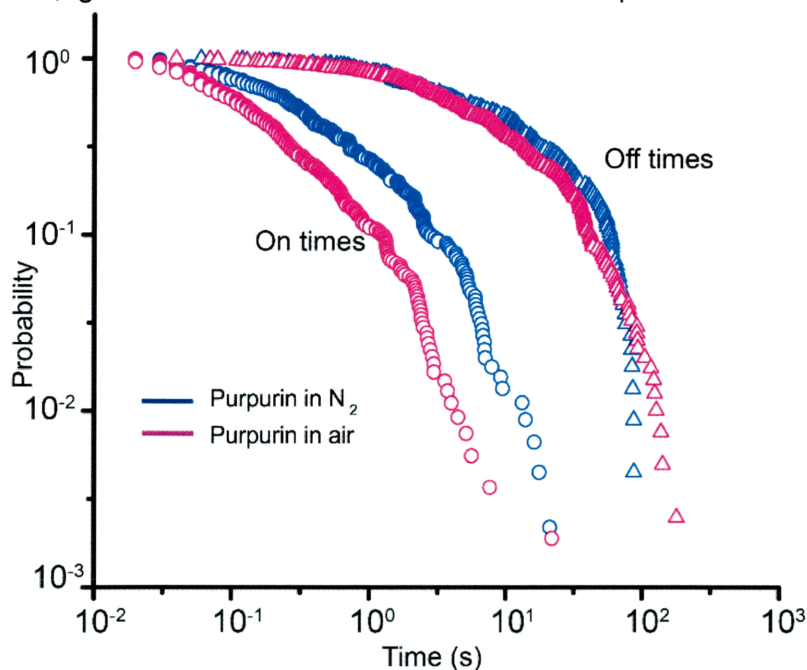


Figure 14 Probability distributions for purpurin in N_2 (blue) and purpurin in air (pink). On time are denoted by circles and off time are denoted with triangles.

purpurin in both air and N₂, we attribute the off times for purpurin in air as best fit by Weibull function ($p = 0.008$). A visual inspection of the data fits validates this assignment (see Appendix III).

Photobleaching

Photobleaching is responsible for the fading of organic colorants in artworks. To examine each molecule that reached photobleaching, blinking traces were analyzed to determine the time photobleaching occurred, the bleach intensity, and the bleach duration. Table 4 shows the average time until photobleaching for purpurin and purpurin lake in N₂. Purpurin dye shows photobleaching parameters distinct from its lake pigment. Appendix IV shows the complete photobleaching data. However, further experiments obtained with similar laser powers are required in order to accurately compare photobleaching parameters. Additional investigations are needed to determine photobleaching

	Fit Parameters		p - value	
	Log-normal $\frac{1}{t\sigma\sqrt{2\pi}} e^{-\frac{(\ln(t)-\mu)^2}{2\sigma^2}}$	Weibull $\frac{A}{B} \left(\frac{t}{B}\right)^{A-1} e^{-\left(\frac{t}{B}\right)^A}$	Log-normal	Weibull
Purpurin (N ₂) ON	$\mu = -1.00 \pm 0.07$ $\sigma = 1.52 \pm 0.05$	A = 0.65 B = 0.80	0.004	0
Purpurin (N ₂) OFF	$\mu = 1.8 \pm 0.1$ $\sigma = 1.2 \pm 0.8$	A = 0.62 B = 15.11	0	0.026
Purpurin (air) ON	$\mu = -1.80 \pm 0.06$ $\sigma = 1.32 \pm 0.04$	A = 0.72 B = 0.34	0	0
Purpurin(air) OFF	$\mu = 1.64 \pm 0.09$ $\sigma = 1.17 \pm 0.06$	A = 0.61 B = 11.61	0.08	0.008

Table 3. Best-fit parameters and p -values for log-normal and Weibull functions for purpurin in N₂ and air on glass. Statistically significant p -values are highlighted and in bold. Errors represent one standard deviation.

mechanisms for these molecules. We are especially interested in the role that $^1\text{O}_2$ plays in fading, since our data suggests that the photophysics of a molecule in air differs in an anoxic environment.

	Purpurin in N ₂ (2.6 μW)	Purpurin in air (2.6 μW)		Purpurin lake in N ₂ (0.8 μW)
N molecules that photobleached	46	16		38
N molecules	91	61		52
% photobleached	51%	26%		73%
Test length (s)	100	100	200	200
Average time until photobleach (s)	48 \pm 31	58 \pm 29	147 \pm 77	34 \pm 29

Table 4: Photobleaching data

Conclusions

The on times for alizarin, purpurin, and purpurin lake are best described by log-normal distributions, and off times are best described by Weibull functions. This data represents the first steps in investigation single lake pigment molecules in heterogeneous paint environments. Future studies of lake pigments will evaluate the effect that different mordant salts have on fading. The intricate photobleaching mechanisms of these colorants requires continued investigation, but their understanding prevents further photodamage to paintings and other objects that represent our cultural heritage.

Acknowledgements

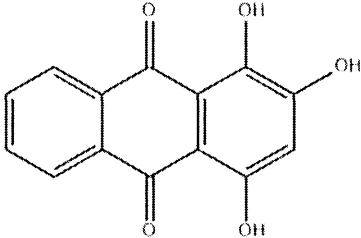
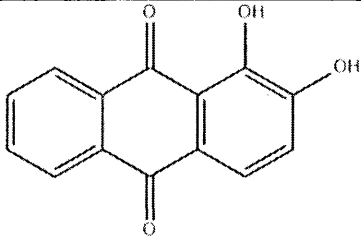
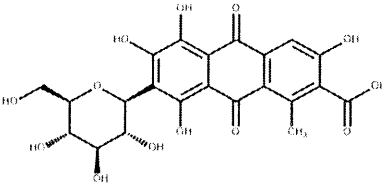
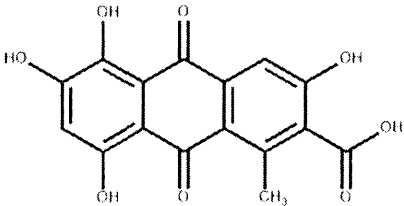
Sofia Garakyaraghi (W&M 2013) previously collected data SMS for alizarin and purpurin. Heidi Crockett and Kan Tagami assisted with purpurin lake SMS studies and data workup.

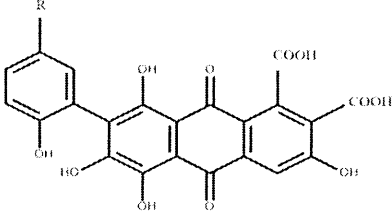
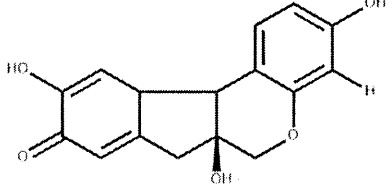
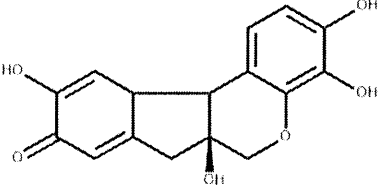
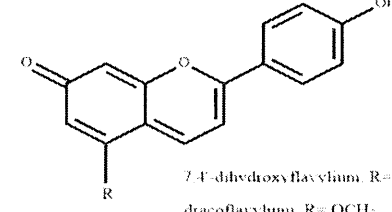
References

- Oakley, L. H.; Dinehart, S. A.; Svoboda, S. A.; Wustholz, K. L. *Anal. Chem.* **2011**, *83*, 3986.
- Allen, N.; McKellar, J. *Journal of Photochemistry* **1976**, *5*, 317.
- Egerton, G.; Morgan, A. *Journal of the Society of Dyers and Colourists* **1970**, *86*, 242.
- Nagaoka, S.; Nagashima, U. *Chem. Phys.* **1996**, *206*, 353.
- Crews, P. C. *Journal of the American Institute for Conservation* **1982**, *21*, 43.
- Koperska, M.; Łojewski, T.; Łojewska, J. *Anal. Bioanal. Chem.* **2011**, *399*, 3271.
- Oakes, J. *Rev. Prog. Color.* **2001**, *31*, 21.
- Favaro, G.; Miliani, C.; Romani, A.; Vagnini, M. *J. Chem. Soc., Perkins Trans. 2* **2002**, 192.
- Borst, H.; Kelemen, J.; Fabian, J.; Nepras, M.; Kramer, H. *J. Photochem. Photobiol. A.* **1992**, *69*, 97.
- Gollnick, K.; Held, S. *J. Photochem. Photobiol. A.* **1993**, *70*, 135.
- Gupta, D.; Gulrajani, M.; Kumari, S. *Color. Technol.* **2004**, *120*, 205.
- Montoya, S. C. N.; Comini, L. R.; Sarmiento, M.; Becerra, C.; Albesa, I.; Argüello, G. A.; Cabrera, J. L. *J. Photochem. Photobiol. B* **2005**, *78*, 77.
- Gutiérrez, I.; Bertolotti, S. G.; Biasutti, M.; Soltermann, A. T.; Garcia, N. A. *Can. J. Chem.* **1997**, *75*, 423.
- Gollnick, K.; Held, S.; Mártire, D. O.; Braslavsky, S. E. *J. Photochem. Photobiol. A.* **1992**, *69*, 155.
- Flom, S. R.; Barbara, P. F. *J. Phys. Chem.* **1985**, *89*, 4489.
- Cho, D. W.; Kim, S. H.; Yoon, M.; Jeoung, S. C. *Chem. Phys. Lett.* **2004**, *391*, 314.
- Moerner, W.; Kador, L. *Phys. Rev. Lett.* **1989**, *62*, 2535.
- Shera, E. B.; Seitzinger, N. K.; Davis, L. M.; Keller, R. A.; Soper, S. A. *Chem. Phys. Lett.* **1990**, *174*, 553.
- Orrit, M.; Bernard, J. *Phys. Rev. Lett.* **1990**, *65*, 2716.
- Weiss, S. *Science* **1999**, *283*, 1676.
- Weiss, S. *Nat. Struct. Biol.* **2000**, *7*, 724.
- Schuler, B.; Lipman, E. A.; Eaton, W. A. *Nature* **2002**, *419*, 743.
- Wong, N. Z.; Ogata, A. F.; Wustholz, K. L. *J. Phys. Chem. C* **2013**, *117*, 21075.
- Bernard, J.; Fleury, L.; Talon, H.; Orrit, M. *J. Chem. Phys.* **1993**, *98*, 850.
- Vosch, T.; Hofkens, J.; Cottlet, M.; Köhn, F.; Fujiwara, H.; Gronheid, R.; Van Der Biest, K.; Weil, T.; Herrmann, A.; Müllen, K.; Mukamel, S.; Van der Auweraer, M.; De Schryver, F. C. *Angewandte Chemie* **2001**, *113*, 4779.
- Bott, E. D.; Riley, E. A.; Kahr, B.; Reid, P. J. *ACS Nano* **2009**, *3*, 2403.
- Chen, R.; Gao, Y.; Zhang, G.; Wu, R.; Xiao, L.; Jia, S. *International journal of molecular sciences* **2012**, *13*, 11130.
- Haase, M.; Hübner, C. G.; Reuther, E.; Herrmann, A.; Müllen, K.; Basché, T. *The Journal of Physical Chemistry B* **2004**, *108*, 10445.
- Grazia, C.; Clementi, C.; Miliani, C.; Romani, A. *Photochem. Photobiol. Sci.* **2011**, *10*, 1249.
- Miliani, C.; Romani, A.; Favaro, G. *J. Phys. Org. Chem.* **2000**, *13*, 141.
- Claro, A.; Melo, M. J.; Schäfer, S.; de Melo, J. S. S.; Pina, F.; van den Berg, K. J.; Burnstock, A. *Talanta* **2008**, *74*, 922.
- Watkins, L. P.; Yang, H. *The Journal of Physical Chemistry B* **2005**, *109*, 617.
- Clauset, A.; Shalizi, C. R.; Newman, M. E. *SIAM Rev* **2009**, *51*, 661.

34. Tomin, V. I.; Demchenko, A. P.; Chou, P. *J. Photochem. Photobiol. C* **2015**, *22*, 1.
35. Miliani, C.; Romani, A.; Favaro, G. *Spectrochim. Acta, Pt. A: Mol. Spectrosc.* **1998**, *54*, 581.
36. Miliani, C.; Romani, A.; Favaro, G. *Journal of Physical Organic Chemistry* **2000**, *13*, 141.
37. Cañamares, M. V.; Garcia-Ramos, J. V.; Domingo, C.; Sanchez-Cortes, S. *J. Raman Spectrosc.* **2004**, *35*, 921.

APPENDIX I: TABLE OF HISTORIC ORGANIC DYES AND PIGMENTS

Dye	Lake pigment?	Description	Chromophore structure(s)
Purpurin	Madder lake	<p>Purpurin and alizarin are anthraquinones found in dyes derived from the root of plants of the Rubiaceae species. Both unmordanted madder dye and madder lake have been used since antiquity. The lake pigment is prepared by adding alum to the madder dye and precipitating it with alkali.</p>	
Alizarin			
Cochineal	Carmine lake	<p>Cochineal is derived from the Coccoidea superfamily of scale insects. New World cochineal and Old World cochineal originate from different genera of these insects. The earliest use of cochineal as a dye was reportedly in Peru in 700 B.C. Carminic acid is the main chromophore of the insect dye. Cochineal lake is referred to as carmine, and is generally mordanted with aluminum.</p>	
Kermes	Yes, referred to as kermes of kermes lake	<p>Kermes is also derived from the Coccoidea superfamily of scale insects, but of the family Kermesidae. Kermesic acid is the chromophore in the insect. Cochineal and kermes are sometimes confused for each other due to the fact that Old World cochineal often contains traces of kermesic acid. Lakes of kermes are made with aluminum, but have been found to have very little significance in paintings.</p>	

Lac dye	Yes, generally known as lac or lac lake, sometimes Indian lake	Lac is also derived from the Coccoidea superfamily of scale insects, but belonging to the kerria lacca species. Lac as a dye has been used since antiquity, but was probably imported to Europe by 1200. The lake pigment is thought to be the primary lake pigment for 15 th century easel painting.	 <p>Laccate acid A R = CH₂CH₂NHCOCH₃ Laccate acid B R = CH₂CH₂OH</p>
Brazilwood	Brazilwood lake	Dye derived from the wood of the genus <i>caesalpinia braziliensis</i> . The dye extract is made by boiling the chipped wood with water and filtered. To make the lake pigment it is precipitated with hot alum. The main chromophores of brazilwood are brazilein and brazilin. Brazilin bears the dye through oxidation to form the dye component brazilein. Brazilwood has had few identifications in paint, probably due in part to their fugitive nature.	
Logwood	Yes, known as logwood	Dye derived from the red wood of the species <i>haematoxylon campechianum</i> . It is extracted by boiling wood chips. The hematoxylin in the raw logwood oxidizes to haematin during the dye making process. A different range of colors can be made depending on the pH of the dye process and the mordant metal. Logwood was mentioned as a cheap watercolor in the 17 th century, but likely not in oil painting.	
Dragon's blood	Maybe, but pigment probably was not successful for painting	Dye that forms as an exudate from plant species belonging to the <i>dracaena</i> and <i>daemonorops</i> genera. Although historically used as a stain for varnishes, it is not commonly used as an artist's colorant in painting.	 <p>7,4'-dihydroxyflavylum R = H dracoflavylum R = OCH₃</p>

APPENDIX II: USING RAMAN SPECTROSCOPY AND SURFACE-ENHANCED RAMAN SCATTERING (SERS): AN EXPERIMENT FOR AN UPPER-LEVEL CHEMISTRY LABORATORY

Introduction

Although surface-enhanced Raman scattering (SERS) spectroscopy has become a powerful technique in analytical and physical chemistry, combining nanoscience and vibrational spectroscopy for the unambiguous and ultrasensitive detection of a wide variety of analytes,¹ SERS is a topic seldom covered in undergraduate curriculum. The application of SERS to art conservation to identify colorants in minute samples from cultural heritage objects represents an excellent method to familiarize undergraduate students with modern spectroscopy and nanoscience. While there are various laboratory experiments designed to introduce undergraduates to art conservation using Raman spectroscopy,² UV/vis spectrometry,³ NIR imaging,⁴ and XRF,⁵ and several experiments designed to demonstrate the SERS effect and estimate enhancement factors,⁶⁻⁹ there are no existing laboratories devoted to the application of SERS to art conservation. The integration of SERS with art conservation enriches the learning experience for undergraduates, combining elements of nanoscience and advanced spectroscopy within the engaging context of art conservation. In this laboratory experiment, undergraduates synthesize silver nanoparticles and perform normal Raman spectroscopy (NRS) and SERS measurements to identify both natural, organic pigments and inorganic pigments in minute samples from four oil paints: carmine lake, madder lake, lac dye, and vermilion. Students are assigned two unknown colorants to identify. To demonstrate the differences between NRS and SERS,

each group is assigned the inorganic, nonfluorescent vermilion paint and then chooses one colorants among the remaining unknown fluorescent paints. NRS measurements are performed on both samples, with students observing either Raman scattering from vermilion, or molecular fluorescence from the organic paint, demonstrating the usefulness of NRS for inorganic pigments and its limitations for organic pigments. If an organic pigment is indicated by molecular fluorescence, students treat the paint sample with silver nanoparticles to obtain a SERS spectrum.

Experimental

Overview

At the beginning of the lab period, students are given a comprehensive explanation of NRS and SERS and their applications to art conservation, and are informed about safety procedures and potential hazards of the lab. A group of 2-3 students obtain two small samples from the oil paints, one from the vermilion paint and one from a paint containing an organic pigment. One student performs the nanoparticle synthesis (<1 hr) while one student obtains paint samples and attempts NRS measurements. Each group then treats their unknown fluorescent sample with nanoparticles and measures SERS. Students' spectra are compared with a correlation value for library spectra to identify the unknown samples.

Silver Nanoparticle Synthesis

Glassware is cleaned with aqua regia and rinsed thoroughly with deionized water prior to the laboratory period. Silver nanoparticles are synthesized by the reduction of AgNO_3 by sodium citrate trihydrate (Sigma Aldrich).¹⁰ Approximately

9 mg of AgNO_3 is added to a 125 mL Erlenmeyer flask containing 50 mL of ultrapure water (Fisher EasyPure, Milli-G, $18.2 \text{ M}\Omega \text{ cm}^{-1}$) with stirring. The solution is heated on a stirring hot plate to $\sim 300 \text{ }^\circ\text{C}$. Upon vigorous boiling of the solution, 1 mL of sodium citrate (1% w/v) is added to initialize nanoparticle growth. The reaction then proceeds for 30 minutes, resulting in an opaque gray-green solution. A centrifuge (Eppendorf MiniSpin) operating at 13.4 rpm for 15 min is used to concentrate 1 mL aliquots of the colloids, with $\sim 100 \text{ }\mu\text{L}$ of colloid solution remaining after supernatant removal.

Art Sample Preparation

Students sample from oil paint to simulate the experience of handling a cultural heritage object. All painting materials were obtained from Kremer Pigments and stored in the dark. Paints were prepared by grinding the pigments into linseed oil with a glass muller. A wood panel was primed with a layer of linseed oil before the four unknown paints were applied. The panel was stored in a closed container in the dark to minimize pigment fading and dust accumulation. Students used surgical razor blades (Feather Safety Razor Company, #15) to remove $\sim 1 \text{ mm}$ paint samples from the wood panel that are placed on glass coverslips (Fisher) for NRS measurements.

NRS and SERS measurements

A DeltaNu (Intevac Photonics) benchtop Raman spectrometer employing a 785 nm diode laser and a right angle attachment was used for all measurements. Laser power is kept $< 10 \text{ mW}$ for the samples and acquisition times are $\sim 10 \text{ s}$. Students identified the unknowns using the reference library created for the laboratory with the DeltaNu NuSpec software. For SERS measurements, art

samples are transferred to centrifuge tubes containing concentrated silver colloid paste and mixed at 13.4 rpm for 15 min. Three 1- μL aliquots of the resulting mixture are applied to a coverslip.

Results and Discussion

The NRS spectra of vermilion, carmine lake, lac dye, and madder lake oil paints are shown in Figure 1. The NRS spectrum of vermilion paint exhibits characteristic peaks at 342, 284, and 252 cm^{-1} .^{11,12} Conversely, Figure 1 demonstrates that upon 785 nm excitation Raman scattering from the organic colorants is overwhelmed by fluorescence. For these fluorescent paints, students treat their samples with silver nanoparticles and perform SERS measurements. Figure 3 shows the corresponding SERS spectra of lac dye,

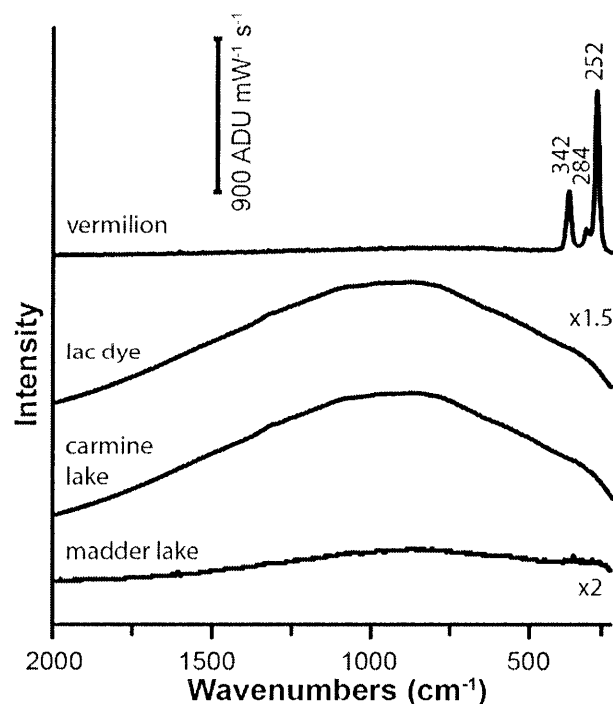


Fig 1 Student spectra for ~ 1 mm samples of vermilion, lac dye, carmine lake, and madder lake oil paints. The Raman spectrum of vermilion paint is evident, but fluorescence impedes the measurement of Raman scattering for the organic colorants

carmine lake, and madder lake paint samples that have been treated with silver nanoparticles. Lac dye exhibits characteristic SERS peaks for laccaic acid at 1464 cm^{-1} , 1276 cm^{-1} , 1225 cm^{-1} , 1098 cm^{-1} , 1056 cm^{-1} , 1010 cm^{-1} , 453 cm^{-1} , and 413 cm^{-1} .¹³ The SERS spectrum of carmine lake paint exhibits major peaks at 1291 cm^{-1} , 460 cm^{-1} , and 428 cm^{-1} , characteristic of carminic acid.¹⁴ The SERS spectrum of madder lake paint contains characteristic peaks for the major chromophores alizarin and purpurin at 1547 cm^{-1} , 1390 cm^{-1} , 1322 cm^{-1} , 1286 cm^{-1} , 1187 cm^{-1} , 1158 cm^{-1} , and 476 cm^{-1} .^{15,16} Although these colorants are all derived from

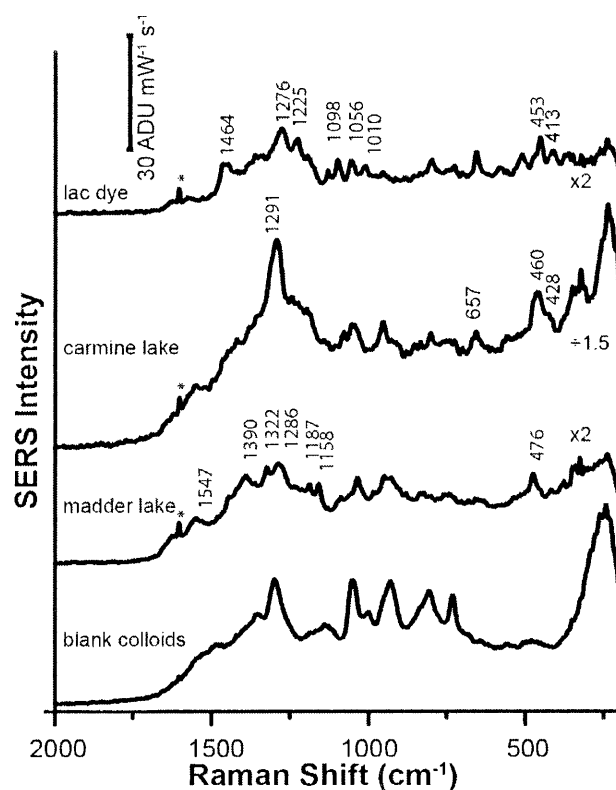


Fig 2 SERS spectra lac dye, carmine lake, and madder lake paint samples obtained by students following treatments with silver nanoparticles. Characteristic peaks for each colorant are labeled and SERS from blank citrate-reduced colloids is shown for comparison. Asterisks denote peaks due to the glass substrate.

substituted anthraquinones, SERS measurements demonstrate unique vibrational fingerprints of chromophores that differentiate these organic colorants.

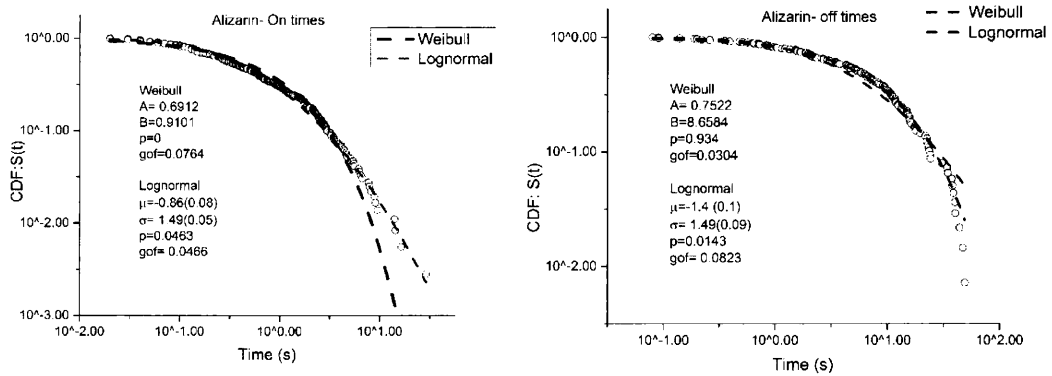
Students identified the unknown by comparing their spectra to a reference database compiled for the laboratory. Students attained spectral correlation values of $97 \pm 2\%$, $77 \pm 10\%$, $70 \pm 10\%$, $71 \pm 7\%$ to vermilion, lac dye, carmine lake, and madder lake paint, respectively, enabling the successful identification of unknowns. Students are tasked with justifying their identification of their unknown. In this laboratory experiment, students problem-solve an investigation of art from beginning to end, which enhances the understanding of the applicability of Raman and SERS spectroscopy to a real-world problem.

References

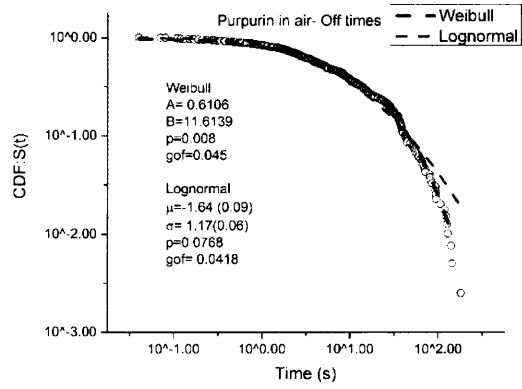
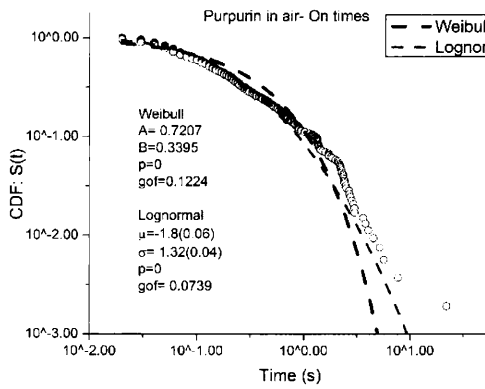
1. Stiles, P. L.; Dieringer, J. A.; Shah, N. C.; Van Duyne, R. P. *Annu. Rev. Anal. Chem.* **2008**, *1*, 601.
2. Nielsen, S.; Scaffidi, J.; Yeziarski, E. *J. Chem. Educ.* **2014**, *91*, 446.
3. Harmon, K. J.; Miller, L. M.; Millard, J. T. *J. Chem. Educ.* **2009**, *86*, 817.
4. Smith, G. D.; Nunan, E.; Walker, C.; Kushel, D. *J. Chem. Educ.* **2009**, *86*, 1382.
5. Nivens, D. A.; Padgett, C. W.; Chase, J. M.; Verges, K. J.; Jamieson, D. S. *J. Chem. Educ.* **2010**, *87*, 1089.
6. Pavel, I. E.; Alnajjar, K. S.; Monahan, J. L.; Stahler, A.; Hunter, N. E.; Weaver, K. M.; Baker, J. D.; Meyerhoefer, A. J.; Dolson, D. A. *J. Chem. Educ.* **2011**, *89*, 286.
7. Weaver, G. C.; Norrod, K. *J. Chem. Educ.* **1998**, *75*, 621.
8. Bright, R. M.; Seney, C. S.; Yelverton, J. C.; Eanes, S.; Patel, V.; Riggs, J.; Wright, S. *J. Chem. Educ.* **2007**, *84*, 132.
9. Schnitzer, C. S.; Reim, C. L.; Sirois, J. J.; House, P. G. *J. Chem. Educ.* **2010**, *87*, 429.
10. Lee, P. C.; Meisel, D. *J. Phys. Chem.* **1982**, *86*, 3391.
11. Bell, I. M.; Clark, R. J. H.; Gibbs, P. J. *Spectrochim. Acta, Pt. A: Mol. Spectrosc.* **1997**, *53*, 2159.
12. Burgio, L.; Clark, R. J. H. *Spectrochim. Acta, Pt. A: Mol. Spectrosc.* **2001**, *57*, 1491.
13. Leona, M. *Proceedings of the National Academy of Sciences* **2009**, *106*, 14757.
14. Oakley, L. H.; Dinehart, S. A.; Svoboda, S. A.; Wustholz, K. L. *Anal. Chem.* **2011**, *83*, 3986.
15. Pozzi, F.; Lombardi, J. R.; Bruni, S.; Leona, M. *Anal. Chem.* **2012**, *84*, 3751.
16. Bruni, S.; Guglielmi, V.; Pozzi, F. *J. Raman Spectrosc.* **2011**, *42*, 1267.

APPENDIX III: ALL SMS FIT PARAMETERS

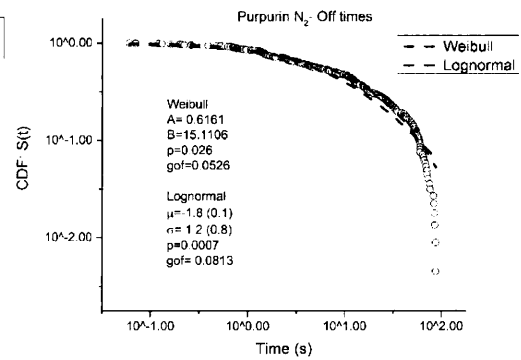
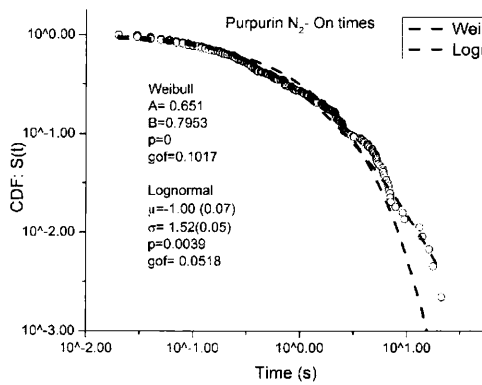
Alizarin in N ₂		
Power Law	On	Off
E	0.0848	0.1408
Alpha	2.6135	2.6537
Xmin	2.14	10.67
L	-119.834	-156.112
P	0.8157	0.0119
gof	0.052	0.1189
Weibull		
A	0.6912	0.7522
B	0.9101	8.6584
p	0	0.934
gof	0.0764	0.0304
Lognormal		
A	-0.86±0.08	-1.4±0.1
B	1.49±0.05	1.49±0.09
p	0.0463	0.0143
gof	0.0466	0.0823
N segments	1897	661
N molecules	138	



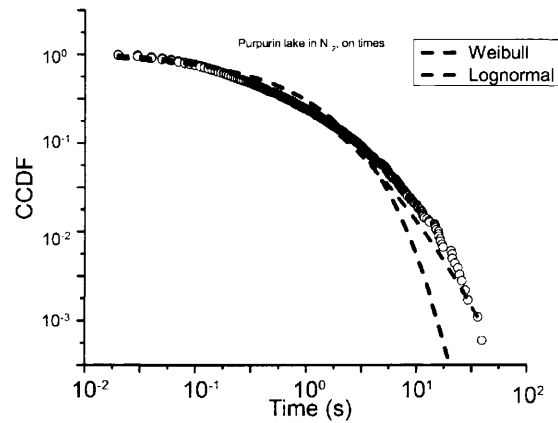
Purpurin in air		
Power Law	On	Off
E	0.0356	0.0953
Alpha	1.8231	2.8985
Xmin	0.13	32.1500
L	-106.356	-291.8552
p	0	0.0917
gof	0.0727	0.0812
Weibull		
A	0.7207	0.6106
B	0.3395	11.6139
p	0	0.008
gof	0.1224	0.045
Lognormal		
A	-1.7978±0.0568	1.6388 ± 0.0859
B	1.3155 ± 0.0402	1.17113 ±0.0607
p	0	0.0768
gof	0.0739	0.0418
N segments		
	533	388
N molecules		
	61	



Purpurin in N ₂		
Power Law	On	Off
E		
Alpha	3.4557	5.9136
Xmin	4.74	54.82
L	-64.0105	-101.236
p	0.4623	0.1655
gof	0.0856	0.1166
Weibull		
A	0.651	0.6161
B	0.7953	15.1106
p	0	0.026
gof	0.1017	0.0526
Lognormal		
A	-1.0011 ±0.0722	-1.8393±0.1
B	1.5248 ±0.0511	1.17333 ±0.8
p	0.0039	0.0007
gof	0.0518	0.0813
N segments	446	224
N molecules	91	



Purpurin lake in N ₂		
Power Law	On	Off
E	0.0393	0.1927
Alpha	2.6699	3.718
Xmin	4.95	33.86
L	-271.228	-62.244
p	0.3678	0
gof	0.0532	0.4584
Weibull		
A	0.6402	0.63
B	0.7563	6.72
p	0	0.003
gof	0.1034	0.0666
Lognormal		
A	-1.0913	1.1255 ±0.1124
B	1.5261±0.0254	1.5857±0.0795
p	0	0.4868
gof	0.061	0.041
N segments	2145	264
N molecules	52	



Power law:

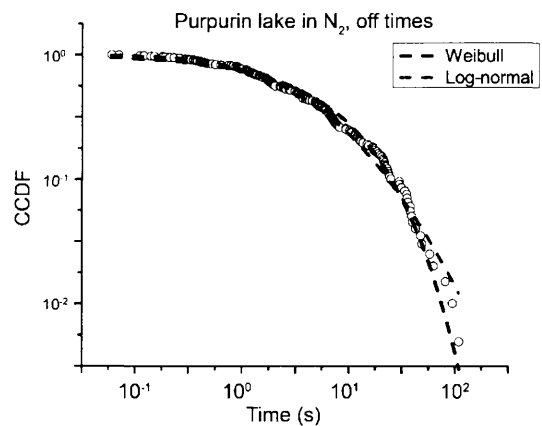
$$\frac{\alpha - 1}{t_{min}} \left(\frac{t}{t_{min}}\right)^{-\alpha}$$

Weibull:

$$\frac{A}{B} \left(\frac{t}{B}\right)^{A-1} e^{-\left(\frac{t}{B}\right)^A}$$

Log-normal:

$$\frac{1}{t\sigma\sqrt{2\pi}} e^{-\frac{(\ln(t)-\mu)^2}{2\sigma^2}}$$



APPENDIX IV: PHOTBLEACHING CPD3 DATA

CPD3bleach	Purpurin in N ₂ (2.6 μW)	Purpurin in air (2.6 μW)		Purpurin lake in N ₂ (0.8 μW)
Average time until bleach	48.2352 (31.27)	57.5628 (29.2336)	146.95 (77.8923)	34 (±29)
Min	0.21	10.72	9.18	0.21
max	96.85	95.12	199.82	162.58
Average bleach intensity	6.2037 (6.0806)	5.3910 (0.7434)	4.4998 (0.5143)	2.494168
Min	3.7841	3.9688	3.8596	1.972
max	41.952	6.0141	5.1404	5.4669
Average bleach duration	51.6352 (31.3514)	42.5285 (29.1843)	53.17 (77.8799)	98.34947
Min	3.17	5.06	0.57	10.86
Max	99.8	61.98	190.91	199.99
Test length (s)	100	100	200	200
N molecules	46	16		38
*Alizarin calculations in progress				